“Molecular Mechanisms of Chinese Herb Formula *Free and Easy Wanderer* In the Treatment of Mental Disorders”

Dissertation

zur Erlangung des Grades

“Doktor der Naturwissenschaften” im

Promotionsfach Pharmazie

am Fachbereich Chemie, Pharmazie und Geowissenschaften der Johannes Gutenberg-Universität in Mainz

vorgelegt von Chunlan Hong

geboren am 2 Januar, 1989

Mainz, November 2017

Betreuer:

Gutachter der Arbeit:

Datum der mündlichen Prüfung: 15. 11. 2017

Prüfungskommission:

D77 (Dissertation Universität Mainz)

Erklärung

Hiermit erkläre ich an Eides statt, dass ich diese Arbeit selbständig verfasst und keine anderen als die angegebenen Quellen und Hilfsmittel verwendet habe.

Mainz, 18.09.2017 Keine Unterschrift zwecks Datenschutz

_____ _____

Ort, Datum Chunlan Hong

Acknowledgement

Abstract

Background: Posttraumatic stress disorder (PTSD) is a mental disorder after traumatic events and is characterized by repeated experience of a trauma with disturbing recurring reflections, avoidance or numbing of memories of the event and hyper-arousal. Due to the high prevalence it has attracted much attention in the past years. The etiology is unclear and new treatment methods are urgently required. Various recipes of Chinese herbs are successfully used in Asian countries against mental disorders. For example, *Free and Easy Wanderer* (FAEW) has been a complex herbal mixture for treating mental disorders in China for centuries, but its mode of action is still unclear. **Method**: We conducted the following studies to elucidate the mechanisms of FAEW: (1) we have chosen a "reverse pharmacology" approach and initially used clinical data to verify identified potential PTSD mechanisms in subsequent *in vitro* and *in silico* studies. For this purpose, microarray-based transcriptome-wide mRNA expression profiles of PTSD patients were analyzed, the effect of FAEW and the clinically established antidepressant fluoxetine on the transcription factor NF-κB using reporter cell assays and Western blotting was investigated. (2) We investigated the neuroprotective effect of FAEW under oxidative stress and the underlying mechanism by microarray and Western blot experiments. (3) We identified various potential drugs by molecular docking and literature research based on the phytochemical components of FAEW. **Results**: FAEW showed high anti-inflammatory activity by inhibiting NF-κB. PTSD-associated oxidative stress was induced by hydrogen peroxide in the experiment. Here it was shown that FAEW counteracts oxidative stress through KEAP1-NRF2/HO-1 pathway. Paeoniflorin, albiflorin, baicalin, isoliquiritin and liquiritin in *silico* bound with high affinity to the proteins IκK, p65 and KEAP1. **Conclusion**: FAEW has a variety of drugs and is active against inflammation by inhibition of NF-κB and against oxidative stress by activation of KEAP1-NRF2/HO-1 signaling pathway, which could be relevant mechanisms of *Free and Easy Wanderer* in the treatment of mental disorders.

Key words: *Free and Easy Wanderer*, posttraumatic stress disorder, inflammation, oxidative stress, NF-κB, KEAP1-NRF2/HO-1

Zusammenfassung

Hintergrund: Die posttraumatische Belastungsstörung (PTSD) ist eine psychische Störung nach traumatischen Ereignissen und ist gekennzeichnet durch wiederholtes Erleben eines Traumas mit störenden wiederkehrenden Rückblenden und Verhinderung oder Betäubung von Erinnerungen an das Ereignis. Aufgrund der hohen Prävalenz hat sie in den vergangene Jahren viel Aufmerksamkeit erregt. Die Ätiologie ist ungeklärt und neue Behandlungsmethoden sind dringend erforderlich. Verschiedene Rezepturen chinesischer Kräuter werden in asiatischen Ländern mit Erfolg gegen psychische Störungen eingesetzt. Beispielsweise stellt Free und Easy Wanderer (FAEW) seit Jahrhunderten in China eine komplexe Kräutermischung zur Behandlung psychischer Störungen dar, deren Wirkungsweise jedoch immer noch unklar ist. **Methode**: Wir haben folgende Untersuchungen durchgeführt, um den Mechanismen von FAEW aufzuklären: (1) Wir haben einen „reverse pharmacology“ Ansatz gewählt und zunächst klinische Daten herangezogen, um identifizierte potenzielle PTSD-Mechanismen in nachfolgenden in vitro und in silico Untersuchungen zu verifizieren. Dazu wurden Mikroarray-basierte Transkriptom-weite mRNA-Expressions-Profile von PTSD-Patienten analysiert und die Wirkung von FAEW und dem klinisch etablierten Antidepressivum Fluoxetin auf den Transkriptionsfaktor NF-κB unter Verwendung von Reporterzell-Assays und Western-Blotting untersucht. (2) Wir haben den neuroprotektiven Effekt von FAEW unter oxidativem Stress und den zugrundeliegenden Mechanismus mittels Mikroarray- und Western-Blot Versuchen untersucht. (3) Wir haben die potenziellen Wirkstoffe durch molekulares Docking und Literaturrecherchen auf der Basis der phytochemischen Bestandteile von FAEW identifiziert. **Ergebnisse**: FAEW zeigte eine hohe anti-entzündliche Aktivität durch Hemmung von NF-κB. PTSD-assoziierter oxidativer Stress wurde durch Wasserstoffperoxid-Applikation im Experiment simuliert. Hier zeigte sich, dass FAEW oxidativem Stress durch den KEAP1-NRF2 / HO-1-Weg entgegenwirkt. Paeoniflorin, Albiflorin, Baicalin, Isoliquiritin und Liquiritin in silico banden mit hoher Affinität an die Proteine IκK, p65 und KEAP1. **Schlussfolgerung**: FAEW hat eine Vielzahl von Wirkstoffen und besitzt eine hohe anti-entzündliche Aktivität durch Hemmung von NF-κB und Aktivierung des anti-oxidativen KEAP1-NRF2 / HO-1 Signalweges. Diese könnten relevante Mechanismen bei der Behandlung von psychischen Störungen darstellen.

Stichwörter: *Free and Easy Wanderer*, posttraumatische Belastungsstörung, Entzündung, oxidativer Stress, NF-κB, KEAP1-NRF2/HO-1

Table of Contents

List of Abbreviations

Abbreviation	Connotation
ATP	adenosine triphosphate
BDNF	brain-derived neurotrophic factor
BTB	bric-a-brac
bZIP	basic leucine zipper
CAPS	Clinician-Administered PTSD Scale
CAT	Catalase
CBT	cognitive-behavioral therapy
CC	coil-coil domains
cDNA	complementary desoxyribonucleic acid
COMT	catechol-O-methyl transferase
CPSS	Child PTSD Symptom Scale
CRH	corticotrophin-releasing hormone
CRHR1	corticotrophin -releasing hormone receptor 1
CRIES	Children's Revised Impact of Event Scale
CTR	C-terminal region
DCF	Dichlorofluoresceine
DMF	Dimethylfumarate
DMSO	dimethyl sulfoxide
DSM	Diagnostic and Statistical Manual
EMDR	exposure therapy, eye movement desensitization and reprocessing
FAEW	*Free and Easy Wanderer*
FDA	Food and Drug Administration
GST	glutathione S-transferase
GWAS	genome-wide association studies
H_2DCFH-DA	2´, 7´-dichlorodihydrofluorescein diacetate
HAMD	Hamilton Depression Scale
HLH	helix-loop-helix
HMOX1	heme oxygenase 1 (alias HO-1)
HO-1	heme oxygenase 1 (alias HMOX1)
HPA	Hypothalamic-pituitary-adrenal
HPLC	high pressure liquid chromatography
ICD	International Classification of Diseases
IES-R	Impact of Event Scale-Revised Scale
IL-1	interleukin-1
IPA	ingenuity pathway analysis
IPT	interpersonal Psychotherapy

Abbreviation	Connotation
IVR	intervening region
IκB	inhibitor of κB
IκK	inhibitor kappa B kinase
KEAP1	Kelch-like ECH-associated protein 1
K-SADS-PL	Kiddie-SADS-Present and Lifetime Version
LPS	Lipopolysaccharide
LZ	leucine zipper
MS	mass spectrometry
NBD	NEMO-binding domain
NEMO	NF-κB essential modulator
NET	Narrative Exposure Therapy
NFE2L2	nuclear factor erythroid 2-like 2 (alias NRF2)
NF-κB	nuclear factor 'kappa light chain enhancer' of activated B-cells
NMR	nuclear magnetic resonance-mass spectrometry
NRF2	NF-E2 related factor 2 (alias NFE2L2)
NTR	N-terminal region
PBS	phosphate buffered saline
PCL-C	PTSD Checklist-Civilian Version
PDB	protein database
PTSD	posttraumatic stress disorder
PTSD-SS	Post-traumatic Stress Disorder Self-Rating Scale
RCTs	Randomized Controlled Trials
ROS	reactive oxygen species
RT-PCR	reverse transcription polymerase chain reaction
SCID-I/P	Structured Clinical Interview for DSM-IV-TR Axis I Disorder-Patient Edition
SNPs	single nucleotide polymorphisms
TBP	TATA-binding protein
TCM	Traditional Chinese Medicine
TFCBT	trauma-focused cognitive behavior therapy
TNF-α	tumor necrosis factor alpha
TSCC-A	Trauma Symptom Checklist for ChildrenAlternate Version
TSR	trauma spectrum response
VMD	Visual Molecular Dynamics
VRET	virtual reality exposure therapy
ZF	zinc finger

1 Introduction

1.1 General information about PTSD

Posttraumatic stress disorder (PTSD) may develop after a person is exposed to a traumatic event, it is characterized by repeatedly experiencing trauma with disturbing recurring flashbacks, avoidance or numbing of memories of the event, and hyper-arousal [1-3]. It was first recognized as a distinct disease among US-American Vietnam veterans and became popular due to high incidence and complex risk factors. The life time prevalence of PTSD in adults is 7.8%, women have a higher risk than men (20.4% vs. 8.2%)[4, 5]. PTSD is widely affected among earthquake survivors and victims who experienced other traumatic events such as sexual abuse in childhood [2], rape [6], accidents, or terroristic acts [1, 7].

PTSD was included into the third edition of the Diagnostic and Statistical Manual of Mental Disorders (DSMIII) by American Psychiatric Association (APA) in 1980 and continued to be listed in the subsequent editions, that is, DSM-III, DSM-III-Revised (DSM-III-R), DSM fourth edition (DSM-IV), and DSM-IV text revision (DSM-IV-TR). The latest edition is DSM fifth edition (DSM-5) published in 2013, superseding the DSM-IV-TR, which was published in 2000. DSM-5 reveals some difference compared to the former versions. PTSD is not enlisted in the chapter ‘‘anxiety disorders’’ but as single chapter entitled ‘‘Trauma- and stressor-related diseases together with acute stress disorder and adaptation disorder’’. In DSM-5, the diagnosis criteria are further elaborated. For instance, Criterion A (stressor criterion) focuses more on the circumstances, how a person experiences a traumatizing event. In addition to DSM-5 produced, the International Classification of Diseases (ICD-10) produced by the World Health Organization (WHO) was also a widely established system to classify mental disorders. For example, the Chinese Classification of Mental Disorders (CCMD-III) edited by the Chinese Psychiatric Association in 2000 was used for PTSD diagnosis in China.

1.2 Epidemiology of PTSD

Incidence and prevalence were two commonly used words in the epidemiology of diseases, to make it clear: Incidence is ‘‘the number of instances of illness commencing or of persons becoming ill’’ (or dying or being hurt in injuries or whatever) ‘‘during a given period in a specified population’’[8]. While prevalence gives a figure for a factor at a single point in time and tells us only what is happening at a certain point[9], most of the reports used the term ‘‘prevalence’’, not “incidence” for several months lasting aftershock period. **Figure 1** shows the prevalence of PTSD among US adult population with 3.5%, which was published in 2005, and the age stage between 45 and 59 took the highest lifetime prevalence rate. **Table 1** gave an overview of the prevalence and risk factors for PTSD among *Wenchuan* earthquake survivors in China. According to the

analysis, **Figure 2** shows the correlation between PTSD prevalence (in percentage) and time after earthquake (in months) in (A) adults and (B) children and adolescents, correlations between PTSD prevalence (in percentage) and distance (in kilometer) from the epicenter of the earthquake in (C) the whole population and (D) children and adults. A variety of factors could increase the risk for PTSD among *Wenchuan* earthquake survivors, such as economic status, physical injury, age and so on.

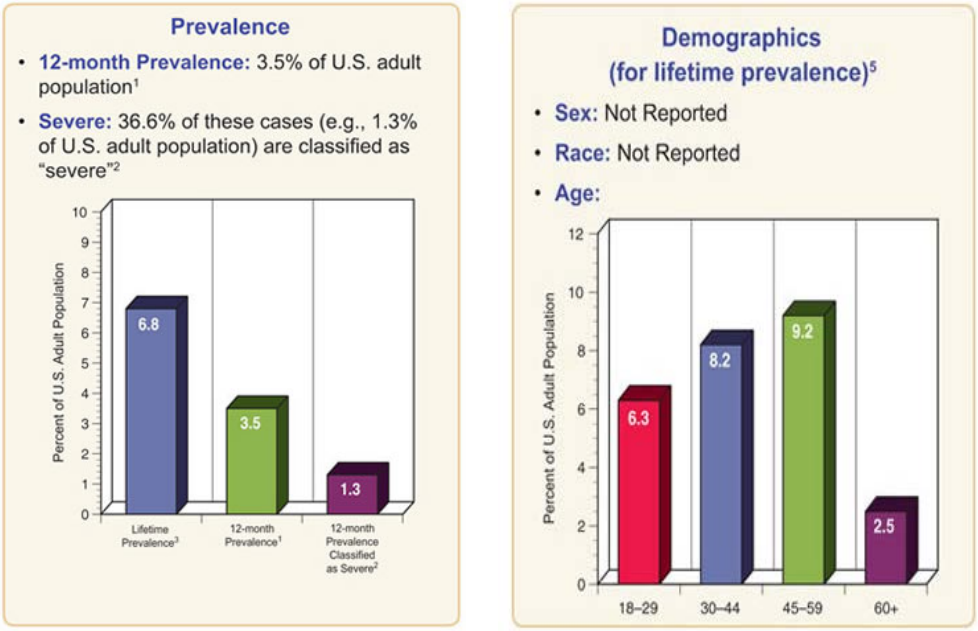

Figure 1. Estimated national PTSD prevalence and demographics for lifetime prevalence in the US in 2012. Image taken from Kessler [10, 11]

Table 1. PTSD Among *Wenchuan* Earthquake Survivors in China.

Time	Place	Sample Size	Population	Estimated PTSD Prevalence	PTSD Diagnositic Tools	Risk factors for PTSD	Associated Disease	Reference
1	Yanjing village of Qingping	1321	Whole	18.7%	IES-R	Low educational level, lacking social support, mudslide exposure, age, living with children under age 6, gender		[12]
1	Qiaozhuang town in Qingchuan county	409	Whole	62.8%	PTSD-SS	Married status, female gender, having deaths or injury of family members, low education level, and losses of possessions		[13]
12	Beichuan County	1195	Whole	26.3%	PCL-C	Bodily injury, loss of livelihood and initial fear	Depression, anxiety	[14]
36	the seriously hard-hit counties; the less-hit counties	2525	Whole	8.8%; 0.5%	PCL-C	Displacement, no regular income, receiving mental health support after the disaster, family members died or missing, injured due to the quake, and person who witnessed someone being killed or injured		[15]
36	Beichuan	287	Whole	22.65%	CAPS	Being female, being widowed, having a low level of education, having low monthly income, suffering bodily injury, being bereaved, and having a low level of social support		[16]
1	Chengdu	324	Secondary students	22.3%	CRIES	Social/emotional support from teachers or peers; exposure to positive news reports, prior experience of severe mental distress and corporal punishment, worry about future aftershocks, absence from school when it was not closed, exposures to scary or sorrowful disaster media coverage, post-disaster visits to affected sites, separation from parents	Depression, suicidal ideation	[17]
1	Chengdu	3323	High school students	22.3%	CRIES	Younger respondents (aged below15 years)		[18]
6	Dujiangyan	2250	Adolescents	15.8%	PTSD-SS	Female gender, older age, and earthquake disaster exposure	Depression, anxiety	[19]
6	Mianzhu	3208	Adolescents	2.5%	K-SADS-PL, CRIES	Social support, cognitive style, being female, being buried / injured during the earthquake, having parents who were severely injured, having classmate(s) who died, having a house destroyed, and witnessing someone buried / wounded /dying during the earthquake		[20]
10	Ningqiang county	1841	Junior middle school students	28.4%	CRIES	Females and in the severe exposure group, house had been destroyed or severely damaged		[21]

(Continued)

Table 1. (Continued)

Time	Place	Sample Size	Population	Estimated PTSD Prevalence	PTSD Diagnositic Tools	Risk factors for PTSD	Associated Disease	Reference
12	Tibetan autonomous region	2987	College students	14.1%	PCL-C	Psychological tutorship, in the severely affected area, injured in the earthquake, those lost their first degree relative, and those confronted with dead bodies, male students		[22]
12	Wenchuan and Maoxian	3052	Children	8.6%	CPSS	Direct exposure, close ones' exposure, fear for the safety of close ones, prior exposure to trauma, living location, and house damage	Depression	[23]
36	Mao County	373	Students	29.6%	IES-R	Witnessed someone being killed, family members being killed, close friends seriously injured or being killed, and felt scared	Depression, anxiety	[24]
6, 12	Qushan Town in Beichuan County	330	Children	11.2%, 13.4%	TSCC-A	Initial exposure to death, bereavement and extreme fear	Depression, anxiety	[25]
4, 6, 9, 12	Wei-Zhou, Mian-Chi, Qi-Pan-Gou	1,474	Students	11.2%, 8.8%, 6.8%, 5.7%	PCL-C	Time duration, school location (the proximity of epicenter), grade, nationality, parent injury, and severe property damage		[26]
6, 12,18	10 km away from the epicenter	548	High school students	9.7%, 1.3%, 1.6%	PCL-C	Home damage, Being a child with siblings	Depression	[27]
3, 6, 9, 12	Wenchuan county	1677	Students	36.6%, 30.7%, 24.8%, 22.2%	PCL-C	Gender and grade, were related with the decreasing trend (the trend for girls and senior school students was sharper than that for boys and junior school students		[28]
3, 6, 24	Chendu, Dujiangyan, Beichuan and Wenchuan districts	7341, 7387, 7395	Students		CRIES	Age (less than 12 years old), gender (female), having family member injury and death, witnessing injury and death, and desperation	Depression	[29]
2	Mianzhu country	228	Adult	43%	IES-R	Being female, having lower educational level, being bereaved, and witnessing death		[30]
6	Dujiangyan, Beichuan and Qingchuan	14207	Adult	15.57%	SCID-I/P	Old age, female gender, living alone, buried in the earthquake, injured in the earthquake, operated on after the earthquake, witnessing someone get injured in the earthquake, witnessing someone get buried in the earthquake, witnessing someone die in the earthquake		[31]
6	Guankou; Jiannan	243;1482	Adult	55.6%; 26.4%	IES-R	Loss of a child, female gender, loss of a parent, loss of friends or neighbors, residential house damage or collapse, and proximity to the epicenter		[32]

(Continued)

Table 1. (Continued)

Time	Place	Sample Size	Population	Estimated PTSD Prevalence	PTSD Diagnositic Tools	Risk factors for PTSD	Associated Disease	Reference
12	19 severally distoryed areas	2080	Adult	40.1%	PCL-C	Gender, age, educational level and degree of earthquake exposure		[33]
12	19 hardest hit counties	2080	Adult	56.8%	IES-R	Being female, younger age, higher level of education, higher degree of earthquake-related exposure		[34]
2, 8, 14, 26, 44	Yongan; Guangji	1066, 1344, 1210, 1174; 1281	Adult	58.20%, 22.10%, 19.80%, 19.0%, 8.0%	IES-R	Female gender, being married, low education, non-drinking, and poor self-perceived health status		[35]
3	Mianzhu and Shifang County	343	Health care workers	19%	IES-R	Being female, being bereaved, being injured, and higher intensity of initial fear		[36]
3	Mianyang; Kunming; Luoyang	17456	Blood donors	13.2%	Screening scale for DSM-IV	Knew someone killed or injured by the earthquake		[37]
8	Mianzhu county and Mianyang city	317	New mothers	19.9%	IES-R	Women with high earthquake exposure; low monthly family income and farm workers	Depression	[38]
12	Beichuan	284	Elderly	26.3%	PCL-C	Loss of livelihood, bereavement, injury and initial fear during the earthquake, being female	Depression, anxiety	[39]
18	Mianzhu	351	Pregnant women	12.2%	IES-R	Living through an earthquake	Depression	[40]

Note. CAPS: Clinician-Administered PTSD Scale; CPSS: Child PTSD Symptom Scale; DSM-IV: Diagnostic and Statistical Manual of Mental Disorders Fourth Edition; IES-R: Impact of Event Scale-Revised Scale; K-SADS-PL, Kiddie-SADS-Present and Lifetime Version; PCL-C, the PTSD Checklist-Civilian Version; PTSD: post-traumatic stress disorder; PTSD-SS, Post-traumatic Stress Disorder Self-Rating Scale; TSCC-A: Trauma Symptom Checklist for Children-Alternate Version. CRIES: Children's Revised Impact of Event Scale; SCID-I/P: Structured Clinical Interview for DSM-IV-TR Axis I Disorder-Patient Edition.

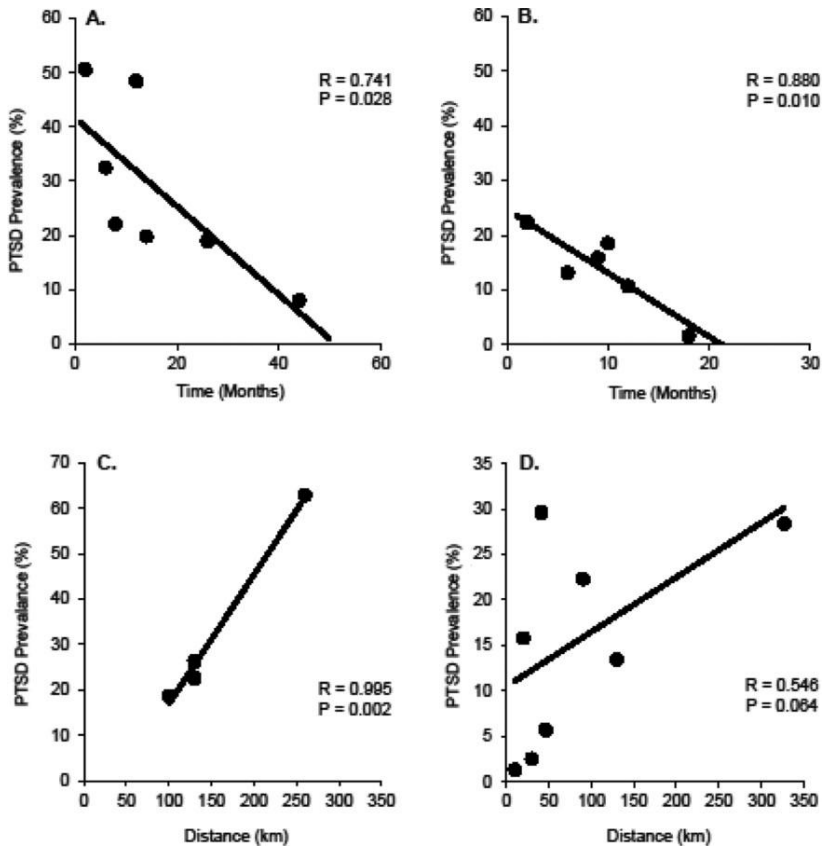

Figure 2. Prevalence of posttraumatic stress disorder (PTSD) among *Wenchuan* earthquake survivors. Image taken from Hong and Efferth [41].

1.3 Mechanisms of PTSD

Dysregulated hypothalamic-pituitary-adrenal (HPA) axis is associated with numerous psychosomatic and psychiatric disorders [42-44]. A wide range of HPA axis changes occurred among PTSD patients, including elevated levels of the corticotrophin-releasing hormone (CRH) / corticotrophin -releasing hormone receptor 1 (CRH type 1 receptor, CRHR1) system [45-47], low cortisol level [48], and increased sensitivity of glucocorticoid [49]. In addition, other biochemical changes were also involved. High catecholamine secretion into urine [50], low serotonin and dopamine levels may also contribute to PTSD [51]. Single nucleotide polymorphisms (SNPs) and epigenetics studies supported their involvement. For instance, DNA methylation in the promoter regions of immune genes, catechol-O-methyl transferase (COMT) and brain-derived neurotrophic factor (BDNF) have been demonstrated to be associated with PTSD [52-54]. In my thesis, I am going to introduce the participation of inflammatory process and oxidative stress, and explore the underlying mechanisms.

1.3.1 Inflammation in PTSD

As a part of the complex biological response of body tissues to harmful stimuli, such as pathogens, damaged cells, or irritants, inflammation is a protective response involving immune cells, blood vessels, and molecular mediators [55]. The function of inflammation is to eliminate the initial

cause of cell injury, clear out necrotic cells and tissues damaged from the original insult, and to initiate tissue repair. Increasing evidence revealed the involvement of immune system in stress-related diseases [56, 57]. Among the diverse diseases, the action mode of inflammation in mental disorders has been demonstrated in previous studies with the participation of C reactive protein or interleukin (IL) [58, 59]. Here in my studies, I am going to focus on nuclear factor of κB (NF-κB) pathway and the underlying mechanism in mental disorders.

1.3.1.1 NF-κB pathway

NF-κB plays a crucial and evolutionarily conserved role in immunity[60, 61]. Under normal conditions, NF-κB is inactivated through interaction with inhibitor protein of the IκB family. Upon activation, NF-κB is involved in the regulation of genes that impact not only on immune responses but also cell proliferation, survival and differentiation.

The NF-κB family of transcription factors can be divided into two classes: the NF-κB proteins (p105/p50 or NFKB1 and p100/p52 or NFKB2) and the Rel proteins (c-Rel, RelB, and RelA/p65)[62]. They are five structurally related protein subunits that share affinity for the κB DNA sequence motif [60, 63]. Through proteasome-mediated proteolysis, p105 and p100 are processed into the shorter DNA-binding subunits called p50 and p52, respectively [64, 65]. The Rel proteins are distinguished by C-terminal transcriptional activation domains (TAD) [66], while all five NF-κB/Rel subunits contain the N-terminal Rel homology domain (RHD), essential for DNA binding, dimerization, inhibitor of κB (IκB) interaction, and nuclear localization [67-69].

The regulation of NF-κB includes the canonical and non-canonical pathways (**Figure 3**). The canonical NF-κB transcription factor, a dimer composed of a p50 and RelA/p65 subunit, will be activated by intracellular or extracellular signals upon the induction of tumor necrosis factor alpha (TNF-α), IL-1, lipopolysaccharide (LPS), viral double-stranded RNA, and ionizing radiation [70, 71], which induced of the IκB kinase (IκK) complex. IκB is phosphorylated at serine 32 and 36 by the IκK complex, and degraded by proteasome, which consequently frees the canonical NF-κB dimer to translocate into the nucleus and activate gene transcription. As well as the canonical pathway, upon the induction of TNF receptor family members, NF-κB-inducing kinase was activated, which promotes an IKKα homodimer, leading to p100 processing into the active p52 subunit. Ultimately, processing of p100 results in the generation of non-canonical transcription factor, a 52-RelB dimer, which is then able to move onto available κB DNA binding sites and control gene expression of its related genes[72].

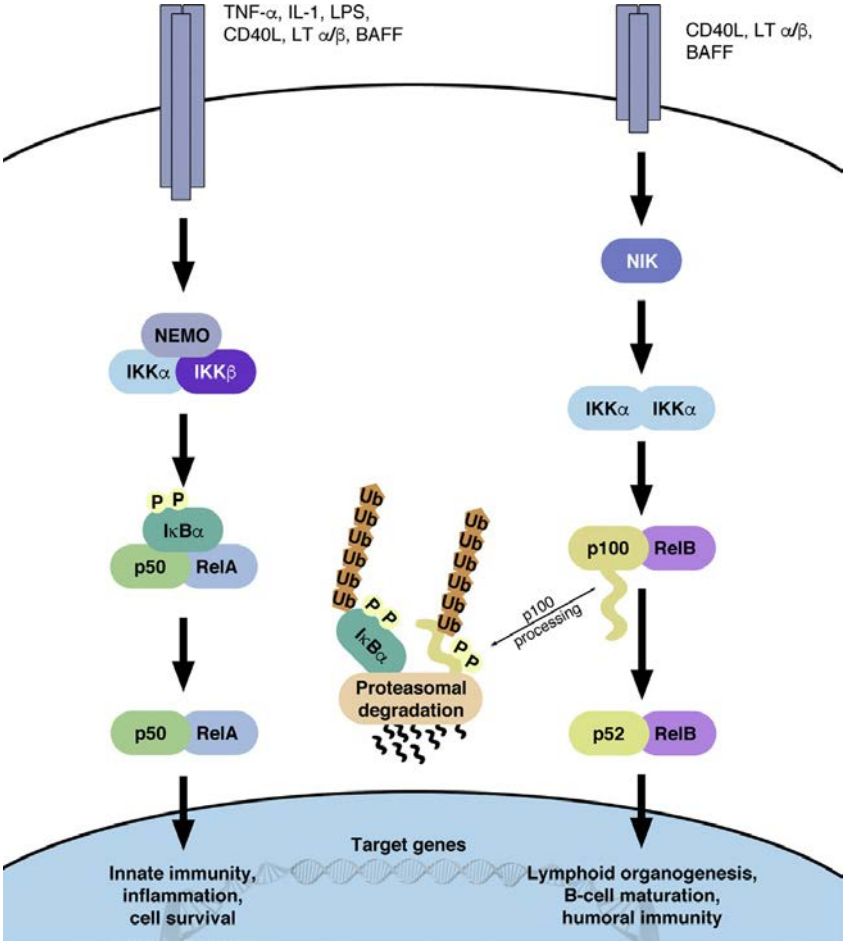

Figure 3. The canonical and non-canonical NF-κB pathways. Image taken from Durand and Baldwin[73].

1.3.1.2 Drug targets towards NF-κB pathway

Due to the prominent role of NF-κB signaling pathway in inflammatory disease and possible links to cancer and autoimmune diseases, drug development to inhibit NF-κB has been widely performed by industry [74]. To achieve the aim, a variety of strategies can be used to inhibit this pathway, shown in **Figure 4**, they are (i) inhibition of the receptors at the cell surface membrane such as IL-1R and TNFR, (ii) inhibition of IκK complex, (iii) stabilizing the suppressor protein IκB[75], (iv) interference with the nuclear transport of NF-κB, (v) inhibition of DNA binding of NF-κB proteins. Among the diverse targets, inhibiting IκK complex and NF-κB are most common and two specific mechanisms among natural products against inflammation.

IκK complex is the essential part of NF-κB translocation, demonstrating the crucial role, which has been an attractive target. IκK complex is composed of three main components, they are IκK1 (IκKα), IκK2 (IκKβ), and NF-κB essential modulator (NEMO) (IκKγ) [76, 77]. The two kinases of the IκK complex, both IκK1 and IκK2 have a kinase domain with two serine residues (S176, S180 for IκK1 and S177, S181 for IκK2) that require phosphorylation for the kinase functions, a predicted leucine zipper (LZ) domain and a helix-loop-helix (HLH) domain (29), and a C-terminus NEMO-binding domain (NBD). They share 51% of their sequence identities with highly homologous [78-81]. Many compounds have been screened to select for inhibition of IκK's kinase

activity. For example, Bay 65-1942 (Compound A) is another highly selective ATP-competitive IκKβ inhibitor that shows broad anti-inflammatory and anticancer activity[82].

Apart from inhibiting the kinase activity of IκK1 and IκK2, another approach is to target protein-protein interactions between the IκK complex members. NEMO is comprised of two coil-coil domains (CC), a LZ, and a zinc finger (ZF) domain. Structural data indicate that dimers of NEMO bind to both IκK1 and IκK2 homo- as well as hetero-dimers [83, 84]. The N-terminal portion of NEMO interacts with the NBD of the IκKs and such interaction is required for IκK activation. Phosphorylation of NEMO on S68, which is located in the region that interacts with IκKs can down-regulate NF-κB activation in the presence of stimuli [85, 86], providing the possibility that phosphorylation of NEMO serves as a negative regulatory event. Cell-permeable NEMO-binding domain (NBD) peptide, derived from the NBD of IκKβ, prevents IκK from binding to NEMO, and inhibits TNF-induced activation of the canonical pathway[87].

In addition, the direct inhibition towards NF-κB transcription factor is another strategy, which could be achieved through inhibiting the DNA binding sites. Dimethylfumarate (DMF) is an anti-inflammatory drug in clinical use for multiple sclerosis through inhibiting the NF-κB pathway[88]. DMF blocks NF-κB activity by covalently modifying RelA/p65 at Cys38, which prevents RelA/p65 nuclear translocation and attenuates its DNA-binding activity [89].

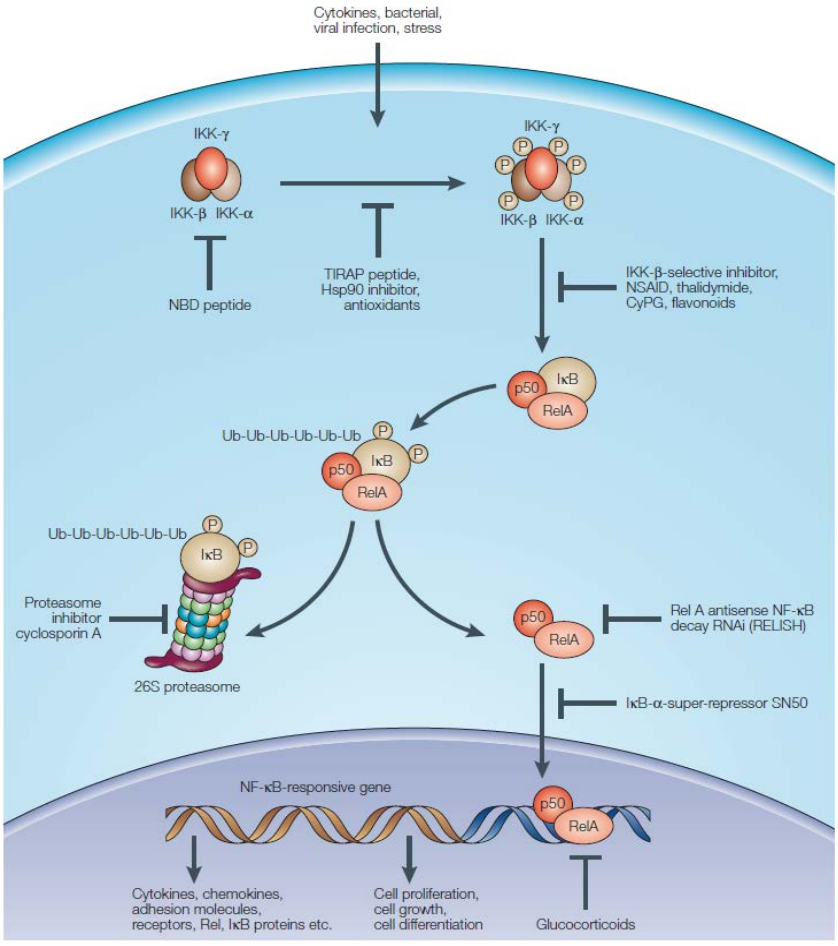

Figure 4. The possible drug targets towards NF-κB pathways. Image taken from Karin, Yumi Yamamoto and Wang[90].

1.3.2 Oxidative stress

Oxidative stress occurs if molecular defense system fails to counteract oxidation caused by endogenous processes such as the mitochondrial breakdown of glucose for energy supply or by exogenous xenobiotic chemicals, air pollution and diet. It reflects the imbalance of a biological system's ability to detoxify reactive intermediates or repair resulting damage. A growing body of studies demonstrated the involvement of oxidative stress in mental disorders, oxidative damage in the brain of the patients suffering from major mental disorders has been demonstrated be one of the major pathological processes[91]. Elevated lipid peroxidation were shown in the patients of generalized anxiety disorder as well as suppressed antioxidant activity in panic disorder[92]. Rats under stressed conditions exhibited anxiety-like behavior and elevated ROS levels, and *vice versa*, induction of ROS generation resulted in anxiety-like behavior [93]. These observations suggest a causative link between ROS and mental disorders. The link between oxidative stress-related genes and stress-related phenotypes have also been determined by a genome-wide association studies (GWAS) of PTSD[94]. Recently, a novel locus in the oxidative stress-related gene *ALOX12* has been identified [95]. In Addition, nuclear factor erythroid 2-related 2 (NFE2L2 or NRF2) -dependent persistent oxidative stress was demonstrated to cause stress-induced vulnerability to depression in rats[96]. In my thesis, I am going to focus on NRF2 as the underlying mechanism of oxidative stress in mental disorders.

1.3.2.1 NRF2

The multifunctional regulator NRF2 is composed of six functional domains with 605 amino acid known as NRF2-ECH homologies (Neh) and designated as Neh1-6, respectively [97]. Neh1 has a bZip motif responsible for hetero-dimerization with small Maf protein, NRF2-Maf heterodimer then binds to ARE activating gene expression. The Neh2 domain at the N -terminus contains DLG and ETGE motifs that bind to the Kelch-like ECH associated protein 1 (KEAP1) Kelch domain, which negatively regulates the transcriptional activity of NRF2. Domains Neh3 at the C-terminus, Neh4, and Neh5 mediate NRF2 trans-activation by binding to histone acetyltransferases. Neh6 has a function of KEAP1-independent negative regulation of NRF2.

NRF2 is a basic leucine zipper (bZIP) transcription factor that regulates the expression of antioxidant proteins to protect against oxidative damage. NRF2 modulates the expression of well-known antioxidant enzymes, such as heme oxygenase-1 (HO-1) and glutathione S-transferases (GST), but also a large number of genes that seemingly control disparate processes such as immune and inflammatory responses, tissue remodeling and fibrosis, even cognitive dysfunction and addictive behavior [98, 99]. To this end, NRF2 is referred to as a "master regulator" of antioxidant response and is involved in many diseases.

1.3.2.2 KEAP1-NRF2-ARE pathway

NRF2 is differently regulated in various situations according to the conditions (Shown in **Figure 5**). Under normal physiological conditions, NRF2 is sequestered in the cytosol and maintained at a low level through KEAP1-dependent ubiquitination and proteasome degradation. In the presence of oxidative stress, such as ROS or electrophilic chemicals, the cysteine residues of KEAP1 are covalently modified. These chemical modifications result in conformational changes in KEAP1 that relieve NRF2 from KEAP1-directed degradation. NRF2 translocates to the nucleus and activates ARE-dependent gene expression of a series of anti-oxidative and cytoprotective proteins, such as HO-1 [100, 101].

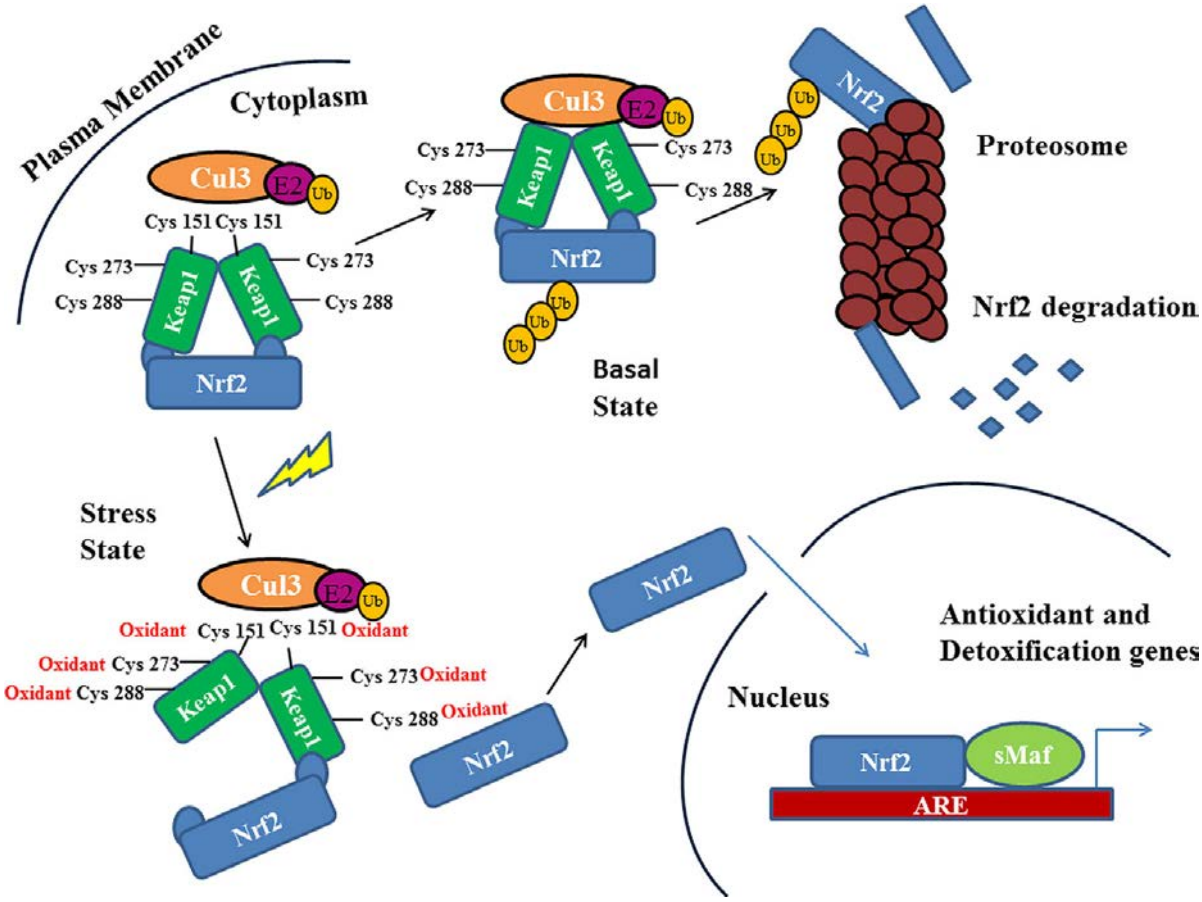

Figure 5. NRF2 is differently regulated in various situations according to the conditions. Under homeostatic conditions, NRF2 is negatively regulated and ubiquitinated through KEAP1, and degraded by the proteasome degradation pathway. Under stressed conditions, NRF2 dissociates from KEAP1, translocates into the nucleus and activates cytoprotective genes. Image taken from Deshmukh & Unni *et al* [102].

KEAP1 is a 69-kDa repressor protein that binds to NRF2 and serves as a negative regulator of NRF2. The human KEAP1 protein sequence contains 627 amino acid residues composed of five domains: i) the N -terminal region (NTR), ii) the Broad complex, Tramtrack, and Bric-a-Brac (BTB), iii) the linker intervening region (IVR), iv) the Kelch domain, and v) the C -terminal region (CTR). BTB domain is responsible for homo-dimerization and interaction with Cullin (Cul3) based ubiquitin E3 ligase complex for NRF2 ubiquitination. IVR are sensitive to oxidation and

nuclear export signal (NES) motif containing some cysteine residues. Kelch domain has six Kelch repeats (KR1-KR6) with multiple protein contact sites that mediate association of KEAP1 with NRF2 (the Kelch domain interacts with Neh2 domain of NRF2) and cytoskeleton proteins actin and/or myosin[103].

KEAP1 forms a homodimer and each dimer binds one molecule of NRF2 via its two Kelch domains, with one weak affinity binding site (DLG motif) and one high affinity binding site (ETGF motif), called "hinge-and-latch"[104]. The KEAP1-NRF2 complex is linked to a functional E3 ubiquitin ligase complex (RBX1) via an adaptor protein, Cullin3. Apart from the general model of KEAP1-CUL3 E3 ligase-mediated NRF2 ubiquitination by targeting KEAP1 cysteine residues, the three-dimensional structure of the KEAP1 Kelch domain, which is responsible for the interaction with NRF2, and the binding cavity of KEAP1 were determined by several groups in mice and humans using X-ray crystallography[105-108]. Therefore, in the pathway of KEAP1-NRF2, KEAP1 possesses dual functions: it senses the redox state using its multiple cysteine residues, and it switches the level of NRF2 ubiquitination according to the redox state. The transcription factor NRF2 acts as the executor of the pathway by inducing gene expression by binding to the cis-regulatory element ARE. While ARE determines the detailed effects of the activation of signaling only the genes with an ARE in the promoter region are involved in KEAP1-NRF2-ARE signaling.

1.3.2.3 Drug targets activating KEAP1-NRF2-ARE pathway

Activation of NRF2 signaling induces the transcriptional regulation of ARE-dependent expression of various detoxifying and antioxidant defense enzymes and proteins. Therefore, KEAP1-NRF2-ARE signaling has been an attractive target for the prevention and treatment of oxidative stress-related diseases and conditions, including cancer, neurodegenerative, cardiovascular, metabolic and inflammatory diseases [109-113]. Subsequently, a variety of KEAP1-NRF2 inhibitors were discovered.

The strategies to modulate KEAP1-NRF2-ARE pathway are multiple. Toxic chemicals, especially electrophiles that can induce oxidative stress, could activate this pathway, therefore, targeting KEAP1 cysteine residues could be an approach to indirectly inhibit KEAP1-NRF2 interaction. As many currently known ARE activators are electrophiles or can be metabolically transformed to become electrophilic, they are indirect inhibitors of KEAP1-NRF2 interaction by forming covalent adducts with the sulfhydryl groups on the cysteines in KEAP1 via oxidation or alkylation. For example, CDDO was demonstrated to covalently bind to Cys151 to inhibit the binding of Cul3 to KEAP1, which leads to the activation of NRF2 through the crystal structure of the CDDO-KEAP1 complex[114].

Compared with indirectly targeting KEAP1 cysteine residues, directly disrupting KEAP1-Cul3 protein-protein interactions seems to be more advantageous, although the specific interaction mechanism needs more structural analysis to confirm which region of KEAP1 directly associates with Cul3.

Besides, directly disrupting KEAP1-NRF2 protein-protein interaction is a novel strategy for modulating NRF2 activity [99]. Shown in Figure 6, the binding cavity in KEAP1 can be divided into five sub-pockets called P1-P5. Diverse methods have been used to explore small molecules targeting KEAP1-NRF2 protein-protein interaction. For example, high-throughput screening using a homogeneous confocal fluorescence anisotropy assay (two-dimensional fluorescence intensity distribution analysis, 2D-FIDA) was performed to discover active hits from the Evotec Lead Discovery library[115]. In addition, virtual screening methods using the receptor-ligand binding model of KEAP1−NRF2 has also been used for the drug discovery of KEAP1-NRF2 protein-protein inhibitors[116].

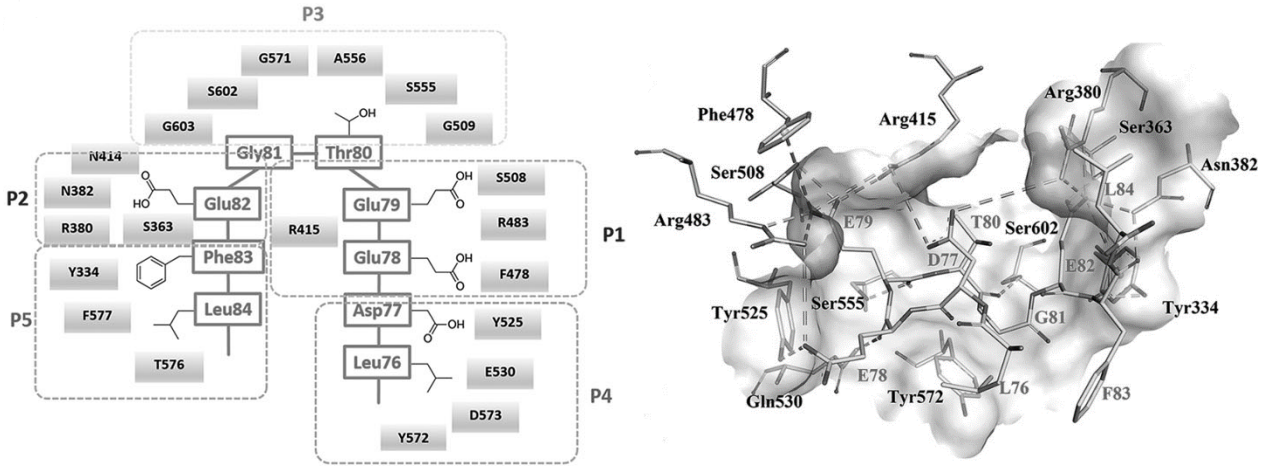

Figure 6. The KEAP1-NRF2 ETGE binding pattern. (A) Sub pocket analysis of the KEAP1 DC domain cavity. The cavity can be divided into five sub pockets: polar sub pockets P1 and P2, hydrophobic sub pockets P4 and P5, and the central sub pocket P5. (B) An interaction model of the KEAP1-NRF2 ETGE peptide. Polar interactions are represented as gray dashed lines. The NRF2 amino acid residues names are abbreviated in one capital letter, whereas the amino acid residues belonging to KEAP1 are represented in three letters. Image taken from Meng-Chen Lu, Jian-Ai Ji, Zheng-Yu Jiang, and Qi-Dong You [117].

1.4 Treatment of PTSD

1.4.1 Psychotherapy

Psychosocial interventions play a crucial role for the management of PTSD, which include trauma-focused cognitive behavior therapy (TFCBT), exposure therapy, eye movement desensitization and reprocessing (EMDR), etc. Among the diverse options, TFCBT and EMDR have the most empirical support [118]. Goncalves et al. performed a systematic review of published articles to evaluate the efficacy of virtual reality exposure therapy (VRET) in the treatment of PTSD, and the results revealed that no differences was found between VRET and

exposure therapy [119]. After the *Wenchuan* earthquake, different psychological approaches have been applied to treat earthquake survivors with PTSD in China. Wu et al. conducted a randomized controlled trial with 2,368 military rescuers for one month according to the "512 Psychological Intervention Model" and then one, two and four months later to follow up changes in PTSD symptoms, anxiety and depression based on the DSM-IV criteria. "512 PIM" was proved to be an effective psychological intervention for military rescuers in reducing symptoms of PTSD, anxiety and depression after this crisis [120]. Wang et al. developed the Chinese My Trauma Recovery approach, a web-based intervention strategy to provide mental health support for traumatized persons [121]. Short-term cognitive-behavioral therapy (CBT) group intervention represents a robust intervention for natural disaster victims [122]. A randomized waiting-list controlled pilot study was conducted at the site of the Sichuan earthquake in Beichuan County between December 2009 and March 2010, to evaluate the efficacy of Narrative Exposure Therapy (NET) as a short-term treatment for PTSD. The results suggested that NET is effective in treating post-earthquake traumatic symptoms among adult Chinese earthquake survivors [123]. In addition, Interpersonal Psychotherapy (IPT) is a 12-week structured psychotherapy developed by Klerman and Weissman in the 1980s, aiming at examining and changing current relationships and social support in order to improve mood and anxiety symptoms. Jiang et al. performed a randomized clinical trial among Sichuan earthquake survivors with IPT, a significantly higher reduction of PTSD and MDD diagnoses was found in the IPT group versus the TAU (treatment as usual) group, indicating that IPT is a promising treatment for reducing PTSD and depression [124].

1.4.2 Pharmacotherapy

Likewise psychotherapy, pharmaco-therapeutic intervention can reduce PTSD symptoms to some extent [125-127]. Different pharmacological classes with different pathogenesis have been investigated, such as selective serotonin reuptake inhibitors, a-adrenergic antagonists, anticonvulsants, mood stabilizers, antipsychotics, b-blockers, benzodiazepines, glucocorticoids, tricyclic antidepressants, and monoamine oxidase inhibitors. Nevertheless, Sertraline (Zoloft®) and paroxetine (Paxil®) are the only two drugs approved by the Food and Drug Administration (FDA) for the treatment of PTSD [128-130]. Therefore, novel effective drugs or alternative medicine are urgently needed, for instance, traditional Chinese herbs might be beneficial for the treatment of PTSD.

1.4.3 Other therapies

Other approaches, such as Yoga and meditation, defined as mind-body practice, were also useful in the treatment of PTSD [131-135]. *Taichi* and *qigong* belong to the repertoire of Traditional Chinese medicine (TCM) and represent effective approaches to treat PTSD although no study

related to *Wenchuan* earthquake has been reported [136]. Remarkably, calligraphy therapy significantly reduced hyperarousal for children among *Wenchuan* earthquake survivors [137].

1.5 Traditional Chinese Medicine

With a specific philosophical background and treatment principles, TCM emphasizes the balance of *yin* and *yang* to achieve harmony between body, mind and soul. With well-developed clinical practice and good written documentation for thousands of years, TCM is especially well suited to treat difficult and complex diseases. The success should be partly attributed to diverse medicinal plants, which have been a valuable source of therapeutic agents in the treatment of cancer, neurodegenerative diseases and malaria [138-140]. The enormous structural and chemical diversity of natural products are evolutionarily optimized for serving different biological functions [141]. In addition, the traditional knowledge on plants and well documented ethno-pharmacological information can be taken as reliable hints for further pharmacological research.

1.5.1 TCM treatment of PTSD

Acupuncture and phytotherapy are two major treatment of TCM. Acupuncture is widely used to treat trauma-related symptoms such as insomnia [142], depression [143, 144], anxiety [145, 146] and other co-morbidities [147]. Lee et al. conducted a systematic review of the effectiveness of acupuncture towards trauma spectrum response (TSR), acupuncture appeared to be effective for treating headaches, anxiety, sleep disturbances, depression and chronic pain [148]. Some trials on acupuncture were performed to treat PTSD patients among *Wenchuan* earthquake survivors. Zhang et al. compared the effectiveness with 24 cases and 67 cases with cognitive-behavior therapy and combination therapy with cognitive-behavior therapy and acupoint stimulation among *Wenchuan* earthquake patients. The total scores of IES-R, the scores of all factors and the total scores of a questionnaire among the two groups after treatment were much lower than those before treatment. The comparison of reduction in the factor scores between the two groups showed that the curative effect in the treatment group was better that in the control group [149]. Wang et al. also performed a clinical study in 138 patients with earthquake-caused PTSD using Randomized Controlled Trials (RCTs) to assess the efficacy and safety of electro-acupuncture. The cases enrolled were randomly assigned to electro-acupuncture group and paroxetine group. The electro-acupuncture group was treated by scalp electro-acupuncture on four points (*Baihui*, *Sishencong*, *Shenting*, and *Fengchi*). The results demonstrated that the total scores of Clinician-Administered PTSD Scale (CAPS), Hamilton Depression Scale (HAMD) in the treatment groups have significant efficacy, of which the electro-acupuncture group was more significant than that of paroxetine group [150].

Chinese herbs have also been demonstrated to significantly improve the symptoms of PTSD [151-154]. It's interesting that a Chinese herb formula (*Xiao-Tan-Jie-Yu-Fang*), which consists of 14 components, has been proved to be useful to treat PTSD in 245 survivors of the 2008 Sichuan earthquake in a randomized, double-blind, placebo-controlled clinical trial. PTSD-related symptoms in patients treated with this Chinese herb formula were significantly improved compared with the placebo group. The herbs can result in the improvement in somatization, obsessive-compulsive behavior, depression, anxiety, hostility, and sleep quality without serious side effects, indicating that *Xiao-Tan-Jie-Yu-Fang* represents a safe and efficient option to improve the generally poor psychological status of PTSD patients [155].

1.5.2 Free and easy wanderer

Free and easy wanderer is originated from the book of Formularies of the Bureau of People's Welfare Pharmacies in Song dynasty of China in 1078 AD. Initially, it was used for women in the treatment of irregular menstruation caused by liver stagnation (TCM languague), and it is orally taken with the form of decoction. According to TCM theory, mood disorders and irregular menstration share the same etiology, caused by liver stagnation. Therefore, FAEW is prescribed to mental patients by TCM doctors and has been widely used in clinic to remove symptoms of depression, premenstrual dysphoric disorder, climacteric syndrome in China.

Free and Easy Wanderer (*Xiao-Yao-Wan*, or *Xiao-Yao-San*, FAEW) is constituted by *Radix Bupleuri Chinensis* (*Chai Hu*), *Radix Angelicae Sinensis* (*Dang Gui*), *Radix Paeoniae Lactiflorae* (*Bai Shao*), *Rhizoma Atractylodis Macrocephalae* (*Bai Zhu*), *Sclerotium Poriae Cocos* (*Fu Ling*), *Radix Glycyrrhizae Uralensis* (*Gan Cao*), *Herba Menthae Haplocalycis* (*Bo He*) and *Rhizoma Zingiberis Officinalis Recens* (*Sheng Jiang*). It has been demonstrated to reverse depressive-like behaviors in rats with type 2 diabetes[156]. FAEW reduced oxidative stress-induced hippocampus neuron apoptosis *in vitro and* change ultrastructure in rat hippocampus[157, 158]. Besides, FAEW can improve learning and memory deficit in rats induced by chronic immobilization stress[159]. Plasma-metabolite-biomarkers for the therapeutic response of FAEW in depressed patients have been identified by the NMR-based metabolomics approach[160]. Although FAEW has a good reputation in the history of Chinese medicine, the cellular and molecular modes of action are still not well-understood.

2 Aims

To understand the mechanisms of FAEW in the treatment of mental disorders, some issues should be elucidated:

(1) PTSD is known to us with loss of capabilities and dissociation symptoms, which are involved with the interruption of the normally integrative functions of consciousness, memory, identity, or perception of the environment. To understand the mechanism of PTSD, genomic analyses of clinical patients may be one potential approach to gain insight into the pathophysiology of such disorders.

(2) FAEW are poly-herbal preparations, frequently consisting of dozens to hundreds of chemical compounds, which might increase safety concerns and hamper the agreement on their clinical usage. To understand how they work in the human body, the molecular mechanisms should be clarified and possible active compounds have to be identified for further drug discovery.

Therefore, in my thesis, we started our studies by analyzing microarray-based transcriptome-wide mRNA expression profiles of PTSD patients. Based on network analyses and associated binding motifs of transcription factors in gene promoters, we hypothesized that inflammatory process may represent a major cause of PTSD. We investigated the cytotoxicity of FAEW and compared its effect with the antidepressant drug fluoxetine against inflammation by assessing the activity of NF-κB and the protein expression of p65. Furthermore, we identified various active compounds of FAEW with molecular docking *in silico*. Finally, we compared our results with published literature and confirmed some pharmaceutical activities of the compounds.

On the other hand, we used hydrogen peroxide to induce oxidative stress in the human glioblastoma T98G and human neuroblastoma SH-SY5Y cell lines as *in vitro* cellular stress model. We examined the effect of FAEW and fluoxetine on ROS levels. To identify underlying cellular mechanisms, we performed transcriptome-wide microarray analyses. In the course of these investigations, we verified the role of KEAP1-NRF2 interaction and their downstream gene HO-1. Finally, molecular docking was performed to explore possible phytochemicals of FAEW *in silico*, which bind to the NRF2-regulator Kelch-like ECH-associated protein 1 (KEAP1).

3 Results

As mentioned previously, PTSD is widely known as a mental disorder, its etiology and pathogenic mechanism are still unknown. Therefore, we performed a systematic analysis on microarray-based transcriptome-wide mRNA expression profiling of patients with posttraumatic stress syndrome to understand the possible mechanisms of PTSD and identify some potential targets for the treatment of PTSD.

3.1 A systematic analysis on microarray-based transcriptome-wide mRNA expression profiling of patients with posttraumatic stress syndrome

3.1.1 Canonical pathways analysis

To identify the common pathways related to PTSD, the top 10 canonical pathway of each dataset was displayed by IPA analyses (**Figure 7**). In general, a variety of pathways were demonstrated to be involved. In dataset 1 and 2, the gene profiles were involved with cancer and tumor pathways. In dataset 3, cellular pathways “change of immune system” and “monocyte among the immune system” were significantly involved. In dataset 4, the main pathways occurred in mitochondria, such as “mitochondrial dysfunction” and “oxidative phosphorylation”.

3.1.2 Diseases and functions analysis of the datasets

As well as canonical pathways analysis, the diseases and functions were classified as well. Top ten relevant diseases and functions to these dysregulated genes were shown in **Figure 8**. Cellular dysfunctions, inflammation and free radical scavenging were highly involved. The dysregulated genes were also associated with diverse diseases, such as cardiovascular diseases, cancer, organismal development and neurological diseases.

3.1.3 Networks analysis of the datasets

Finally, network analyses were performed to investigate the protein-protein relationship within the dysregulated genes (**Figure 9**). Among the four datasets, NF-κB played a central role in the networks of dysregulated genes in four datasets, implying that the inflammation might be a mechanism of PTSD.

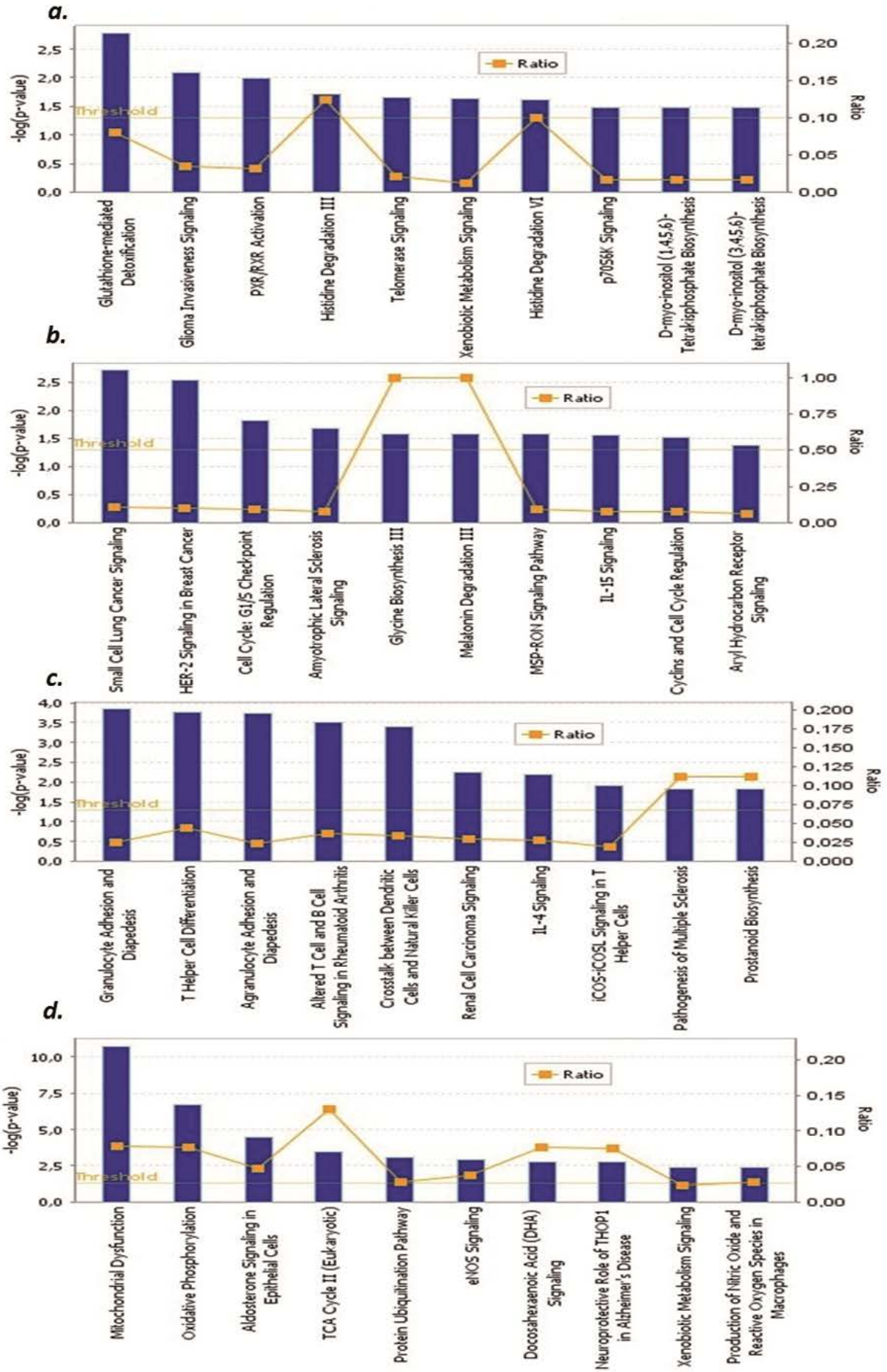

Figure 7. The top 10 canonical pathways significantly affected by PTSD. *a*) Blood-based gene-expression according to [161]**;** *b*) Peripheral blood mononuclear cell gene expression profiles according to [162]**;** *c*) Monocyte gene expression profiles according to [163]; *d*) Post mortem brain biopsy gene expression profiles according to [164]**.**

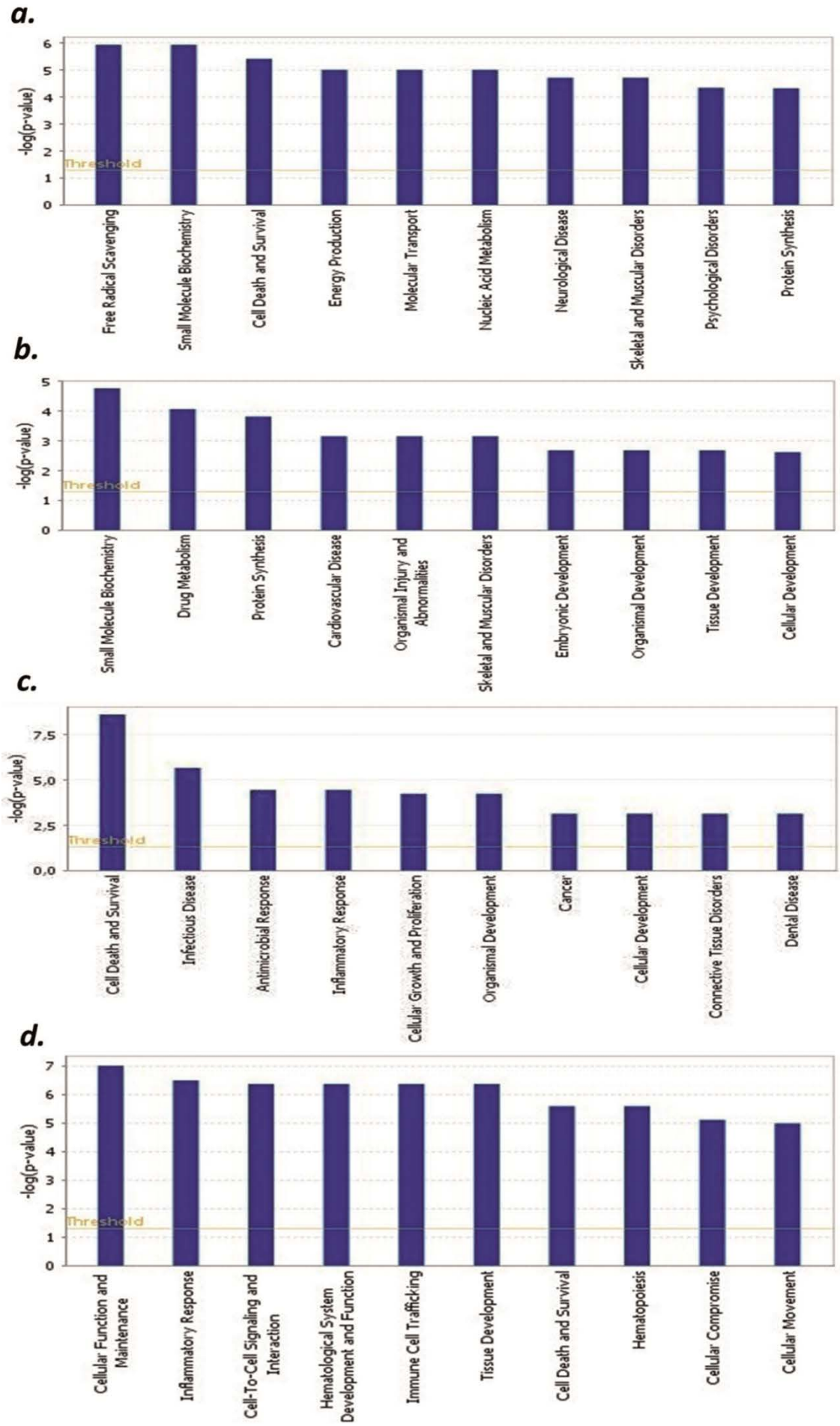

Figure 8. Top 10 diseases and functions significantly affected by PTSD. *a*) Blood-based gene-expression according to [161]**;** *b*) Peripheral blood mononuclear cell gene expression profiles according to [162]; *c*) Monocyte gene expression profiles according to [163]; *d*) *Post mortem* brain biopsy gene expression profiles according to [164].

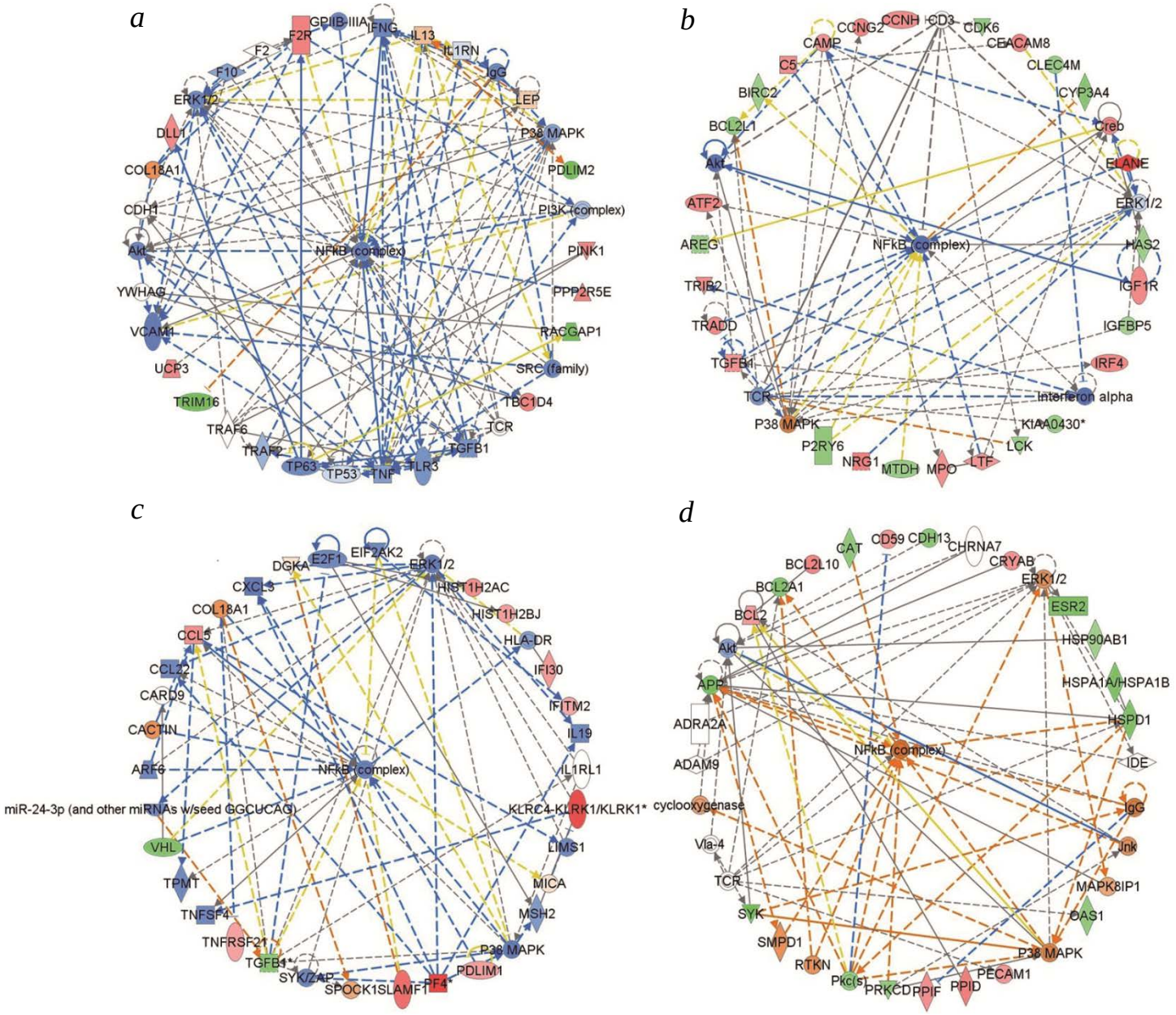

Figure 9. Deregulated genes among PTSD patients. Red colored genes were up-regulated, green colored ones were down-regulated. The arrows indicted effects of deregulated genes on other genes. Continuous lines show direct interactions, dotted lines indirect interactions. *a*) Blood-based gene-expression according to [161]; *b*) Peripheral blood mononuclear cell gene expression profiles according to[162]; *c*) Monocyte gene expression profiles according to [163]; *d*) Post mortem brain biopsy gene expression profiles according to [164]

3.1.4 Analysis of binding motifs for transcription factors in gene promoters

Integrative gene promoter analyses were performed to investigate common binding motifs for transcription factors in the promoter sequences of dysregulated genes among the datasets. **Table 2** shows the top ranked transcription factors. Among them was the NF-κB binding motif with a z-score of -4.39. **Figure 10** shows detailed information of the NF-κB.

Table 2. The most pronounced gene promoter binding motifs depending on the integrative analysis of Galaxy /Cistrome.

ID	Factor	hits	cutoff	zscore	-10*log(pval)
1	IKZF2|Ikzf2	33	8.733	-5.25	163.693
2	CAT8	21	8.035	-5.16	159.248
3	CCDC16	70	6.592	-5.09	155.157
4	HOXA1	285	5.666	-4.94	147.672
5	HOXD10|Hoxd10	175	7.493	-4.90	145.427
6	Meox1	235	6.41	-4.87	144.123
7	E2F1::TFDP1	569	4.626	-4.85	143.061
8	Sfpi1	179	6.952	-4.72	136.281
9	Mox1|MEOX1|CD200| NOX1	245	6.333	-4.66	133.664
10	CBFA2T2	233	4.945	-4.65	133.291
11	DAL81	72	4.577	-4.61	130.914
12	Etv1	137	6.035	-4.60	130.538
13	Hoxa1	267	5.713	-4.57	129.11
14	FOXP4	211	5.907	-4.55	128.263
15	Nkx1-1	104	6.226	-4.54	127.587
16	lhx6.1|LHX6	499	4.368	-4.43	122.535
17	MET4	340	5.212	-4.41	121.631
18	**NF-kappaB |NFKB1**	954	2.651	-4.39	120.777
19	ACE2	537	6.774	-4.25	114.451
20	Muscle TATA box	1242	1.144	-4.23	113.4

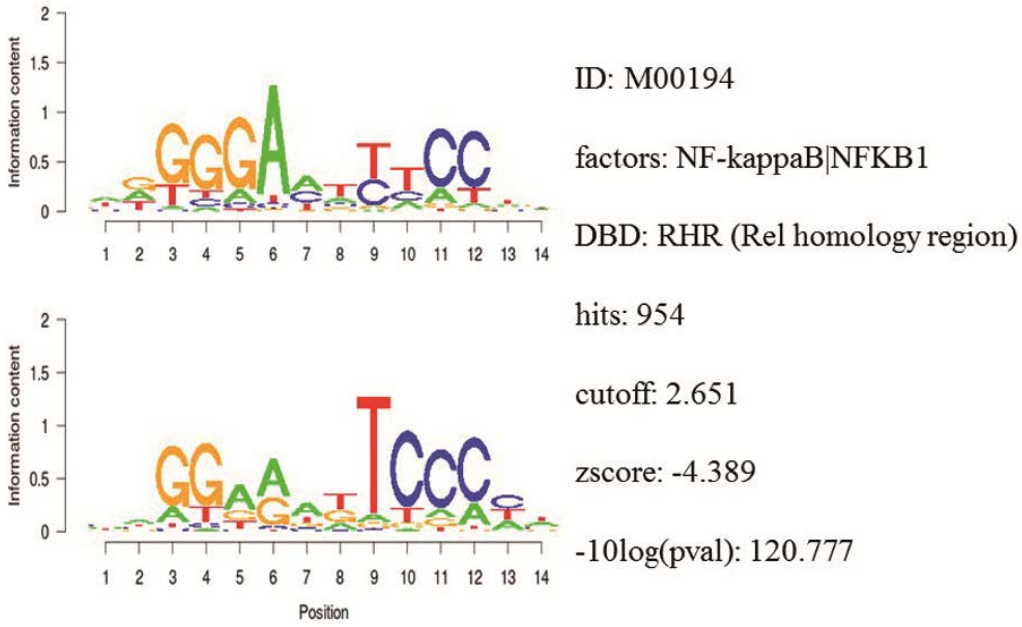

Figure 10. Detailed information of the NF-κB binding motif in gene promoter sequences.

3.1.5 Summary

In the present investigation of our studies, the dysregulated genes of PTSD patients were involved with a wide array of pathways, diseases and functions, such as psychological or physiological diseases, which might be taken as a general hint for common pathogenic factors between PTSD and metabolic syndrome, cardiovascular diseases, cancer, as well as psychological diseases, *e.g*. depression, suicidality and anxiety [109, 165, 166], implying that a holistic way to investigate PTSD might be one approach to achieve multiple-targets. In addition, network analyses revealed that NF-κB was involved in both blood cells and central nervous system. Furthermore, the participation of NF-κB has also been demonstrated in the promoter binding motif search analysis, suggesting that NF-κB may be an important immunological component of inflammatory processes in PTSD.

As well as inflammation, it is also worthwhile to notice that oxidative stress-related pathways, such as mitochondrial dysfunction and oxidative phosphorylation, have also been demonstrated to be involved with PTSD, which could be suggested by the diseases and functions analysis, and pathway analysis. Although the specific pathway was not indicated in the network analysis, the role of oxidative stress and its signal pathway could also be one point for the following studies.

3.2 NF-κB was inhibited by the Chinese herbal remedy *Free and Easy Wanderer*

The previous chapter gave an overview of PTSD with clinical datasets. Inflammatory process has been demonstrated to participate in PTSD, suggested by the pathway analysis, diseases and functions analysis. The network analysis stressed the important role of NF-κB. In addition, promoter binding motif search of genes revealed that NF-κB was among the most important transcription factors. These findings showed a strong signal that NF-κB could be a target in the treatment of PTSD. Therefore, in this part, we aimed to validate the effect of FAEW with the link between the therapeutic effect of FAEW on PTSD, and NF-κB as relevant underlying mechanism.

3.2.1 Cytotoxicity of FAEW and fluoxetine

To identify the role of NF-κB in the acting model of FAEW, firstly, resazurin assays in HEK293 cells were performed to investigate, whether or not FAEW reveals cytotoxic effects. As shown in **Figure 11,** FAEW was indeed not cytotoxic at concentrations up to 2000 µg/ml. For comparison, fluoxetine was non-toxic up to 6 µM and inhibited HEK293 cells at higher concentrations.

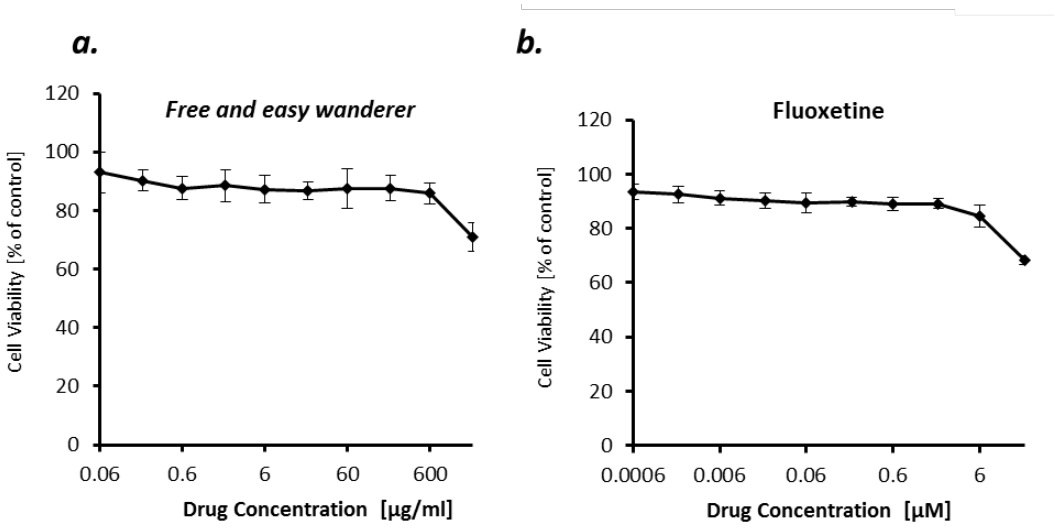

Figure 11. Cytotoxicity of FAEW and fluoxetine as determined by the resazurin assay. Shown are mean values ± SD of three independent experiments.

3.2.2 Inhibition of NF-κB activity by FAEW and fluoxetine

To investigate whether FAEW affects PTSD through NF-κB-mediated inflammatory effects, NF-κB reporter cell assays were performed. As shown in **Figure 12**, FAEW inhibited NF-κB activity in a dose-dependent manner. In addition, the inhibitory effect strengthened in a time-dependent manner from 24 to 72 h, reaching the similar inhibitory level caused by MG-132. Fluoxetine revealed the same trend as FAEW.

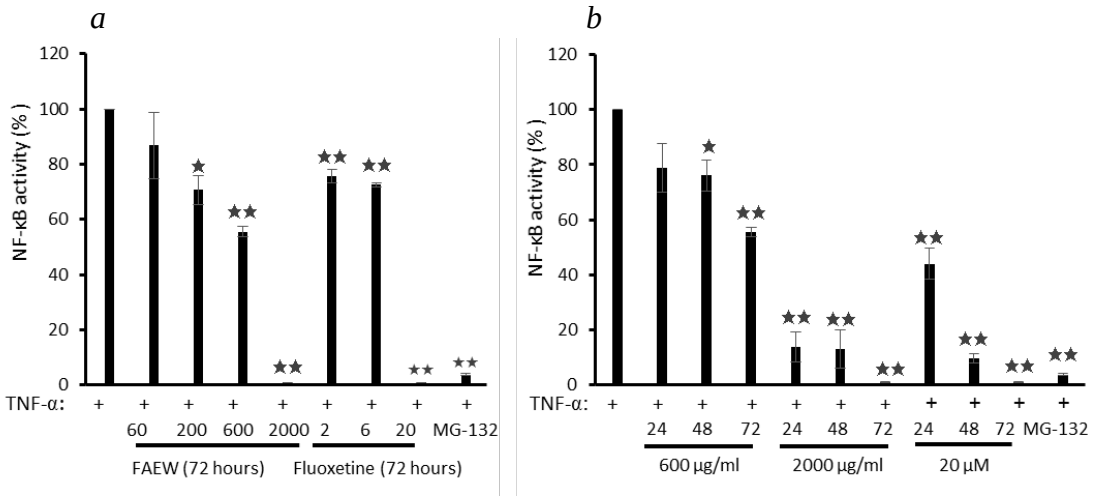

Figure 12. Inhibition of NF-κB activity by FAEW and fluoxetine in HEK293 reporter cells. (*a*) Concentration kinetics and (*b*) time kinetics shown are mean values ± SD of three independent experiments. ★ $p < 0.05$, ★★ $p < 0.01$. The inhibition effects of FAEW and fluoxetine towards NF-κB activity were calculated by comparison with untreated TNF-α induction group.

3.2.3 Inhibition of p65 protein expression by FAEW and fluoxetine

To further confirm the inhibition of NF-κB, western blot assays were performed to investigate the role of FAEW on p65 protein expression in T98G brain cells. According to the cytotoxic assays in **Figure 13,** three non-cytotoxic concentrations (200, 40, 8 μg/ml) were selected. As shown in **Figures 13a** and **Figures 13c**, with treatment for 24 h, both FAEW and fluoxetine inhibited p65 expression in a dose-dependent manner. Fixed concentrations of 200 μg/ml FAEW or 20 μM fluoxetine inhibited p65 expression in a time-dependent manner from 24 to 72 h (**Figures 13b** and **Figures 13d**).

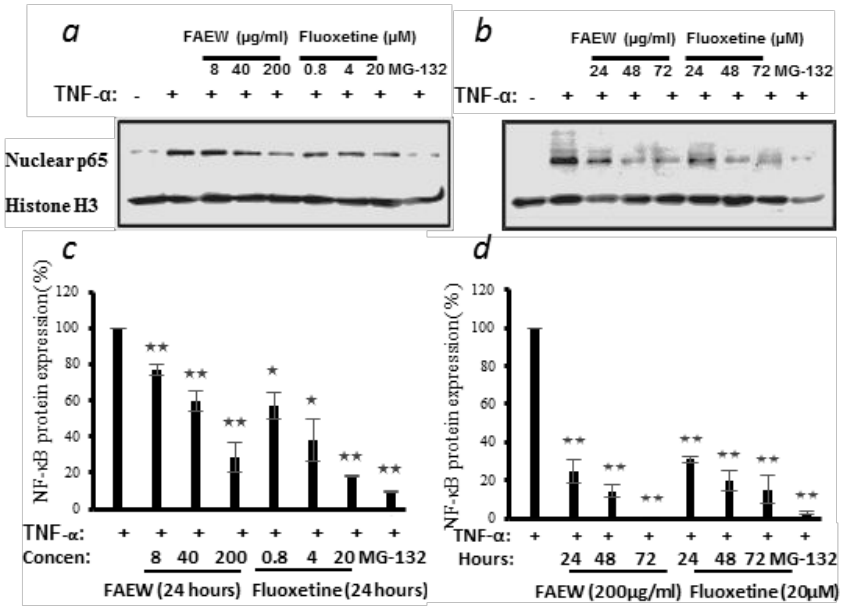

Figure 13. Inhibition of p65 expression by FAEW and fluoxetine in T98G brain cells. (*a*) Concentration kinetics and (*b*) time kinetics. Histone was used as loading control. (*c*) and (*d*) show inhibition effects of FAEW and fluoxetine towards p65 protein expression were compared with TNF-α group after using the control group without TNF-a for the quantification of western blots shown in (*a*) and (*b*), respectively. Shown are mean values ± SD of three independent experiments. ★ $p < 0.05$, ★★ $p < 0.01$.

3.2.4 Structures of 10 phytochemicals from FAEW

Ten compounds were isolated from the herb mixture of FAEW, and their structures were identified by HPLC-NMR and MS, as shown in **Figure 14.**

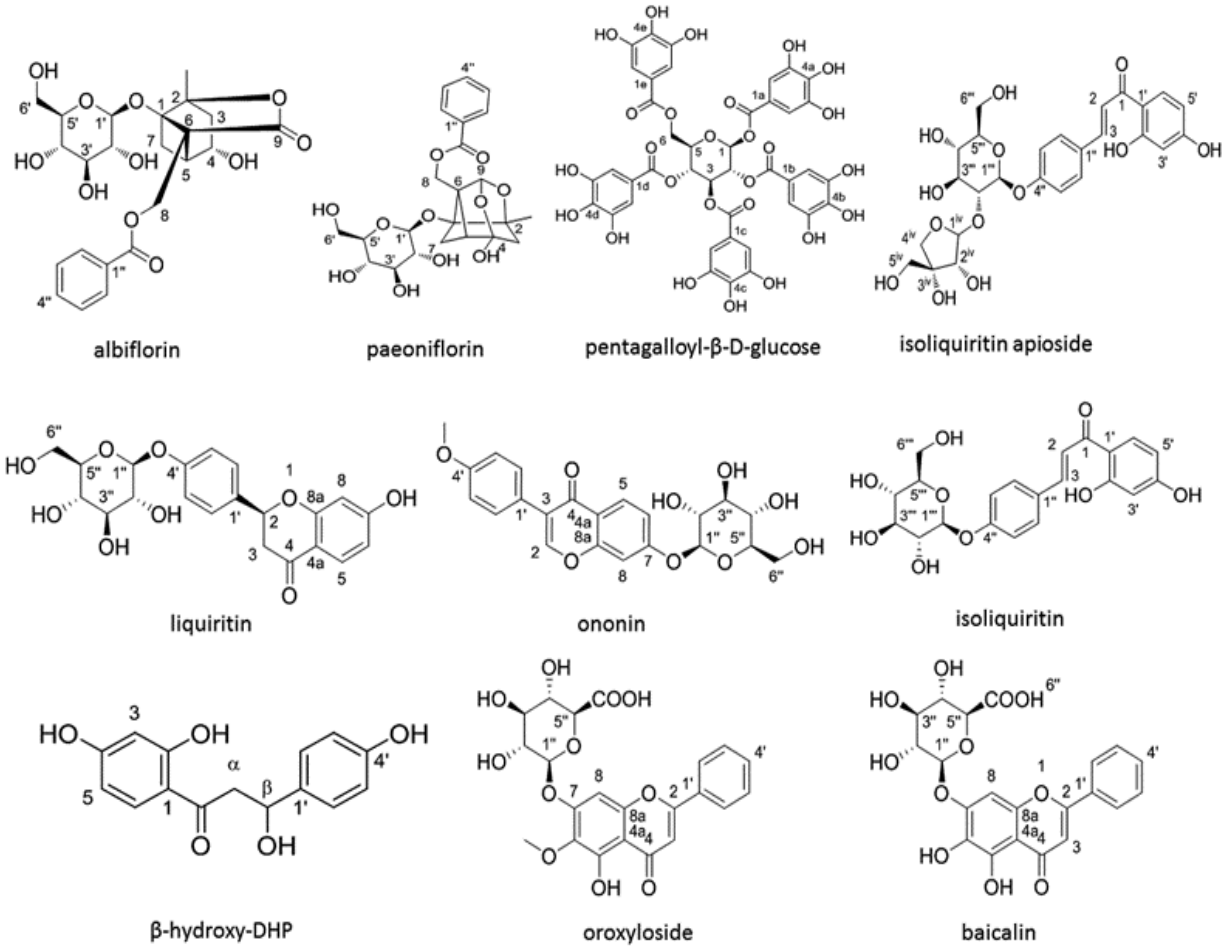

Figure 14. The structures of 10 compounds isolated from FAEW

3.2.5 *In silico* molecular docking of compounds from FAEW binding to the proteins of the NF-κB pathway

In order to explore possible interactions of compounds known to be in FAEW with the proteins of the NF-κB pathway, *in silico* molecular docking analysis were performed with 10 compounds (shown in **Figure 14**) in the remedy to IκK-NEMO, IκK and p65-RelA. As shown in **Table 3** and **Table 4**, paeoniflorin and ononin bound to IκK and p65-RelA with low binding energies, which were comparable to the binding of MG-132. In addition, isoliquiritin apioside, albiflorin, baicalin, isoliquiritin, liquiritin and oroxyside mainly bound to p65-RelA through DNA and ATP binding sites (**Figures 15** and **Figure 16**). The control fluoxetine (S) bound to p65-RelA with high affinity.

Table 3. Binding energies of molecular docking of chemical compounds of FAEW to proteins of the NF-κB pathway.

Ligand	IκK-NEMO		IκK		p65-Rel A	
	Lowest binding energy (kcal/mol)	pKi (μM)	Lowest binding energy (kcal/mol)	pKi (μM)	Lowest binding energy (kcal/mol)	pKi (nM)
Baicalin	-3.79±0.50	1690±155.56	-5.97±0.04	42.47±2.43	-9.68±0.09	79.88±11.99
β-hydroxy-DHP	-5.04±0.05	203.52±18.09	-5.87±0.18	52.24±14.46	-8.54±0.04	553.70±33.52
Isoliquiritin	-3.59±0.17	2390.00±692.97	-7.04±0.08	6.92±0.98	-9.97±0.22	61.00±4.24
Isoliquiritin apioside	-1.20±0.12	132.78±28.65	-6.90±0.15	9.00±2.28	-10.10±0.74	56.59±8.56
Liquiritin	-4.12±0.28	1155.00±247.49	-6.10±0.19	34.91±11.08	-9.20±0.04	180.31±14.99
Ononin	-3.82±0.02	1600.00±70.71	-7.33±0.01	4.24±0.07	-11.55±0.08	3.43±0.50
Oroxyloside	-3.32±0.08	3690.00±551.54	-6.16±0.04	30.84±1.90	-9.41±0.02	127.50±4.95
Fluoxetine (R)	-4.35±0.05	652.97±54.98	-5.61±0.06	77.65±8.25	-7.35±0.07	4093.33±475.01
Fluoxetine (S)	-4.14±0.05	928.59±79.41	-5.90±0.03	47.15±2.48	-7.63±0.03	2543.33±123.42
Albiflorin	-5.05±0.30	211.37±52.00	-6.63±0.16	14.23±3.77	-10.66±0.50	23.85±3.12
Paeonflorin	-4.41±0.04	591.13±29.66	-7.83±0.21	2.09±0.27	-11.25±0.03	5.45±0.07
Pentagalloyl-β-D-glucose	-0.67±0.01	320580.00±150.00	-2.39±0.49	19090.00±3490.00	-6.09±0.21	35.50±1.27
MG-132	-3.50±0.63	47053.00±1090.00	-7.75±0.35	2.31±0.33	-9.07±0.29	172.10±27.01

IκK, IκB kinase; IκK-NEMO, NF-κB essential modulator; NF-κB, nuclear factor kappa - light - chain - enhancer of activated B cells. Shown are mean values ± SD of three independent experiments

Table 4. Hydrogen bonds and amino acid residues identified by molecular docking of chemical compounds of FAEW to proteins of the NF-κB pathway

Protein	Ligand	Residues forming H bonds	Residues involved in hydrophobic interactions
IκK	Baicalin		Thr23, Val29, Ala42, Lys44, Met65, Met96, Glu97, Tyr98, Cys99, Asp103, Val152, Ile165, Asp166, Leu167
	β-hydroxy-DHP	Lys44	Thr23, Val29, Ala42, Lys44, Met96, Glu97, Ile165, Asp166, Leu167
	Isoliquiritin	Cys99, Lys147	Leu21, Thr23, Gly24, Val29, Ala42, Glu97, Tyr98, Cys99, Lys147, Glu149, Ile165, Asp166, Gly184
	Isoliquiritin apioside	Lys44, Cys99	Thr23, Gly24, Val29, Ala42, Lys44, Met96, Glu97, Tyr98, Cys99, Lys147, Glu149, Ile165, Asp166, Leu167, Gly184
	Liquiritin	Lys147	Leu21, Thr23, Gly24, Ala42, Glu97, Cys99, Lys147, Glu149, Val152, Ile165, Asp166
	Ononin	Cys99, Lys147	Leu21, Gly22, Thr23, Val29, Ala42, Val74, Met96, Glu97, Tyr98, Cys99, Lys147, Val152, Ile165, Thr185
	Oroxyloside	Cys99	Thr23, Val29, Ala42, Lys44, Met65, Met96, Glu97, Tyr98, Cys99, Asp103, Glu149, Val152, Ile165, Asp166, Leu167
	Fluoxetine (R)		Gly24, Val29, Ala42, Lys44, Met65, Met96, Tyr98, Ile165, Asp166, Leu167
	Fluoxetine (S)		Gly24, Val29, Lys44, Met96, Tyr98, Cys99, Ile165, Asp166, Leu167
	Albiflorin	Cys99	Gly22, Val29, Lys44, Met 65, Val74, Met96, Glu97, Tyr98, Cys99, Asp103, Glu149, Asn150, Ile165, Asp166, Leu167
	Paeoniflorin		Gly22, Val29, Lys44, Met65, Val74, Met96, Glu97, Tyr98, Cys99, Asp103, Glu149, Asn150, Ile165, Asp166, Leu167
	Pentagalloyl-β-D-glucose	Glu100	Leu21, Gly22, Thr23, Val29, Ala42, Lys44, Glu61, Met65, Val73, Val74, Ala76, Leu94, Met96, Tyr98, Cys99, Glu100, Gly102, Asp103, Glu149, Asn150, Ile151, Val152, Ile165, Asp166, Leu167
	MG-132		Leu21, Thr23, Val29, Ala42, Met65, Val73, Val74, Met96, Glu97, Tyr98, Asp103, Val152, Ile164, Ile165, Asp166, Leu167
p65-RelA	Baicalin	DA18, Lys122	DT8, DT9, DT10, DA18, DG19, DT20, DC21, Lys122, Arg124
	β-hydroxy-DHP	DG19	DT8, DT9,DT10, DA18, DG19, DT20, DC21
	Isoliquiritin	DA18, DG19	DC7, DT8, DT9, DT10, DA18, DG19, DT20, DC21, Lys123
	Isoliquiritin apioside	DA18	DT8, DT10, DA18, DG19, DC21
	Liquiritin	DG19	DT8, DT9, DA18, DG19, DT20, DC21, Lys123
	Ononin	DG19	DC7, DT8, DT9, DT10, DA18, DG19, DT20, DC21, Lys445
	Oroxyloside	DG19, Lys122, Arg124	DT8, DT9, DT10, DG19, DT20, DC21, Lys122, Lys123, Arg124
	Fluoxetine (R)	DA18, DG19	DC7, DT8, DT9, DT10, DA18, DG19, DT20, DC21
	Fluoxetine (S)	DG19	DC7, DT8, DT9,DT10, DG19, DT20, DC21
	Albiflorin	DG19	DC7, DT8, DT9, DT10, DA18, DG19, DT20, DC21, Arg124
	Paeoniflorin	DG19	DC7,DT8, DT9, DT10, DA18, DG19, DC21, DC22, Arg124
	Pentagalloyl-β-D-glucose	DG19	DC7, DC8, DT9, DG19, DT20, DC21, DC22, Lys123, Arg124
	MG-132	DG19	DA6, DC7, DT8, DT9, DT10, DA18, DG19, DT20, DC21, DC22, Lys123

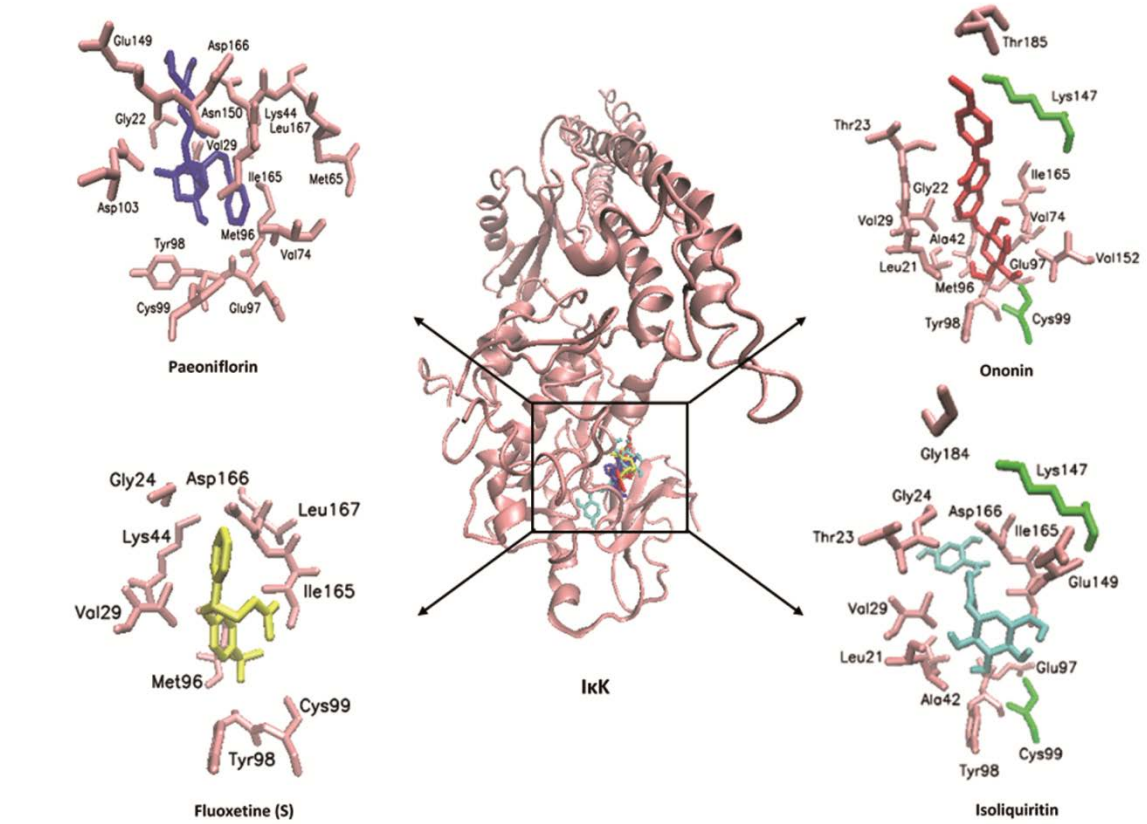

Figure 15. Visualization of molecular docking of chemical compounds of FAEW to IκK.

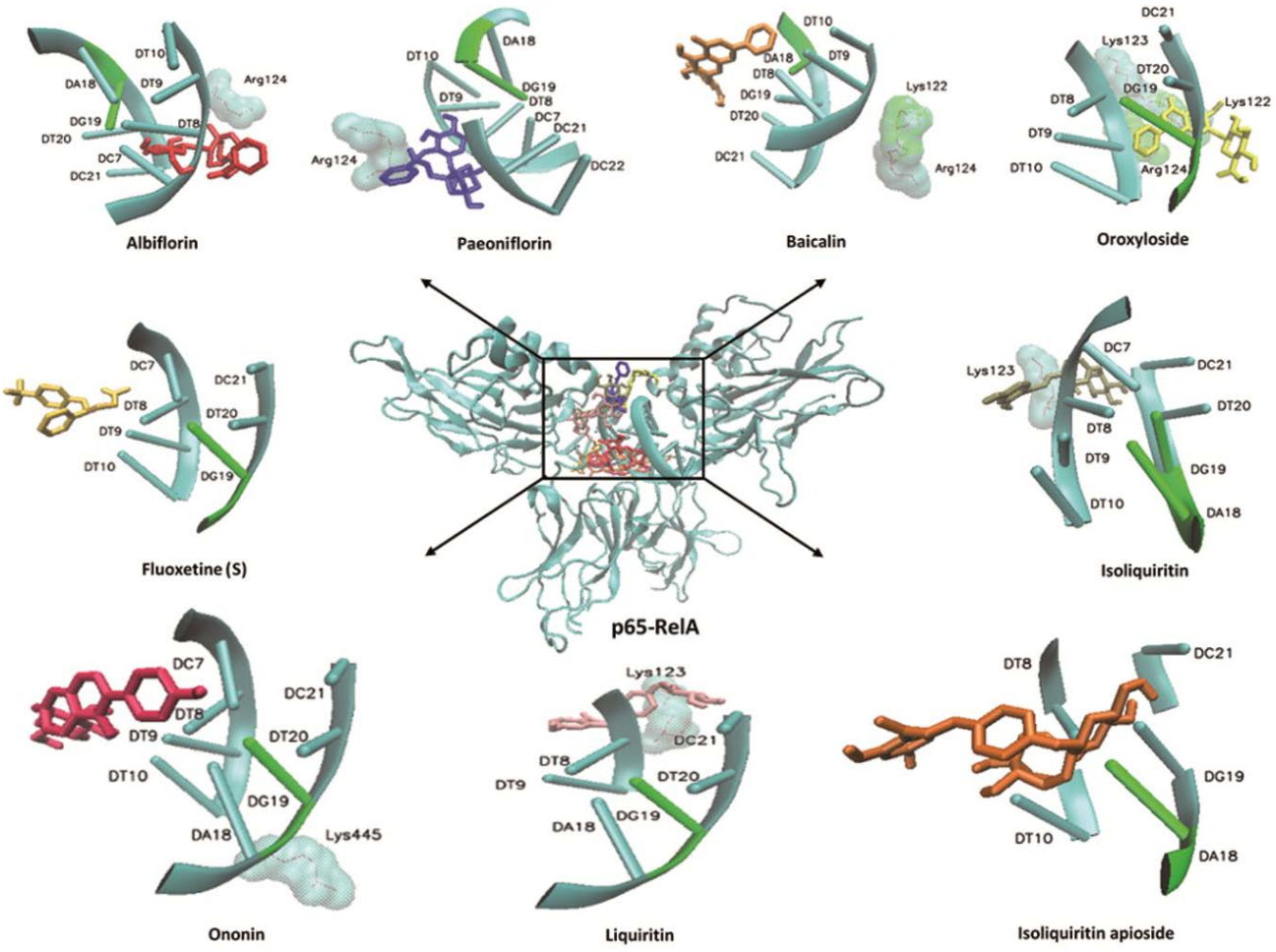

Figure 16. Visualization of molecular docking of chemical compounds of FAEW to p65.

3.2.6 Literature review on the pharmacological activity and anti-inflammation of the compounds from FAEW

To further characterize the therapeutic potential of the candidate compounds investigated by molecular docking, we performed literature review of the current research on the isolated compounds of FAEW. As shown in **Table 5**, paeoniflorin, albiflorin and baicalin were reported to *in vitro* act against inflammation and oxidative stress, and to be effective *in vivo* against depression, and Parkinson's disease. Furthermore, clinical trials were carried out among herbal formulae in inflammation-related diseases, such as Japanese traditional recipe *Shakuyakukanzoto*, and the Chinese herb formula *Xiongshao capsule*. *In vivo* studies on isoliquiritin and liquiritin showed their activities against depression and cognitive-related diseases, for instance, Parkinson's disease. As shown in **Table 6**, paeoniflorin, baicalin and liquiritin have been demonstrated to reduce inflammatory processes related to numerous diseases *in vitro* and *in vivo* through inhibiting NF-κB, which implies their role as constituents of FAEW acting against inflammatory reactions related to PTSD.

Table 5. Literature review on the pharmacological activity of the compounds from FAEW

Compounds	**pharmacological activity**		
	In vitro	***In vivo***	**Clinical studies**
Paeoniflorin	Anti-inflammation and oxidative stress [167]; neuroprotection [168]; apoptosis [169]	Parkinson's disease [170]; depression [171]; neuropathic pain [172]; non-alcoholic steatohepatitis [173]	Rheumatoid arthritis [174]; muscle cramps and abdominal pains [175]; restenosis after percutaneous coronary intervention [176]
Albiflorin	Oxidative stress [177]; neuroprotection [178]	Anti-depression [179]; Parkinson's disease [180]; neuropathic pain [172, 181]	Muscle cramps and abdominal pains [175]
Baicalin	Inflammation[182]; apoptosis[183]; oxidative stress[184]	Alcoholic liver injury[185]; depression /anxiety [55]; renal damage [56]; memory impairment[57]	Ulcerative colitis[186]
Liquiritin	Neuroprotection [187]	Cognitive deficits [188]; Parkinson's disease [189]; depression [190]; focal cerebral ischemia [191]	Melisma [192]
β-hydroxy-DHP	Apoptosis [193]		
Isoliquiritin apioside	Anti-genotoxic [194]		
Isoliquiritin	Anti-allergic activity [194]	Depression [195]; antifungal activity [196]	Depression [197]
Oroxyloside		Colitis [198]; inflammation-related diseases [199]	

Table 6. Literature review of the effect of chemical constituents of FAEW against NF-κB.

Compounds	pharmacological activity on NF-κB	
	In vitro	***In vivo***
Paeoniflorin	Parkinson's disease [200]; immunomodulation [201]; Alzheimer's disease [202]; apoptosis [167]; morphine tolerance [203]; anti-inflammation and immunomodulation [204]; sepsis [205]; obesity [206]; cardiac remodeling [207]	Renal function [208];non-alcoholic steatohepatitis[173]; cardiac dysfunction [209]; vascular dementia [210]; Alzheimer's Disease [211]; arthritis [212] ; hepatitis [213]; colitis [214]; learning dysfunction and brain damage [215]; lung injury [216]
Baicalin	Myofibroblast differentiation [217]; atherosclerosis [218]; haemophilus parasuis infection [219]; mastitis [220]; apoptosis [221]	Asthma[222]; periodontitis [223]; allergic diseases [224]; arthritis [225]; brain edema [226]; lung injury [227]; liver injury [228]; ischemic stroke [229]; cerebral ischemia[230]
Isoliquiritin	Inflammatory responses [231]	
Liquiritin	Endothelial dysfunction [232]	Myocardial fibrosis [233]; acute Lung Injury [234]
Oroxyloside		Colitis [198]

3.2.7 Summary

In this part, we observed that FAEW was not cytotoxic with a wide range, it was indeed not cytotoxic in HEK293 cells at concentrations up to 2000 μg/ml. FAEW significantly inhibited NF-κB activity in a dose-dependent manner and time-dependent manner from 24 to 72 h, reaching the similar inhibitory level caused by MG-132 at 72 h. Its effect in inhibiting NF-κB has also been demonstrated in the protein level in T98G brain cells. Hence, FAEW might exert anti-anxiety effects through inhibiting NF-κB-mediated inflammatory process.

In the investigation of this section, 10 compounds were identified in the extract of FAEW, they were baicalin, β-hydroxy-DHP, isoliquiritin, isoliquiritin apioside, liquiritin, ononin, oroxyloside, albiflorin, paeoniflorin, and pentagalloyl-β-D-glucose. To identify the active compounds, we performed molecular docking to investigate the binding modes of the identified FAEW compounds with NF-κB pathway related proteins

Among a panel of 10 compounds, paeoniflorin, isoliquiritin apioside and ononin exerted high affinity to IκK and p65-RelA. Baicalin, isoliquiritin, liquiritin and oroxyloside strongly bound to p65-RelA. Paeoniflorin, albiflorin, baicalin, isoliquiritin and liquiritin were reported to be active against depression and Parkinson's disease in *in vivo* studies and clinical trials, and paeoniflorin, baicalin and liquiritin were reported to inhibit NF-κB *in vitro* and *in vivo*. These data demonstrated that FAEW is constituted by a wide array of diverse anti-depressant natural drugs with strong anti-inflammatory activity.

3.3 The Chinese herb formula *Free and Easy Wanderer* ameliorates oxidative stress through KEAP1-NRF2/HO-1 pathway

3.3.1 Cytotoxicity of FAEW and fluoxetine

As the first step, we performed resazurin assays in human glioblastoma T98G and human neuroblastoma SH-SY5Y cell lines to investigate whether FAEW reveals cytotoxic effects or not. As expected, FAEW was indeed not cytotoxic towards T98G cells at concentrations up to 300 µg/ml (**Figure 17A1**). For comparison, fluoxetine was non-toxic up to 3.1 µg/ml (10 µM) and inhibited T98G cells at higher concentrations (**Figure 17A2**). However, both FAEW and fluoxetine have no cytotoxicity towards SH-SY5Y cell, even at higher concentrations (**Figure 17B1, Figure 17B2**).

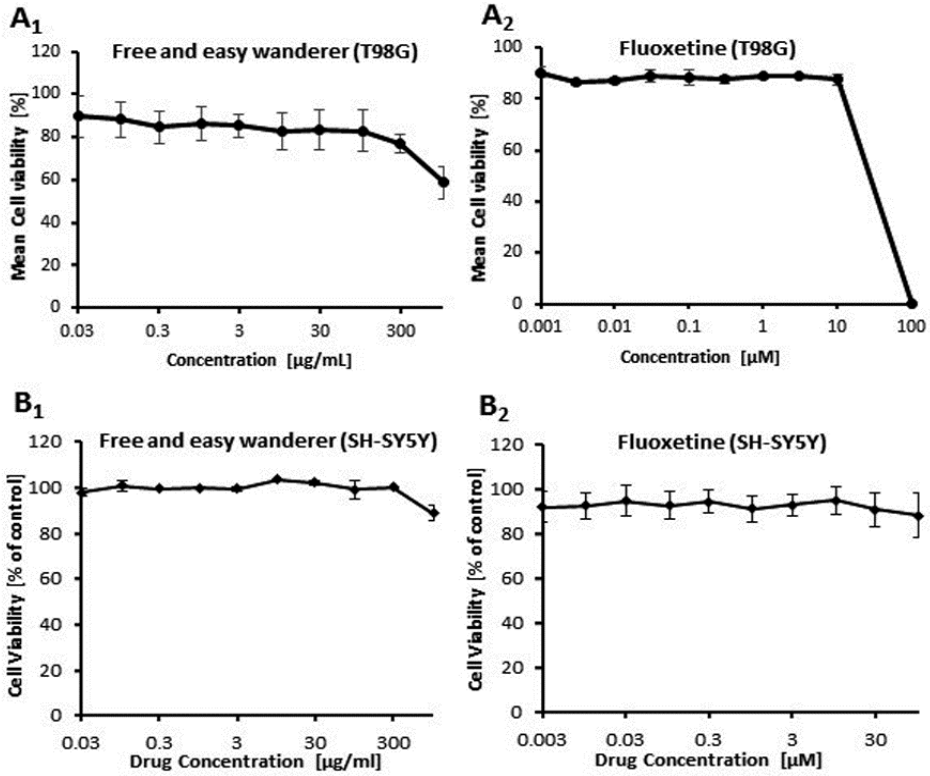

Figure 17. Cytotoxicity of FAEW (1) and fluoxetine (2) as determined by the resazurin assay in the human glioblastoma T98G (A) and human neuroblastoma SH-SY5Y (B) cells. Shown are mean values ± SD of three independent experiments.

3.3.2 Inhibition of ROS generation by FAEW and fluoxetine

We selected several non-cytotoxic concentrations of FAEW and fluoxetine, and performed flow cytometric experiments to investigate ROS levels. Firstly, we used H_2O_2 to induce oxidative stress *in vitro*. As shown in **Figure 18A1** and **Figure 18B1**, FAEW strongly reduced the levels of ROS induced by H_2O_2 and the levels of ROS in untreated T98G and SH-SY5Y cells, indicating that FAEW diminished exogenous H_2O_2-induced ROS and also protected against endogenous ROS. Fluoxetine showed the same effect as FAEW shown in **Figure 18A2** and **Figure 18B2**.

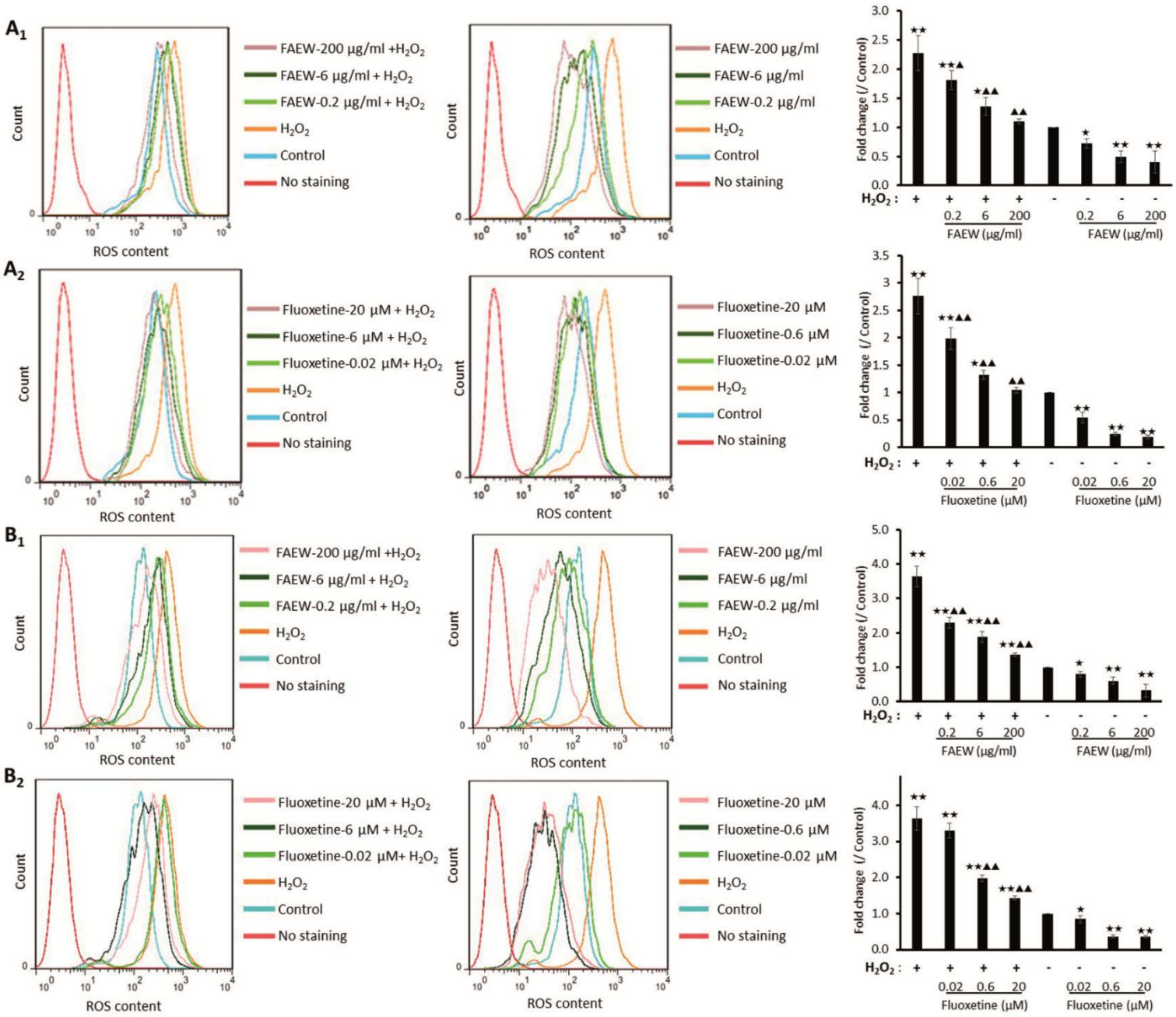

Figure 18. Inhibition of reactive oxygen species by FAEW (1) or fluoxetine (2) in the human glioblastoma T98G (A) and human neuroblastoma SH-SY5Y (B) cells. Shown are mean values ± SD of three independent experiments. ★ $p < 0.05$, ★★ $p < 0.01$, compared with control; ▲ $p < 0.05$, ▲▲ $p < 0.01$, compared with H_2O_2.

3.3.3 Gene expression profiling caused by FAEW and fluoxetine

Gene expression profiling was performed to obtain deeper insight into the mechanisms of FAEW and fluoxetine against oxidative stress. Therefore, total RNA was extracted to perform transcriptome-wide microarray analyses, after human glioblastoma T98G cells were treated with FAEW or fluoxetine for 48 h, and oxidative stress was induced with H_2O_2 for 6 h.

All data obtained by microarray analyses were subjected to pathway analysis. The deregulated genes were correlated with several molecular and cellular functions and pathways. As shown in **Figure 19A** and **Figure 19B**, NRF2-mediated oxidative stress was the top-ranked pathway upon FAEW treatment. Furthermore, an upstream regulator analysis was performed with IPA to identify transcriptional regulators, kinases, or enzymes that may be responsible for gene expression changes in T98G cells after treatment. **Table 7** shows the upstream transcriptional factors predicted by IPA to be affected by FAEW and fluoxetine. Remarkably, NFE2L2 (alias NRF2) (underlined) was found to be a commonly activated transcription regulator by both FAEW and fluoxetine, implying that NRF2-mediated stress response may be involved with the mechanisms of the two drugs. **Table 8** displays the targeted genes downstream of NRF2 upon different treatment models. Most interestingly, *HMOX1* (alias *HO-1*) was commonly targeted by FAEW and fluoxetine with or without oxidative stress. Six deregulated downstream genes of NRF2, including *HMOX1* were quantified by real-time RT-PCR to technically validate the microarray results. KEAP1 was identified as a cytoplasmic NRF2-interacting protein that negatively regulates NRF2 activity, but recent studies revealed that alternative mechanisms of NRF2 activation that do not rely on KEAP1[235]. Therefore, we also investigated the transcriptional levels of NRF2 and KEAP1. The correlation coefficients (R-values) between mRNA expression values determined by microarray hybridization and real-time RT-PCR were in the range of 0.83 to 0.97 for each compound (Pearson correlation test), indicating a high degree of concordance between the data obtained from the two different methods (**Table 9**). The levels of KEAP1 and NRF2 were not affected, which excluded the transcription regulation and autoregulation, and suggested the possibility of participation of KEAP1-NRF2 protein-protein interaction. **Figure 19C** shows the deregulated genes controlled by NRF2 upon treatment by FAEW and fluoxetine, respectively.

Table 7. Most pronounced upstream transcription factors for deregulated genes upon different treatments.

Comparison with control					Comparison with H_2O_2	
FAEW	Fluoxetine	H_2O_2	H_2O_2+FAEW	H_2O_2 +Fluoxetine	H_2O_2 +FAEW	H_2O_2 +Fluoxetine
RBPJ	SOX2	KDM5B	NUPR1	TP53	JUN	***NFE2L2***
HMGA1	EGR2	TP53	KDM5B	FOXO1	RELA	PDX1
HLX	ATF4	***NFE2L2***	RELA	TCF7L2	FOXO1	TCF3
CEBPD	TCF3	FOXM1	JUN	NEUROG1	CREB1	HMGA1
NFE2L2	GFI1	MYC	CREB1	TFEB	DDIT3	MED1
CTNNB1	SPI1	TBX2	***NFE2L2***	IRF4	NUPR1	MYC
CEBPA	SMAD4	CCND1	REL	RELA	ECSIT	FOXM1
SOX2	HIF1A	TAL1	PPRC1	SRF	JUNB	ERG
EGR1	GATA1	ATF4	RELB	CREBBP	REL	ATF6
RELB	SMARCB1	ATF6	TP53	SP1	***NFE2L2***	RUNX2
JUNB	E2F3	REL	ECSIT	XBP1	STAT3	NUPR1
EBF1	JUN	MED1	SPI1	NUPR1	ATF2	FOS
NKX2-3	MTPN	MITF	WT1	NFKBIA	SOX2	BRCA1
YY1	MDM2	NUPR1	ATF4	***NFE2L2***	FOXL2	SMARCE1
MITF	RUNX2	CEBPB	TP63	NOTCH1	CEBPB	STAT5B
ETS2	KLF4	XBP1	RUNX1	CREB1	RBPJ	SREBF1
GLI1	NKX2-3	BRCA1	NCOA3	VDR	FOXO3	CTNNB1
SRF	IRF3	SRF	TBX2	MEF2C	HIF1A	TFEB
STAT3	HIC1	E2F1	YY1	CTNNB1	TP53	SOX2
SPDEF	TFEB	GPS2	FLI1	BRCA1	CREBBP	TP63
CCND1	MYC	IFI16	CARM1	JUN	NFKB1	NKX2-3
EP300	HMGA1	FOXO1	TFAP2C	HOXA10	RB1	SIRT1
TCF7L2	STAT1	FOS	MEF2D	TAL1	EP300	FOXO4
HDAC6	RB1	IRF3	POU2F1	FOS	NKX2-3	TP73
DACH1	E2F1	STAT3	GATA3	HIC1	EZH2	NFKBIA
FOSL1	NRF1	RB1	IRF6	ELK1	USF1	DDIT3
TP53	BRCA1	CREB1	ATF2	IKZF1	CDKN2A	FOXO3
SMARCA4	TP63	HIF1A	CTNNB1	IFI16	CEBPA	HIF1A
BRCA1	ETS2	HIC1	FOXL2	FOXO3	TP73	CREB1
CITED2	***NFE2L2***	EGR1	MITF	GLI1	SIRT1	GLI1

Table 8. Target genes in the corresponding dataset regulated by NRF2.

Comparison	Treatment	Activation z-score	P-value of overlap	Target molecules in dataset
Compared with control	FAEW	1.790	1.49E-02	CXCL8, GCLM, **HMOX1**, GPX1, IL6, SAT1, SCG2, COL1A1
	Fluoxetine	1.000	3.64E-04	ATF4, BRCA1, DDX50, DHCR7, ERP29, **HMOX1**, LGALS8, MAFG, MGST3, NOCT, NQO1, PSMD12, SNAI2, TXNRD1
	H_2O_2	2.390	7.08E-02	ATF4, CXCL8, **HMOX1**, PSAT1, RRS1, VCAM1
	H_2O_2+FAEW	2.674	3.04E-03	AHR, ATF4, BNIP3, CREG1, CXCL8, GCLM, GPX1, **HMOX1**, IL6, MAFF, MGST1, NQO1, PAFAH1B1, RRS1, S100P, SLC6A9, SLC7A11, SOD2, TXNRD1, VCAM1
	H_2O_2+Fluoxetine	1.685	2.58E-04	ALDH3A1, CREG1, DAD1, GCLM, HERPUD1, IL6, MGST1, MGST3, SCG2, SRXN1, **HMOX1**
Compared with H_2O_2	H_2O_2+FAEW	1.837	4.25E-03	CXCL8, **HMOX1**, IL6, MAFF, SOD2
	H_2O_2+Fluoxetine	2.250	8.91E-02	CTSD, DDIT3, DHCR7, GCLM, IL6, SRXN1

Table 9. Comparison of mRNA expressions (fold change) obtained by microarray gene expression profiling and real-time RT-qPCR for selected genes.

Genes	FAEW		Fluoxetine		H_2O_2		H_2O_2 +FAEW		H_2O_2 +Fluoxetine	
	RT-qPCR	Micro-array	RT-qPCR	Micro-array	RT-qPCR	Micro-array	RT-qPCR	Micro-array	RT-qPCR	Micro-array
HMOX1	2.36	1.72	3.74	1.75	1.91	1.69	5.23	3.46	1.81	1.45
MGST1	1.42	1.25	-1.08	-1.15	1.44	1.25	1.50	1.61	1.37	1.75
TXNRD1	1.88	1.26	2.87	2.14	2.31	1.45	2.68	1.51	1.75	1.44
HERPUD1	1.47	1.28	1.33	1.11	1.68	1.44	2.02	1.46	1.59	1.46
KEAP1	1.19	1.14	1.24	1.15	1.16	1.02	2.23	1.40	1.44	1.32
GCLM	1.99	1.51	2.42	1.48	1.30	1.12	1.48	1.60	1.97	1.65
NFE2L2	-1.20	-1.15	1.22	1.08	1.21	1.13	-1.15	-1.04	-1.06	-1.12
ATF4	1.05	1.22	2.38	1.80	1.79	1.52	2.25	1.84	1.45	1.22
R-value	**0.97**		**0.92**		**0.83**		**0.96**		**0.97**	

Real time qPCR results are shown with mean values of two independent experiments.

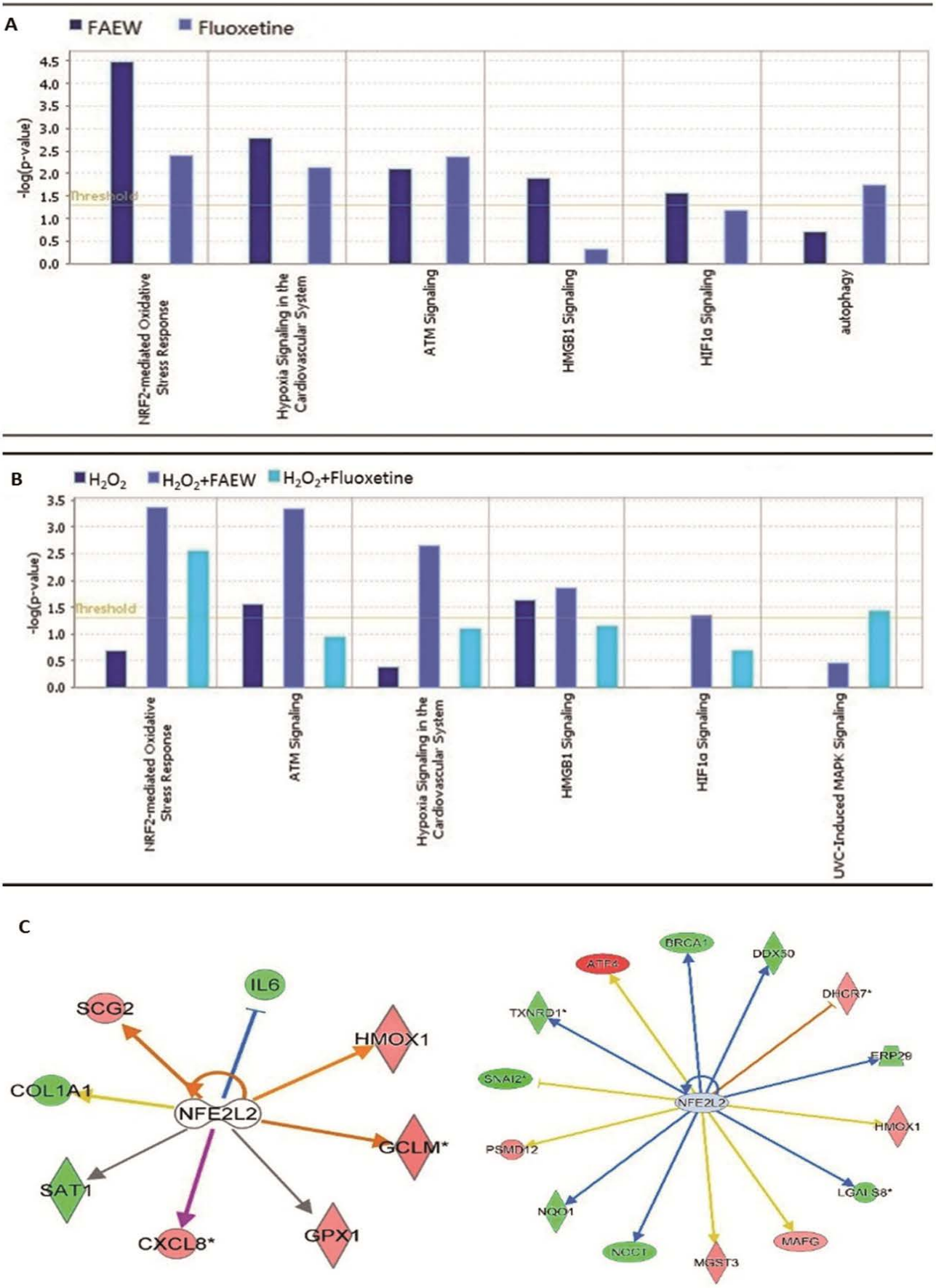

Figure 19. Gene expression profiling of T98G cells upon treatment of FAEW or fluoxetine. (A and B). Pathway analyses: Top cellular pathways affected by FAEW and fluoxetine examined by mRNA microarray hybridization. (A) shows the comparison between FAEW and fluoxetine. (B) shows the comparison between H_2O_2, H_2O_2 and FAEW, H_2O_2 and fluoxetine. P-values were calculated using right-tailed Fisher's exact test. (C) Deregulated genes under the influence of the common upstream regulator NFE2L2 (NRF2) inhibited by FAEW (left) and fluoxetine (right).

3.3.4 Inhibition of KEAP1-NRF2 interaction by FAEW and fluoxetine

To further investigate the protective mechanism of FAEW against oxidative stress, we performed western blotting with NRF2 pathway-related proteins to clarify the participation of the NRF2-HO-1 pathway. As shown in **Figure 20A, Figure 20B, Figure 20C** and **Figure 20D**, FAEW and fluoxetine both promoted nuclear NRF2 translocation. The expression levels of NRF2 in the nucleus were significantly increased with or without stressed conditions induced by H_2O_2. Meanwhile, the levels of total HO-1 also significantly increased, which confirmed the prediction by microarray analysis. H_2O_2 also triggered NRF2 translocation at short times, *i.e*. 10 min and 6 h. The effects diminished with longer times of H_2O_2-induced stress, *i.e*. 12 to 24 h. The HO-1 levels significantly increased after stress induction for 6 h, the trend lasted for 24 h. While, there is no significant change for the protein expression of catalase (CAT) upon the different treatment. Interestingly, in parallel with the translocation of NRF2 from the cytoplasm, cytosolic KEAP1 levels decreased, indicating a correlation between KEAP1 and NRF2. **Figure 20E** and **Figure 20F** display the dose-response relation of nuclear NRF2, cytoplasmic NRF2, cytoplasmic KEAP1 and HO-1 upon treatment with FAEW or fluoxetine among human glioblastoma T98G and human neuroblastoma SH-SY5Y cell lines, respectively.

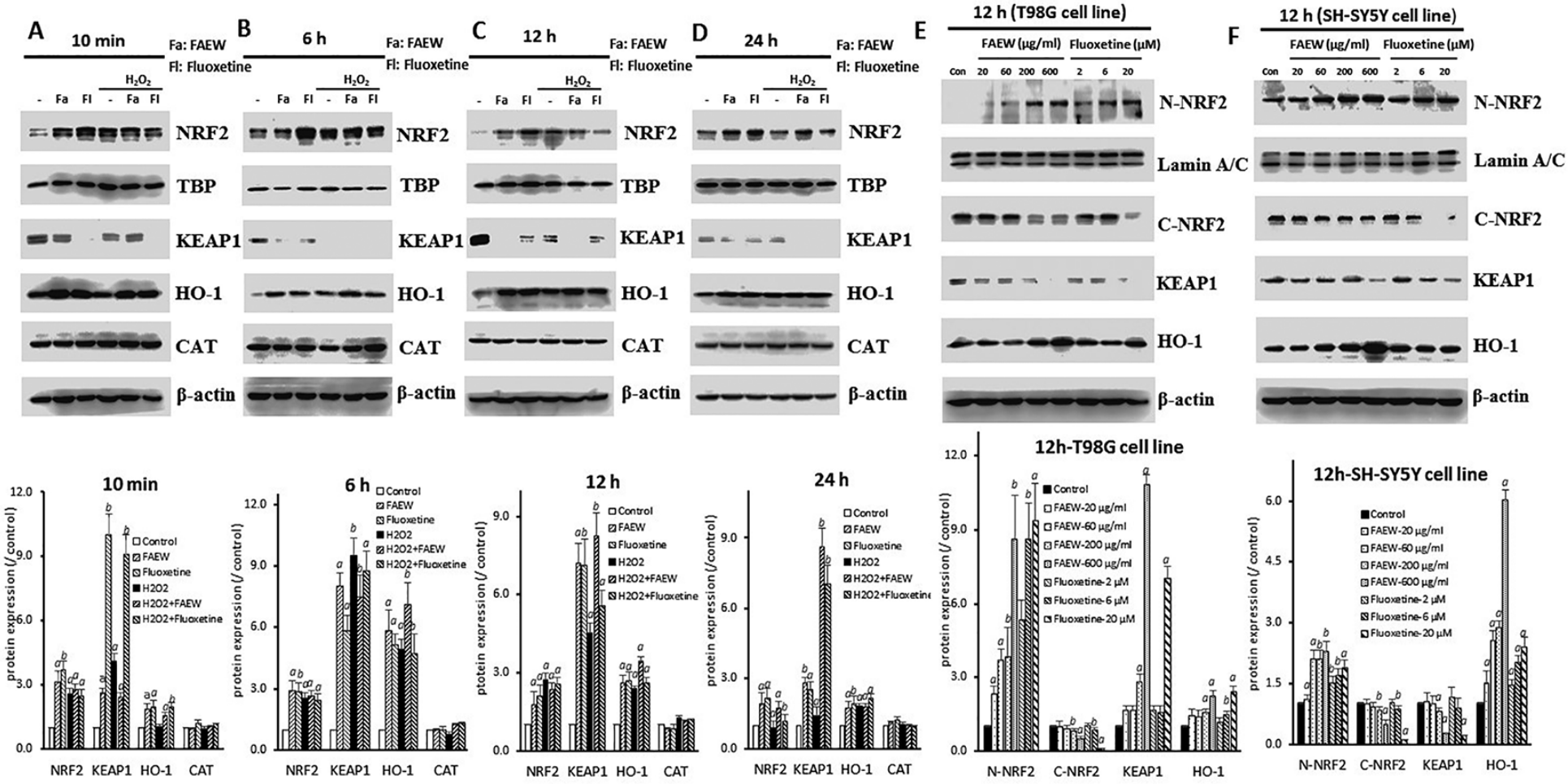

Figure 20. NRF2, HO-1, CAT and KEAP1 protein expression affected by FAEW or fluoxetine in human glioblastoma T98G cells and human neuroblastoma SH-SY5Y cells. A, B, C and D show NRF2, HO-1, CAT and KEAP1 protein expression affected by FAEW or fluoxetine in human glioblastoma T98G cells with different induction times for H_2O_2 (A, 10 min; B, 6 h; C, 12 h; D, 24 h, respectively). TBP was used as loading control for nuclear proteins and β-actin was used as loading control for cytoplasmic proteins. E and F show cytoplasmic and nuclear NRF2, cytoplasmic KEAP1 and total HO-1 protein expression in human glioblastoma T98G (E) and human neuroblastoma SH-SY5Y (F) cells with different concentrations of FAEW and fluoxetine for 12 h. Lamin A/C was used as loading control for nuclear protein, β-actin was used as loading control for cytoplasmic protein. Shown are mean values ± SD of three independent experiments. ^{a} $p < 0.01$, ^{b} $p < 0.05$.

3.3.5 *In silico* molecular docking of compounds from FAEW to KEAP1

Initially, we performed molecular dockings to predict binding energies of 10 compounds from FAEW, the antidepressant control drug fluoxetine and another control drug, IQK, which is a KEAP1-NRF2 interaction inhibitor. Except for isoliquiritin apioside and pentagalloyl-β-D-glucose, the other compounds were predicted to exhibit higher binding affinities than fluoxetine (-5.01 kcal/mol for fluoxetine (S)), especially baicalin (-7.45 kcal/mol), oroxyloside (-7.89 kcal/mol) and liquiritin (-6.86 kcal/mol). **Figure 21** shows the predicted binding sites of the compounds to KEAP1.

Table 10. *In silico* molecular docking of chemical compounds isolated from FAEW to KEAP1.

Ligands	Binding energy (kcal/mol)	Ki (μM)	Residues forming H-bonds	Residues involved in hydrophobic interactions
Baicalin	-7.45±0.04	3.47±0.23	Asn382, Asn414, Arg415, Ser555, Ser602	Tyr334, Arg380, Ile461, Gly462, Phe478, Ser508, Ala556, Tyr572
Ononin	-5.57±0.08	83.58±10.40	Ser602	Tyr334, Ser363, Gly364, Arg415, Ile416, Gly462, Ala556, Tyr572, Phe577, Gly603
Isoliquiritin	-5.87±0.19	51.78±15.65	Asn382, Ser602	Tyr334, Gly364, Arg415, Ile416, Gly462, Gly509, Ala510, Ala556, Phe577, Gly603
Liquiritin	-6.86±0.06	9.46±0.93	Arg380, Arg415, Ser555	Tyr334, Ser363, Gly364, Asn382, Asn414, Gly462, Arg483, Gly509, Tyr525, Gln530, Ala556, Ser602
Isoliquiritin apioside	-4.42±0.19	592.15±191.29	Tyr334, Asn414, Arg415	Ser363, Asn382, Ile461, Gly462, Arg483, Ser508, Gly509, Tyr525, Tyr572, Phe577, Ser602
β-hydroxy-DHP	-5.32±0.34	139.60±25.36	Asn382	Tyr334, Ser363, Gly364, Arg380, Asn414, Arg415, Ile416, Gly462, Ala556, Gly603
Pentagalloyl-β-D-glucose	-2.68±0.14	11.15±2.51	Asn382, Arg483	Tyr334, Ser363, Arg415, Gly509, Tyr525, Gln528, Asp529, Gln530, Ser555, Ala556, Tyr572, Phe577, Ser602
Oroxyloside	-7.89±0.27	1.73±0.45	Ser363, Arg380, Asn382, Arg415, Ser602	Tyr334, Gly364, Leu365, Asn414, Ile416, Gly462, Gly509, Ala556, Gly603
Albiflorin	-5.93±0.14	45.95±11.73	Asn382	Tyr334, Ser363, Gly364, Arg380, Asn414, Arg415, Arg483, Tyr525,Gln530, Ser555, Ala556, Tyr572, Phe577, Ser602
Paeoniflorin	-6.00±0.08	68.01±5.23	Arg415	Tyr334, Ser363, Asn414, Gly462, Ser508, Gly509, Tyr525, Ala556, Ser602
Fluoxetine (R)	-4.99±0.07	221.02±24.87	Asn382, Asn414, Arg415, Ser555, Ser602	Gly364, Arg415, Gly462, Val463, Ser508, Gly509, Ala510, Tyr525, Ala556, Gly603, Val604
Fluoxetine (S)	-5.01±0.20	220.93±80.57	Ser602	Gly364, Arg415, Ile461, Gly462, Phe478, Arg483, Ser508, Gly509, Ser555, Ala556,
IQK	-9.52±0.18	0.11±0.03	Arg415, Gln530, Ser555	Ser363, Gly364, Asn414, Ile461, Arg483, Ser508, Gly509, Tyr525, Gln530, Ser555, Ala556, Phe577, Ser602, Gly603

Shown are mean values ± SD of three independent experiments

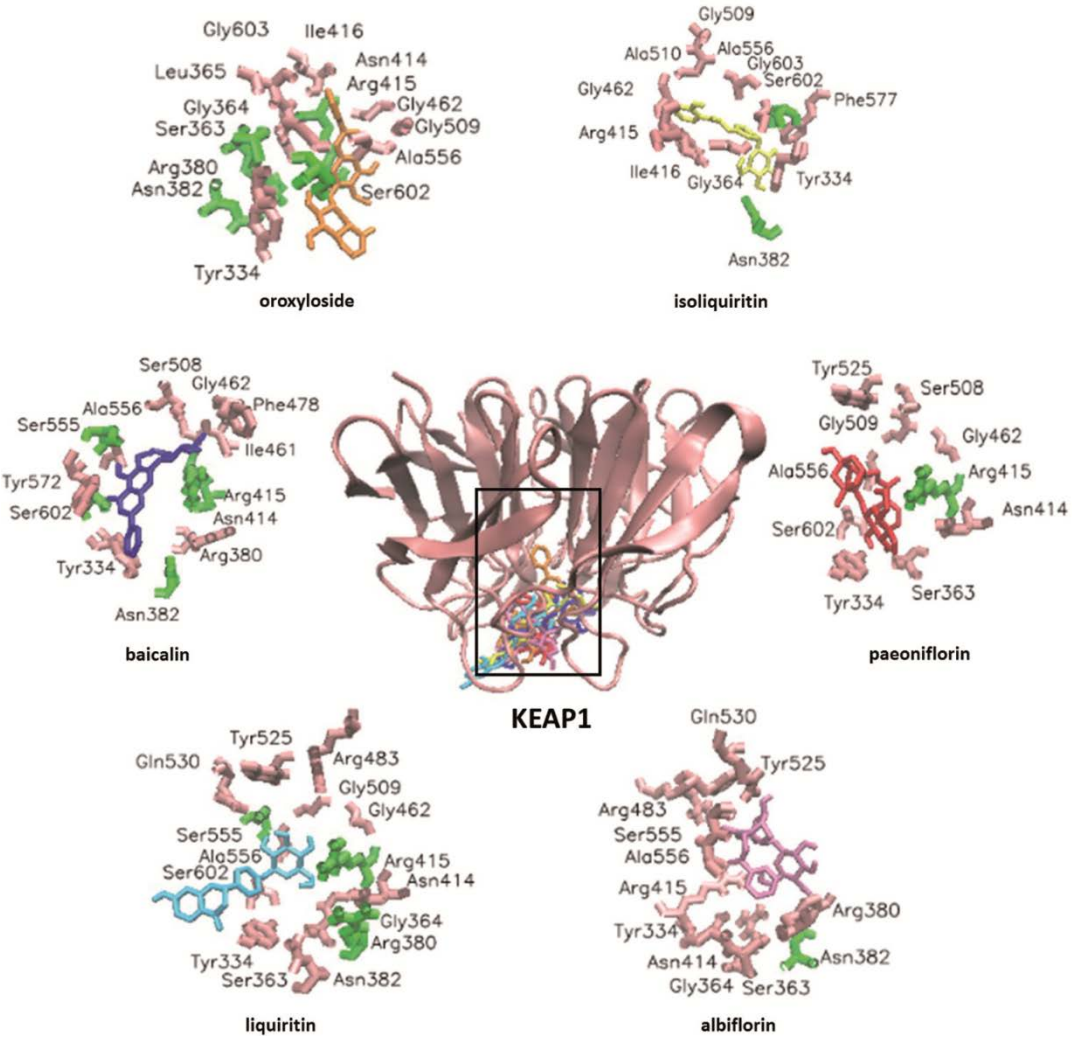

Figure 21. Visualization of molecular docking of chemical compounds of FAEW to KEAP1.

3.3.6 Anti-oxidative effect of the compounds isolated from FAEW extract

Among the compounds isolated from FAEW, paeoniflorin, albiflorin, baicalin, and isoliquiritin have been reported against oxidative stress *in vitro*, they are active against apoptosis, neurotoxicity and oxidative injury, *In vivo* experiments revealed their effect in quite many diseases, such as chronic obstructive pulmonary disease, diabetics, colitis. In addition, liquiritin, isoliquiritin apioside were active towards oxidative stress-induced genotoxicity, as shown in **Table 11**.

Table 11. Literature review of the effect of chemical constituents of FAEW against oxidative stress

Compounds	*In vitro*	*In vivo*
Paeonifloirin	Neurotoxicity[200]; apoptosis[167, 236, 237]; oxidative injury[238]; cell damage[239]; osteoblast cytotoxicity[240]	Cholestasis[241], chronic obstructive pulmonary disease[242]
Albiflorin	Neurotoxicity[177, 180], oxidative stress[177]	Diabetics[243]
Baicalin	Oxidative injury[244, 245]; apoptosis[246]	Colitis[247]; *Haemophilus parasuis* infection[219]; vascular inflammation[248]; neurotoxicity[249]; skin fibroblast[250]
Isoliquiritin	Neurotoxicity[251]	Oxidative stress-induced genotoxicity[194]
Isoliquiritin apioside		Oxidative stress-induced genotoxicity[194]
Liquiritin		Myocardial fibrosis[233], depression[252], lung epithelial cell injury[253], cognitive deficits[254], endothelial dysfunction[232]

3.3.7 Summary

In the investigation of this section, we employed exogenous H_2O_2 for ROS induction in human glioblastoma T98G and human neuroblastoma SH-SY5Y cell lines as the cellular stress model to investigate the effect of FAEW and fluoxetine on oxidative stress. Our results indicated that ROS levels significantly increased upon H_2O_2 treatment. Both FAEW and fluoxetine effectively diminished ROS generated by H_2O_2. Furthermore, they also significantly reduced the levels of endogenous ROS in untreated cells, suggesting their capability against oxidative stress by removing both endogenous and exogenous ROS. Furthermore, the nuclear levels of NRF2 increased upon the induction by H_2O_2. In parallel, cytoplasmic KEAP1 levels decreased accordingly, which confirmed the interaction of KEAP1 and NRF2 under stress situations shown in previous studies [255]. Compared with the H_2O_2-induced dissociation of NRF2 from KEAP1, both FAEW and fluoxetine alone resulted in the translocation of NRF2 from cytoplasm to the nucleus, as the levels of cytoplasmic NRF2 decreased with the occurrence of the elevation of nuclear NRF2 levels. Besides, the level of nuclear NRF2 increased in a KEAP1-dependent manner, and the antioxidant response element HO-1 significantly elevated at transcriptional and translational levels upon treatment of FAEW or fluoxetine. In addition, the transcriptional levels of *NRF2* and *KEAP1* were not affected by the treatment of FAEW or fluoxetine. This can be taken as another hint for the capability of FAEW and fluoxetine to inhibit the KEAP1-NRF2 protein-protein interaction.

In this study, we proved that FAEW exerted strong activity against oxidative stress in human glioblastoma T98G and human neuroblastoma SH-SY5Y cell lines. The herbal mixture treatment reduced both endogenous and exogenous ROS, strongly promoted NRF2 translocation to the

nucleus in a KEAP1-dependent manner and, hence, HO-1 levels increased. The underlying mechanism for FAEW against oxidative stress may be related to multiple compounds, which bound to KEAP1-NRF2 protein-protein interaction sites and lead to the release of NRF2 from KEAP1 and NRF2 translocation to the nucleus, implying FAEW might be active against psychiatric disorders by reducing oxidative stress. Furthermore, oroxyloside, baicalin, liquiritin, paeoniflorin, albiflorin etc. revealed high affinities to KEAP1, which might be the effective substances of FAEW against oxidative stress. *In vivo* experiments revealed their effect in quite many diseases, such as chronic obstructive pulmonary disease, diabetics, colitis. These data demonstrated that FAEW is constituted by a wide array of diverse anti-depressant natural compounds with activity against oxidative stress.

4 Discussion

4.1 Identification of NF-κB as determinant of posttraumatic stress disorder and its inhibition by the Chinese herbal remedy *Free and Easy Wanderer*

4.1.1 Identification of NF-κB as determinant of PTSD

Increasing evidence indicated an involvement of immune system in fear- and anxiety-based disorders. Recent studies suggested that inflammation is associated with increased basal ganglia glutamate in patients in depression [110]. Furthermore, inflammasome signaling affects anxiety- and depressive-like behavior and gut microbiome composition, and suggesting that the gut microbiota-inflammasome-brain axis could be novel therapeutic targets for psychiatric disorders [111]. In our studies, network analyses revealed that NF-κB was activated in both the peripheral and central nervous system. In addition, promoter binding motif search of genes revealed that NF-κB was among the most important transcription factors. These results indicated that NF-κB may be an important immunological component of inflammatory processes in PTSD. Therefore, we hypothesized a link between the therapeutic effect of FAEW on PTSD, and NF-κB as relevant underlying mechanism.

4.1.2 Inhibition of NF-κB by FAEW and Structure Activity relationship of FAEW compounds

In our studies, we observed that FAEW was not cytotoxic with a wide range and showed a dose and time-dependent inhibition of NF-κB activity in HEK293 cells as well as of protein expression of NF-κB in T98G brain cells. Among the panel of 10 compounds, paeoniflorin, isoliquiritin apioside and ononin exerted high affinity to IκK and p65-RelA. Baicalin, isoliquiritin, liquiritin and oroxyloside strongly bound to p65-RelA. For example, paeoniflorin bound with IκK and p65 through multiple hydrogen bonds involving the OH groups of its glucose moiety. The hemiacetal OH-group in the core (position 5) and the 3'- and 4'-OH of paeoniflorin are predicted to bind to IκK residues Thr23, Met 96 and Glu 97, respectively. In the interaction of the same compound with p65, the 5-OH and the glucose OH groups in positions 3', 4', and 6' bound to the p65 residues DT9, DC22, DT8 and DC21, respectively. Besides, p65 residue DG 19 donates a hydrogen bond to the benzoate carbonyl of paeoniflorin. The same type of interactions for the other compounds from FAEW can be applied to explain their activities towards NF-κB, such as ononin, isoliquiritin. Furthermore, paeoniflorin, albiflorin, baicalin, isoliquiritin and liquiritin were reported to be active against depression and Parkinson's disease in *in vivo* studies and clinical studies, and paeoniflorin, baicalin and liquiritin were demonstrated to inhibit NF-κB *in vitro* and *in vivo*. These data suggested that FAEW is constituted by various natural compounds with high activity against inflammation. Importantly, some compounds have been indeed demonstrated to pass the blood-

brain barrier and reach brain tissue, e.g. albiflorin, paeoniflorin, liquiritin, which might explain the effect of FAEW in the central nervous system [256]. In addition, it is also quite interesting to observe that some compounds were used to treat colitis *in vivo* and in clinic studies, which might imply their participation in the balance of the gut- microbiota-inflammasome-brain axis [186, 198].

4.1.3 Summary and conclusion

In our studies, we observed that, with diverse active compounds, FAEW has high activity against inflammation by inhibiting NF-κB, which were comparable to the antidepressant drug, fluoxetine. It is not cytotoxic and approachable for the treatment of inflammation-related diseases. The literature review provided us some hints for future studies, to confirm and investigate the activity of different components of FAEW. To conclude the above results and discussions, *Free and easy wanderer* is active against inflammation by inhibiting NF-κB, the mechanism might be related to the multiple natural products binding to IκK and p65 through hydrogen bonds, which might also be the mechanism in the treatment of mental disorders.

4.2 The Chinese herb formula *Free and Easy Wanderer* ameliorates oxidative stress through KEAP1-NRF2/HO-1 pathway

4.2.1 Reactive oxygen species removal by *Free and Easy Wanderer*

Oxidative stress occurs if molecular defense systems fail to counteract oxidation caused by endogenous processes such as the mitochondrial breakdown of glucose for energy supply or by exogenous xenobiotic chemicals, air pollution and diet. It reflects an imbalance of a biological system's ability to detoxify reactive intermediates or repair resulting damage. Due to the essential role for physical well-being, longevity and survival, oxidative stress is involved in a variety of diseases, including diabetes, cardiovascular illnesses and neurodegenerative conditions. ROS are byproducts of aerobic metabolism, including the superoxide anion (O2-), hydrogen peroxide (H_2O_2), and hydroxyl radicals (OH-). All of them have inherent chemical properties that confer reactivity to different biological targets. Rats under stress conditions exhibited greater anxiety-like behavior and increased ROS levels than corresponding control animals, and vice versa, induction of ROS generation resulted in anxiety-like behavior [93]. These observations suggest a causative link between ROS and mental disorders.

In our studies, we therefore, employed exogenous H_2O_2 for ROS induction in human glioblastoma T98G and human neuroblastoma SH-SY5Y cell lines as the cellular stress model to investigate the effect of FAEW and fluoxetine upon oxidative stress. Our results indicated that ROS levels significantly increased upon H_2O_2 treatment. Both FAEW and fluoxetine effectively diminished ROS generated by H_2O_2. Furthermore, they also significantly reduced the levels of endogenous

ROS in untreated cells, suggesting their capability against oxidative stress by removing both endogenous and exogenous ROS.

4.2.2 NRF2-KEAP1-ARE pathway activation upon oxidative stress

NRF2 is composed of six functional domains known as NRF2-ECH homologies (Neh) and designated as Neh1-6, respectively [97]. Under normal physiological conditions, NRF2 is sequestered in the cytosol and maintained at a low level through KEAP1-dependent ubiquitination and proteasome degradation. Human KEAP1 are highly reactive towards ROS and electrophiles and are believed to be involved in redox sensing with the existence of seven active cysteine residues (i.e., Cys151, Cys257, Cys273, Cys288, Cys297, Cys434, and Cys613) [109, 165, 166]. In the presence of oxidative stress, such as ROS or electrophilic chemicals, the cysteine residues of KEAP1 are covalently modified. These chemical modifications result in conformational changes in KEAP1 that relieve NRF2 from KEAP1-directed degradation. NRF2 translocates to the nucleus and activates ARE-dependent gene expression of a series of anti-oxidative and cytoprotective proteins, such as HO-1[98]. In our studies, the nuclear levels of NRF2 increased upon the induction by H_2O_2. In parallel, cytoplasmic KEAP1 levels decreased accordingly, which confirmed the interaction of KEAP1 and NRF2 under stressed situations shown in previous studies [100, 101].

4.2.3 KEAP1-NRF2-ARE pathway activation by *Free and Easy Wanderer*

KEAP1-NRF2-ARE pathway represents one of the most important cellular defense mechanisms against oxidative stress and xenobiotic damage. Activation of NRF2 signaling induces the transcriptional regulation of ARE-dependent expression of various detoxifying and antioxidant defense enzymes and proteins. KEAP1-NRF2-ARE signaling has become an attractive target for the prevention and treatment of oxidative stress-related diseases and conditions including cancer, neurodegenerative, cardiovascular, metabolic and inflammatory diseases. Recent studies indicated that NRF2 may play an essential role in the central nervous system. NRF2-dependent persistent oxidative stress resulted in stress-induced vulnerability to depression in rats [96]. KEAP1-NRF2 signaling is involved in depression in a mice model [257], implying that interruption the KEAP1-NRF2 protein-protein interaction might be a potential therapeutic approach against depression.

Subsequently, a variety of KEAP1-NRF2 protein-protein interaction inhibitors were discovered, and the disruption of KEAP1-NRF2 protein-protein interactions became a novel approach for drug discovery of antioxidant agents[99]. In my studies, compared with the H_2O_2-induced dissociation of NRF2 from KEAP1, both FAEW and fluoxetine alone resulted in the translocation of NRF2 from cytoplasm to the nucleus, as the levels of cytoplasmic NRF2 decreased with the occurrence of the elevation of nuclear NRF2 levels. Besides, the level of nuclear NRF2 increased

in a KEAP1-dependent manner, and the antioxidant response element HO-1 significantly elevated at transcriptional and translational levels upon treatment of FAEW or fluoxetine. In addition, the transcriptional levels of NRF2 and KEAP1 were not affected by the treatment of FAEW or fluoxetine. This can be taken as another hint for the capability of FAEW and fluoxetine to inhibit the KEAP1-NRF2 protein-protein interaction. Furthermore, we performed molecular docking to investigate the binding modes of the identified FAEW compounds with KEAP1. Indeed, oroxyloside, baicalin, liquiritin, paeoniflorin, albiflorin etc. revealed strong affinities to KEAP1, which might be the effective substances of FAEW against oxidative stress. Importantly, some compounds have been indeed demonstrated to pass the blood-brain barrier and to reach the brain tissue (*e.g.* albiflorin, paeoniflorin and liquiritin), which may further explain the effect of FAEW on the central nervous system [256].

4.2.4 Summary and conclusion

In this study, we proved that FAEW exerted high activity against oxidative stress in human glioblastoma T98G and human neuroblastoma SH-SY5Y cell lines. The herbal mixture reduced both endogenous and exogenous ROS, strongly promoted NRF2 translocation to the nucleus in a KEAP1-dependent manner and, hence, caused elevated HO-1 levels. The underlying mechanism for FAEW against oxidative stress may be related to multiple compounds, which bound to KEAP1-NRF2 protein-protein interaction sites and lead to the release of NRF2 from KEAP1 and NRF2 translocation to the nucleus, implying FAEW might be clinically effective in the treatment of mental disorders through reducing oxidative stress.

4.3 Limitations and recommendations for future work

Free and Easy Wanderer is called *Xiao-Yao-Wan*, or *Xiao-Yao-San* in China, depending on the dosage forms it was made. On the market, FAEW is commonly sold by pills or powder, with the names *Xiao-Yao-Wan* and *Xiao-Yao-San*, respectively. It is constituted by *Radix Bupleuri Chinensis* (*Chai Hu*), *Radix Angelicae Sinensis* (*Dang Gui*), *Radix Paeoniae Lactiflorae* (*Bai Shao*), *Rhizoma Atractylodis Macrocephalae* (*Bai Zhu*), *Sclerotium Poriae Cocos* (*Fu Ling*), *Radix Glycyrrhizae Uralensis* (*Gan Cao*), *Herba Menthae Haplocalycis* (*Bo He*) and *Rhizoma Zingiberis Officinalis Recens* (*Sheng Jiang*).

FAEW contains doses of natural compounds, the ingredients that can be identified quite depend on the extraction method and isolation techniques. In my experiment, we used *Xiao-Yao-Wan* with the form of pills and ten compounds were identified by using HPLC/MS techniques. Although the quantity control of FAEW in Chinese Pharmacopeia only mentioned two ingredients paeoniflorin and albiforin, other approaches have been demonstrated to improve the identification and quality control for FAEW. A room-temperature super-extraction system (RTSES) was

applied to extract the major active components of FAEW and enhance their psycho-pharmacological effect by improving the regulation of blood glucose and increasing the insulin sensitivity in reserpine-induced anxiety and depression as well as activating cerebral 5-HT1A receptors [258]. Besides, capillary electrophoresis fingerprints was established to optimize applied to the background electrolyte in capillary zone electrophoresis and can be served as a novel reference to identify and control the quality of FAEW[259]. Therefore, other methods can be applied and compared to explore the active compounds in future studies.

In my studies, we performed biological experiments with the extract of FAEW *in vitro*. It demonstrated that FAEW is active against inflammation and oxidative stress, through inhibiting NFκB and activating KEAP1-NRF2/HO-1 pathway, repspectively, which might be one part of the future *in vivo* and clinical studies. Other activities of FAEW have been also reported. For example, FAEW improved depressive-like behavior in rats through modulation of β-arrestin 2-mediated pathways in hippocampus[260]. Another study indicated that FAEW treatment can effectively improve depressive-like behaviors in rats through inhibition of locus coeruleus-norepinephrine neurons activity[261]. FAEW has also been demonstrated to act against corticosterone-induced stress injury via upregulating glucocorticoid receptor reaction element transcriptional activity, and improve the anxiety-like behaviors of rats induced by chronic immobilization stress with the involvement of the JNK signaling pathway in the hippocampus [262, 263]. In addition, the endogenous metabolites in depressed patients treated with TCM formula FAEW were dynamically analyzed using urinary (1)H NMR-based metabolomics and the data suggested the involvement of energy metabolism, gut microbes, tryptophan metabolism and taurine metabolism[264]. A similar research on the plasma-metabolite-biomarkers for the therapeutic response in depressed patients by the traditional Chinese medicine formula FAEW confirmed the results[160]. The following experiment demontrated that FAEW could effectively adjust the gut dysbacteriosis in functional dyspepsia[265].

The limitations of my study can provide some hints for future studies. The conclusion that FAEW might be effective in the treatment of mental disorders through the activity against inflammation and oxidative stress is performed *in vitro*. An integrated investigations on the activity of FAEW *in vivo* and in clinic could be part of future work. FAEW is a poly-herb with multiple compounds, in our studies, only ten compounds were isolated due to the limitations of isolation methods. On one hand, standardized fingerprint methods could be applied to improve the quality and identify the active compounds of FAEW. On the other hand, future studies, should, therefore, focus on the individual roles of the identified compounds from FAEW and their binding modes to the proteins involved. Finally, more *in vivo* and clinical studies should be performed to validate the multiple targets of FAEW with respect to mental disorders such as PTSD and to explore the underlying mechanisms.

5 Material and Methods

5.1 Gene expression profiling and network analysis of PTSD patients

Gene expression profiling from PTSD patients were searched from Pubmed, GEO dataset and Google Scholar database. Among all the results, only four were related to our analysis with data available [161-164]. Among the datasets we have chosen for our study, three were derived from blood samples[161-163], and one was originated from *post mortem* collected brain tissue biopsies[164]. To allow comparisons between the four datasets, consistent fold-change ratios were calculated between the control and PTSD groups. Gene symbols (or IDs) and fold-change values were uploaded into the Ingenuity Pathway Analysis (IPA) software[266] to determine canonical signal transduction pathways, gene functions and signaling networks predicted by dysregulated gene expressions.

5.2 Binding motif search for transcription profiles in gene promoter sequences

Transcription factor binding site analyses were performed by the Cistrome analysis software [267]. Briefly, regulated genes were input and BED formats, a tab-delimited text file defining data lines displayed in an annotation track, were retrieved with an upstream setting (promoter region) at 2 kb[268]. SeqPos motif analyses were used to screen for enriched motifs in given regions (http://cistrome.org). Using SeqPos, we scanned all the motifs not only in Transfac, JASPAR, UniPROBE (pbm), hPDI database, but also attempted to identify de novo motifs using MDscan algorithm. The output of genes was ranked by -log10 (p-value).

5.3 Chemicals and equipment

FAEW and fluoxetine

The FAEW extract was prepared from commercial pills (Xiaoyao wan) purchased from Wanxi Pharmaceutical Company (Henan Province, China). Five bottles of FAEW pills were mixed and dissolved in H_2O：MeOH：DCM in a ratio of 1：4：5 for three days. A rotary evaporator was used to remove the solvents and the final extracts were stored at -20℃. Fluoxetine was purchased from Sigma-Aldrich (Steinheim, Germany).

Cell culture media, reagents and disposable material

Table 12. Cell culture media, reagents and disposable material

Product	**Supplier**
96-well, flat bottom cell culture microplate, clear, Nunclon®	Thermo Scientific, Germany
Cell culture flasks (25 cm^2), Nunclon®	Thermo Scientific, Germany
Cell culture flasks (75 cm^2), Nunclon®	Thermo Scientific, Germany
Cell scraper	Greiner Bio-One, Germany
Centrifuge tube (15 ml)	Sarstedt, Germany
Centrifuge tube (50 ml)	Sarstedt, Germany
Cover Glass 24 × 32 mm	VWR International, Austria
DMEM, High Glucose, GlutaMAXTM, Pyruvate	Life Technologies, Germany
DMEM/F-12	Life Technologies, Germany
DPBS, no calcium, no magnesium	Life Technologies, Germany
FACS tubes	BD Biosciences, USA; Sarstedt, Germany
Fetal Bovine Serum (FBS)	Life Technologies, Germany
HEK293 cell line	InvivoGen, USA
L-Glutamine	PAA Laboratories, Germany
Micro tubes (1.5 mL, 2.0 mL)	Sarstedt, Germany
Normocin™ - Antimicrobial Reagent	InvivoGen, USA
PCR plate sealing foils	Axon Labortechnik, Germany
PCR plates (384-well)	Axon Labortechnik, Germany
Penicillin (10000 U/mL) /Streptomycin (10000 µg/mL)	Life Technologies, Germany
Phytohemagglutinin M form	Life Technologies, Germany
Pipette tip (10, 200 and 1250 µL)	Sarstedt, Germany
Pipette with tip (5 and 10 mL)	Greiner BIO-ONE, Germany
Roti® PVDF blot membrane (0.45 µm)	Roth, Germany
Trypsin-EDTA 0.25% (1×), phenol red	Life Technologies, Germany
Zeocin™	InvivoGen, USA

Chemicals, dyes, antibodies and kits

Table 13. Chemicals, dyes, antibodies and kits

Product	**Supplier**
30% acrylamide/bis solution 29:1	Bio-Rad, Germany
5 × Hot Start Taq EvaGreen qPCR Mix (no ROX)	Axon Labortechnik, Germany
Ammonium persulfate (APS)	Sigma-Aldrich, Germany
Biotin-16-UTP	Roche, Germany
Bovine serum albumin (BSA)	Sigma-Aldrich, MO, USA
Bromophenol Blue	Merck, Germany
Catalase (D4P7B) XP® Rabbit mAb	Cell Signalling, Germany
c-Myc (D84C12) Rabbit mAb	Cell Signalling, Germany
Complete Mini Protease Inhibitor	Roche, Germany
Dimethyl sulfoxide (DMSO)	Sigma-Aldrich, Germany
Ethanol (EtOH)	Sigma-Aldrich, Germany
Glycerol	AppliChem, Germany
Glycine	AppliChem, Germany
HO-1 (D60G11) Rabbit mAb	Cell Signalling, Germany
HRP-linked anti-mouse IgG	Cell Signaling, Germany
HRP-linked anti-rabbit IgG	Cell Signaling, Germany
Hydrochloric Acid 37% (HCl)	AppliChem, Germany
Illumina® TotalPrep™ RNA Amplification Kit	Life Technologies, Germany
InviTrap® Spin Universal RNA Mini kit	STRATEC Biomedical, Germany
KEAP1 (D6B12) Rabbit mAb	Cell Signalling, Germany
LuminataTM Classico Western HRP substrate	Merck Millipore, Germany
Lamin A/C (4C11) Mouse mAb	Cell Signalling, Germany
MagicMark™ XP Western Standard	Life Technologies, CA, USA
MessageAmp II aRNA Amplification kit	Ambion, TX, USA
Methanol	J. T. Baker, NJ, USA
M-PER® Mammalian Protein Extraction Reagent	Thermo Scientific, IL, USA
NE-PER® Nuclear and Cytoplasmic Extraction Reagents	Thermo Scientific, IL, USA
NRF2 (D1Z9C) XP® Rabbit mAb	Cell Signalling, Germany

QUANTI-Blue™	InvivoGen, USA
Resazurin	Sigma-Aldrich, Germany
RevertAid H Minus First Strand cDNA Synthesis Kit	Thermo Scientific, Germany
RevertAid H Minus First Strand cDNA Synthesis Kit	Thermo Scientific, Germany
Sodium chloride (NaCl)	Grüssing, Germany
Sodium dodecyl sulfate (SDS)	J. T. Baker, NJ, USA
Sodium hydroxide (NaOH)	Sigma-Aldrich, Germany
TBP (D5G7Y) Rabbit mAb	Cell Signalling, Germany
Tetramethylethylenediamine (TEMED)	AppliChem, Germany
Tumor necrosis factor-α	Sino Biological Inc, China
TotalPrep™ RNA Amplification Kit	Life Technologies, Germany
Tween20	Sigma-Aldrich, Germany
Ultravision Quanto Detection System HRP	Thermo Scientific, Germany
β-Actin (13E5) rabbit mAb	Cell Signalling, Germany
β-Mercaptoethanol	AppliChem, Germany
Water, nuclease-free	Thermo Scientific, Germany

Technical equipment and software

Table 14. Technical equipment and software

Device	**Supplier**
Agilent 2100 Bioanalyzer	Agilent Technologies GmbH, Germany
Alpha Innotech FluorChem Q system	Biozym, Germany
AutoDock 4.2 software	Molecular Graphics Laboratory, CA, USA
AutoDockTools 1.5.6rc3 software	Molecular Graphics Laboratory, CA, USA
AutoGrid 4.2 software	Molecular Graphics Laboratory, CA, USA
BD Calibur Flow Cytometer	Becton-Dickinson Biosciences, CA, USA
BD CellQuest™ software	Becton-Dickinson Biosciences, CA, USA
BeadStudio software	Illumina Inc., CA, USA
C1000™ Thermal Cycler	Bio-Rad, Germany
Centrifuge 5424	Eppendorf, Germany
CFX384™ Real-Time PCR Detection System	Bio-Rad, Germany
ChemSketch	ACD, Canada
Chipster software	CSC, Finland
Coulter Counter Z1	Beckman Coulter, Germany

ENVAIR eco air V 0.8m vertical laminar flow workbench	ENVAIR, Germany
Eppendorf 8-channel electric pipette	Eppendrof, Germany
FlowJo software	FlowJo LLC, OR, USA
FluorChem® Q imaging system	Alpha Innotech, CA, USA
Forma Steri-Cult 3310 CO2-Incubator	Thermo Scientific, Germany
Heraeus Cytospin	Thermo Scientific, Germany
Heraeus Fresco 21 microcentrifuge	Thermo Scientific, Germany
Heraeus Labofuge 400 R centrifuge	Thermo Scientific, Germany
ImageJ 1.4.6	NIH, MD, USA
Illumina Human HT-12 v4 BeadChip array	Illumina Inc., CA, USA
Illumina BeadStation array scanner	Illumina Inc., CA, USA
Infinite M2000 Pro™ plate reader	Tecan, Germany
Ingenuity Pathway Analysis (IPA)	Ingenuity Systems Inc., CA, USA
Maxisafe 2020 laminar flow hood	Thermo Scientific, Germany
Microsoft Office	Microsoft Corporation, WA, USA
Milli-Q ultrapure water purification system	Millipore, Germany
Mini-PROTEAN® Tetra Cell	Bio-Rad, Germany
MODELLER 9.11	University of California, CA, USA
Molecular Operating Environment (MOE) 2012.10	Chemical Computing Group Inc., Canada
NanoDrop 1000 Spectrophotometer	PEQLAB, Germany
Neubauer counting chamber	Marienfeld, Germany
Optika XDS-2 trinocular inverted microscope	Optika, Italy
Precisa BJ2200C balance	Precisa Gravimetrics AG, Switzerland
PyMOL 1.3	Schroedinger LLC, USA
REAX 2000 vortexer	Heidolph, Germany
Safe 2020 Biological Safety Cabinets	Thermo Scientific, Germany
Sartorius R 160 P balance	Sartorius, Germany
Sonorex RK 102 H Ultrasonic Cleaning Unit	Babdelin, Germany
Spectrafuge™ Mini Centrifuge	Labnet, Germany
SUB Aqua 26 waterbath	Grant Scientific, Germany
Thermomixer comfort	Eppendorf, Germany
TopMix vortexer	Fisher Scientific, Germany
VMD 1.9 software	University of Illinois at Urbana Champaign, IL, USA

5.4 Cell cultures

5.4.1 T98G cell line

Human glioblastoma T98G cell line was obtained from the German Cancer Research Center (DKFZ, Heidelberg, Germany). The original source of these two cell lines is the American Type

Culture Collection (ATCC). Human glioblastoma T98G cell line was cultivated under standard conditions (37°C, 5% CO_2) in DMEM medium supplemented with 10% fetal bovine serum (Life Technologies, Darmstadt, Germany), 1% penicillin/streptomycin (Life Technologies, Darmstadt, Germany). Cells were passaged twice a week. All experiments were performed with logarithmically growing cells.

5.4.2 HEK 293 cell line

HEK293 cells stably expressing the HEK-Blue-Null vector and secreted embryonic alkaline phosphatase (SEAP) reporter gene on NF-κB promoter were purchased from Invivogen. The cells were cultured according to the recommendations from the company and passaged twice per week.

5.4.3 SH-SY5Y cell line

Human neuroblastoma SH-SY5Y cell line was obtained from University Medical Center of the Johannes Gutenberg University (Mainz, Germany). The original source of these two cell lines is the American Type Culture Collection (ATCC). Human neuroblastoma cell line SH-SY5Y was cultivated under standard conditions (37°C, 5% CO_2) in DMEM/F-12 (without phenol red, with 1% glutamine, Life Technologies, Darmstadt, Germany) supplemented with 10% fetal bovine serum. Cells were passaged twice a week. All experiments were performed with logarithmically growing cells.

5.5 Cytotoxicity assay

Cell viability was evaluated by resazurin assay. One hundred microliters of cell suspension with 5000 or 10000 cells per well (T98G and HEK293 cells: 5000 cells per well; SH-SY5Y cells: 10000 per well) were seeded into 96-well plates one day before the treatment with different concentrations of FAEW and fluoxetine. All these different concentrations of drugs were diluted with 200 fold medium from the stock solution. Distilled water was used as solvent control with the same dilution ratio. After 48 h, 20 µl resazurin (Sigma-Aldrich, Steinheim, Germany) 0.01% w/v in ddH2O was added to each well and the plates were incubated at 37℃ for 4 h. The fluorescence was measured with an Infinite M200 Proplate Reader (Tecan, Crailsheim, Germany) using an excitation wavelength of 544 nm and an emission wavelength of 590 nm. The toxicity of compounds was determined by means of the formula:

$$\text{Cell Viability (\% of control)} = \frac{\text{Absorption from sample well - absorption from medium}}{\text{Absorption from solvent treated cells - absorption from medium}} \times 100$$

The calculated cell viability (y-axis) was plotted against the log drug concentration (x-axis) using Microsoft Excel.

5.6 NF-κB reporter assay

HEK293 cells stably expressing the HEK-Blue-Null vector and secreted embryonic alkaline phosphatase (SEAP) reporter gene on NF-κB promoter were purchased from Invitrogen. The cells were cultured according to the recommendations from the company and passaged twice per week. The cells were treated with different concentrations of FAEW (60, 200, 600, 2000 µg/ml) and fluoxetine (2, 6, 20 µM) for 24, 48 or 72 h followed by TNF-α induction for 3 h. MG-132 was used as a positive control with treatment for only 1 h. The fluorescence was measured with an Infinite M200 Proplate Reader (Tecan, Crailsheim, Germany) with the wavelength of 630 nm. Background value caused by the medium was deducted for all the wells. The inhibition effects of FAEW and fluoxetine towards NF-κB activity were calculated by comparison with untreated TNF-α control.

5.7 Measurement of reactive oxygen species with flow cytometry

H_2DCFH-DA (Sigma-Aldrich, Steinheim, Germany) is an indicator dye used for the highly sensitive and quantifiable detection of ROS. H_2DCFH-DA is cleaved by cytoplasmic esterases into 2´, 7´-dichlorodihydrofluorescein (H_2DCF), if it diffuses into the cells. In the presence of hydrogen peroxide, H_2DCF is oxidized to the fluorescent molecule dichlorofluorescein (DCF) by peroxidases. The fluorescent signal emanating from DCF can be measured and quantified by flow cytometry [269-271]. Briefly, 2×10^5/well T98G cells or 4×10^5/well SH-SY5Y cells were cultured in 6-well plates, and FAEW extract and fluoxetine with different concentrations were added to the medium the day after the cells attached. Distilled water was used as solvent control.

After 24 h incubation, the medium was removed and the cells were washed three times with PBS, 10 µM H_2DCFH-DA was incubated for 30 min in the dark at 37 ℃. Subsequently, the cells were washed with PBS three times and resuspended in PBS containing hydrogen peroxide (H_2O_2, 200 µM) (Sigma-Aldrich, Steinheim, Germany) or only PBS, respectively, for 15 min. The samples were immediately measured in a FACS Calibur flow cytometer (Becton-Dickinson, Heidelberg, Germany). For each sample, 1×10^4 cells were counted. DCF was measured at 488 nm excitation and detected using a 530/30 nm bandpass filter. All parameters were plotted on a logarithmic scale. Cryptographs were analyzed using FlowJo software (Celeza). All experiments were performed at least in triplicate.

5.8 Microarray gene expression profiling

5.8.1 RNA isolation

T98G cells were treated with 200 µg/ml FAEW and 20 µM fluoxetine or distilled water as solvent control for 48 h, and H_2O_2 (200 µM) was added to induce oxidative stress for 6 h before total

RNA was isolated using InviTrap spin Universal RNA Mini kit (STRATEC Molecular, Berlin, Germany) according to the manufacturer's instruction. RNA concentrations were determined using a nanodrop spectrophotometer (Nanodrop Technologies, Thermo Fisher).

5.8.2 Probe labeling and hybridization

Microarray hybridizations were performed in duplicates for treated samples and for control samples by the Genomics and Proteomics Core Facility at the German Cancer Research Center (DKFZ, Heidelberg, Germany).

Briefly, 1 µg total RNA was used for complementary DNA (cDNA) synthesis, followed by an amplification/labeling step (in vitro transcription) to synthesize biotin-labeled cRNA according to the MessageAmp II aRNA Amplification kit (Ambion). Biotin-labeled cRNA samples for hybridization on Illumina Human HT-12 BeadChip arrays were prepared according to Illumina's recommended sample labeling procedure based on the modified Eberwine protocol [272]. The cRNA was column purified according to TotalPrep™ RNA Amplification Kit (Life Technologies) and eluted in 60-80 µL water. Hybridization was performed according to the manufacturer's instructions.

5.8.3 Scanning and data processing

Microarray scanning was done by the Genomics and Proteomics Core Facility at the German Cancer Research Center using an Illumina® BeadStation array scanner (Illumina), setting adjusted to a scaling factor of 1 and PMT settings at 430. Data was extracted for each individually, and outliers were removed, if the median absolute deviation (MAD) exceeded 2.5. Then, mean average signals and standard deviations were calculated for each probe. Data analysis was done by using the quantile normalization algorithm without background subtraction, and differentially regulated genes were defined by calculating the standard deviation differences of a given probe in a one-by-one comparison of samples or groups.

5.8.4 Data analysis

5.8.4.1 Chipster analysis

The expression data sets obtained were further filtered with Chipster software, which is an analysis platform for high-throughput data. It includes the steps that filtering of genes by two times standard deviation and a subsequent assessment of significance using empirical Bayes t-test ($p < 0.05$) with Bonferroni correction.

5.8.4.2 Ingenuity pathway analysis

Filtered genes were fed into Ingenuity Pathway Analysis software (IPA; Ingenuity Systems Inc.), which allows to integrate the experimental data to known biological and chemical interactions,

mechanisms and functions. It relies on the Ingenuity Knowledge Base, a frequently updated giant database of biological interactions and functional annotations gathered from literatures. Only molecules with an expression fold changes ≥ ±1.65 were used for IPA analysis. Core Analyses using the Core Analysis tool were performed for all datasets to determine cellular networks and functions associated with deregulated mRNA that affected by each drug treatment. The results of the core analyses were further studied using the comparison analysis tool, offering the possibility to compare datasets of samples treated by different compounds.

5.8.4.3 Real-time reverse transcription-PCR

Real-time RT-PCR was performed with the same samples used for microarray experiments. Total RNA samples were converted to cDNA with random hexamer primers by RevertAid H Minus First Strand cDNA Synthesis Kit (Thermo Scientific, Darmstadt, Germany). Oligonucleotides were synthesized by Eurofins MWG Operon (Ebersberg, Germany). The efficiency of all primer pairs used for real-time PCR expression was better than 90%. Quantification of cDNA was performed on CFX384 Real-Time PCR Detection System (Bio-Rad, München, Germany) using a Hot Start Taq EvaGreen qPCR Mix (Axon scientific, Göttingen, Germany). RT-PCR was performed with an initial denaturation at 95°C for 10 min followed by 40 cycles including strand separation at 95°C for 15 s, annealing at 57.5°C for 40 s and extension at 72°C for 1 min. After PCR product amplification, melting curves were computed. The expression levels were normalized to the transcription level of the housekeeping gene, *RPS13*. All samples were run in duplicates and the experiment was repeated once.

Table 15. Primers for the investigated genes

Genes	Forward Primer	Reverse Primer
GCLM	CTAGACAAAACACAGTTGGAACA	ATGCAGTCAAATCTGGTGGCAT
HMOX1	GCCAGCAACAAAGTGCAAGATTC	CACCAGAAAGCTGAGTGTAAGGAC
NFE2L2	GAGAGCCCAGTCTTCATTGC	TGCTCAATGTCCTGTTGCAT
KEAP1	CAACTTCGCTGAGCAGATTGGC	TGATGAGGGTCACCAGTTGGCA
MGST1	TGTACGCAGAGCCCACCT	GTAGATCCGTGCTCCGACAAATAG
ATF4	TGACCTGGAAACCATGCCAG	AATGATCTGGAGTGGAGGAC
TXNRD1	ACCCAATTAGGAGCTCTCAGC	GGCTAACTGCCAGAGTCAGAA
HERPUD1	CTAGATGGCGAGCAGACC	GAGTCAGGTGATCCAGTCC
RPS13	GGTTGAAGTTGACATCTGACGA	CTTGTGCAACACATGTGAAT

5.9 Analysis of protein expression by Western blotting

5.9.1 Sample preparation

For adherent cells, some amount of cells (16×10^4, 32×10^4, and 64×10^4 for 72h, 48h and 24h, respectively) were sowed into the wells of a small flask (Thermo Scientific) one day before treatment. The cells were washed twice with PBS after treated with the indicated concentrations of the compound of interest for 24 h, 48h and 72h. Lysis buffer (M-PER Mammalian Protein Extraction Reagent, Thermo Scientific, plus protease inhibitor, Roche) containing phosphatase inhibitor (Roche) was used to extract the total protein. After shaking 30 min at 4 °C, the lysate was centrifuged at 14,000 × g for 15 min. The nuclear protein extracts were prepared according to the NE-PER nuclear and cytoplasmic extraction reagent (Thermo Scientific, USA) supplemented with EDTA-free Halt Protease Inhibitor Cocktail (Thermo Scientific) according to the kit protocol. The supernatant was quantified by NanoDrop 1000 spectrophotometer. 45 µg protein were mixed with 4 µL 6 × sample loading buffer and H_2O to a final volume of 24 µL and denatured at 95°C for 10 min. All the proteins were stored for use in freezers.

5.9.2 SDS-PAGE and blotting

20 µL protein extracts were separated on SDS-PAGE (The gel concentrations depend on the protein molecular weight, 12% for Histone, the other proteins used 10% gels) and electro blotted onto a PVDF membrane using the Mini-PROTEAN® Tetra Cell system (Bio-Rad). 3 µL of Magic Mark Western Blot Standard protein ladder (Life Technologies) was loaded asides and run in parallel to estimate molecular weights of the protein. Samples were run through the stacking gel under 55 V and the voltage was increased up to 100 V and maintained till the end of electrophoresis. Then the separating samples were transferred to a Roti® PVDF blot membrane (Roth) by wet sandwich method at a 250 mA current for 2 h.

5.9.3 Antibody incubation and detection

After blotting, the membrane was first rinsed with TBST and then blocked with 5% (w/v) bovine serum albumin in TBST for 1 h at room temperature. The blocked membrane was subsequently incubated overnight at 4 °C with specific primary antibodies (Cell Signaling) that diluted 1：2000 in blocking solution. After washing for three times with TBST for 10 min, the membrane was incubated for 1 h at room temperature with HRP-conjugated secondary antibody (Cell Signaling) (1：3000 in blocking solution). After the membrane was washed with TBST (3 × 10 min), the immunoreactivity was revealed by use of a Luminata Classico Western HRP Substrate (Millipore Corporation), and the densities of the protein bands were quantified by FluorChem Q software (Biozym Scientific Company). β-actin served as the internal control for total and

cytoplasmic protein. Histone, TATA-binding protein (TBP) and Lamin A/C levels served as the internal control for nuclear protein.

5.10 Chromatography analysis

5.10.1 Isolation of compounds from FAEW

The FAEW extract (2 g) was dissolved in DMSO and bound to 2 g of C18 material (Merck Lichroprep RP-18, 25-40 µm), which was then dried by lyophilization. Solid phase extraction (Agilent MegaBE-C18, 10 g) was performed by using a step gradient. The first fraction was eluted with 100% H_2O and discarded. Intermediate I (227.5 mg) was eluted with 15% MeCN and intermediate II (81.9 mg) with 30% MeCN. Preparative HPLC with intermediate I (MeCN/H_2O with 0.1% TFA gradient, 5% MeCN to 25% MeCN in 40 min, 21.2 ml/min, Agilent Eclipse XDB-Phenyl, 5 µm, 21.2 × 150 mm) yielded FAEW-1 (3.2 mg, RT 18-18.5 min), FAEW-2 (18.3 mg, RT 18.75-19.5 min), FAEW-3 (6.4 mg, RT 27.75 min), and FAEW-4 (1.1 mg, RT 36 min). FAEW-5 (2.3 mg, RT 15.5 min), FAEW-6 (1.9 mg, RT 20.6 min), FAEW-7 (2.1 mg, RT 22.3 mg), FAEW-8 (1.3 mg, RT 27.3 min), and FAEW-9 (1.0 mg, RT 31.8 min) were isolated by semi-preparative HPLC with intermediate II (MeCN / H_2O with 0.1% TFA gradient, 17% MeCN to 33.2 % MeCN in 38 min, 4 ml/min, Agilent Eclipse XDB-Phenyl, 5 µm, 9.4 × 250 mm).

5.10.2 Structure identification

NMR and MS methods were used to identify the structures of the isolated compounds, the method and results were attached as **supplementary information**.

5.11 Molecular Docking

Ten compounds identified in the FAEW extract (albiflorin, paeoniflorin, baicalin, 1- (2, 4-dihydroxyphenyl) - 3 - hydroxyl - 3 - (4 - hydroxyphenyl) - 1 - propanone (β - hydroxyl - DHP), ononin, isoliquiritin, isoliquiritin apioside, liquiritin, oroxyloside, pentagalloyl-β-D-glucose) were selected for the *in silico* molecular docking analyses together with the anti-depressant drug fluoxetine and the known KEAP1 inhibitor, *N*, *N* '- naphthalene - 1, 4 - diylbis (4 - methoxybenzenesulfonamide) (PubChem ID: IQK) [115] in order to compare their binding affinity and docking poses on KEAP1. The known inhibitor for IκK, MG-132 (PubChem ID: 462382) was selected as a standard to compare its binding modes with other compounds [273]. The PDB structure file of the protein was downloaded from RCSB Protein Data Bank (http://www.rcsb.org/pdb/home/home.do). All bound water molecules and ligands were eliminated from the protein and polar hydrogen was added. 3D structures of these compounds were downloaded from PubChem, ChemSpider was used to convert mol files to pdb file after checking absolute and relative configuration. Molecular docking was then carried out with

AutoDock 4.2 (The Scripps Research Institute, La Jolla, CA) following a protocol previously reported by us[274]. Docking parameters were set to 250 runs and 25,000,000 energy evaluations for each cycle. VMD (Visual Molecular Dynamics) was used for visualization of the binding modes obtained from docking. The average of the lowest binding energy of three runs was taken into account.

5.12 Literature search

The PubMed database was searched with the corresponding compound name as the key word. Identified literature was classified into *in vitro*, *in vivo* or clinical studies to give a retrospective summary of the current state of knowledge. To search the published studies of the compounds from FAEW on NF-κB or ROS, NF-κB and the corresponding compound name were used as the key words.

6 Reference

1. Cavanagh, S.R., E.J. Fitzgerald, and H.L. Urry, *Emotion reactivity and regulation are associated with psychological functioning following the 2011 earthquake, tsunami, and nuclear crisis in Japan.* Emotion, 2014. **14**(2): p. 235.
2. McLean, C.P., et al., *Trauma characteristics and posttraumatic stress disorder among adolescent survivors of childhood sexual abuse.* Journal of family violence, 2014. **29**(5): p. 559-566.
3. Weaver, T.L., M.G. Griffin, and E.R. Mitchell, *Symptoms of posttraumatic stress, depression, and body image distress in female victims of physical and sexual assault: exploring integrated responses.* Health care for women international, 2014. **35**(4): p. 458-475.
4. Kessler, R.C., et al., *Lifetime prevalence and age-of-onset distributions of DSM-IV disorders in the National Comorbidity Survey Replication.* Arch Gen Psychiatry, 2005. **62**(6): p. 593-602.
5. Ditlevsen, D.N. and A. Elklit, *Gender, trauma type, and PTSD prevalence: a re-analysis of 18 nordic convenience samples.* Ann Gen Psychiatry, 2012. **11**(1): p. 26.
6. Armour, C., et al., *The DSM-5 dissociative-PTSD subtype: Can levels of depression, anxiety, hostility, and sleeping difficulties differentiate between dissociative-PTSD and PTSD in rape and sexual assault victims?* Journal of anxiety disorders, 2014. **28**(4): p. 418-426.
7. Küçükoğlu, S., N. Yıldırım, and O.B. Dursun, *Posttraumatic stress symptoms seen in children within the 3‐month period after the Van earthquake in Turkey.* International journal of nursing practice, 2015. **21**(5): p. 542-549.
8. St Leger, A., *A Dictionary of Epidemiology.* Journal of epidemiology and community health, 2001. **50**(2): p. 229.
9. Jekel, J.F., et al., *Epidemiology, biostatistics and preventive medicine*. 2007: Elsevier Health Sciences.
10. Kessler, R.C., et al., *Lifetime prevalence and age-of-onset distributions of DSM-IV disorders in the National Comorbidity Survey Replication.* Archives of general psychiatry, 2005. **62**(6): p. 593-602.
11. Kessler, R.C., et al., *Prevalence, severity, and comorbidity of 12-month DSM-IV disorders in the National Comorbidity Survey Replication.* Archives of general psychiatry, 2005. **62**(6): p. 617-627.
12. Chen, H., et al., *The presence of post-traumatic stress disorder symptoms in earthquake survivors one month after a mudslide in southwest China.* Nurs Health Sci, 2014. **16**(1): p. 39-45.
13. Wang, B., et al., *Posttraumatic stress disorder 1 month after 2008 earthquake in China: Wenchuan earthquake survey.* Psychiatry Res, 2011. **187**(3): p. 392-6.
14. Zhang, Z., et al., *One year later: Mental health problems among survivors in hard-hit areas of the Wenchuan earthquake.* Public Health, 2011. **125**(5): p. 293-300.
15. Wen, J., et al., *Quality of life, physical diseases, and psychological impairment among survivors 3 years after Wenchuan earthquake: a population based survey.* PLoS One, 2012. **7**(8): p. e43081.
16. Chen, G., H. Shen, and G. Chen, *A cross-sectional study on posttraumatic stress disorder among elderly Qiang citizens 3 years after the Wenchuan earthquake in China.* Can J Psychiatry, 2012. **57**(9): p. 547-53.

17. Lau, J.T., et al., *Psychological distress among adolescents in Chengdu, Sichuan at 1 month after the 2008 Sichuan earthquake.* J Urban Health, 2010. **87**(3): p. 504-23.

18. Yu, X.N., et al., *Posttraumatic growth and reduced suicidal ideation among adolescents at month 1 after the Sichuan Earthquake.* J Affect Disord, 2010. **123**(1-3): p. 327-31.

19. Fan, F., et al., *Symptoms of posttraumatic stress disorder, depression, and anxiety among adolescents following the 2008 Wenchuan earthquake in China.* J Trauma Stress, 2011. **24**(1): p. 44-53.

20. Ma, X., et al., *Risk indicators for post-traumatic stress disorder in adolescents exposed to the 5.12 Wenchuan earthquake in China.* Psychiatry Res, 2011. **189**(3): p. 385-91.

21. Wang, W., et al., *Prevalence of PTSD and depression among junior middle school students in a rural town far from the epicenter of the Wenchuan earthquake in China.* PLoS One, 2012. **7**(7): p. e41665.

22. Fu, Y., et al., *Analysis of prevalence of PTSD and its influencing factors among college students after the Wenchuan earthquake.* Child Adolesc Psychiatry Ment Health, 2013. **7**(1): p. 1.

23. Ying, L.H., et al., *Prevalence and predictors of posttraumatic stress disorder and depressive symptoms among child survivors 1 year following the Wenchuan earthquake in China.* Eur Child Adolesc Psychiatry, 2013. **22**(9): p. 567-75.

24. Pan, X., et al., *Symptoms of Posttraumatic Stress Disorder, Depression, and Anxiety Among Junior High School Students in Worst-Hit Areas 3 Years After the Wenchuan Earthquake in China.* Asia Pac J Public Health, 2013.

25. Liu, M., et al., *Mental health problems among children one-year after Sichuan earthquake in China: a follow-up study.* PLoS One, 2011. **6**(2): p. e14706.

26. Liu, Z.Y., et al., *One-year follow-up study of post-traumatic stress disorder among adolescents following the Wen-Chuan earthquake in China.* Biosci Trends, 2010. **4**(3): p. 96-102.

27. Zhang, Z., et al., *Prevalence of post-traumatic stress disorder among adolescents after the Wenchuan earthquake in China.* Psychol Med, 2012. **42**(8): p. 1687-93.

28. Yang, Y.F., et al., *[A follow-up study on the post-traumatic stress disorders among middle school students in Wenchuan earthquake region].* Zhonghua Yu Fang Yi Xue Za Zhi, 2011. **45**(4): p. 354-8.

29. Zhu, C.Z., et al., *[Influence factors of post-traumatic stress disorder (PTSD) and depression symptoms in children and adolescents after Wenchuan earthquake in China].* Zhonghua Yu Fang Yi Xue Za Zhi, 2011. **45**(6): p. 531-6.

30. Wang, L., et al., *Symptoms of posttraumatic stress disorder among adult survivors two months after the Wenchuan earthquake.* Psychol Rep, 2009. **105**(3 Pt 1): p. 879-85.

31. Zhou, X., et al., *Prevalence and risk factors of post-traumatic stress disorder among adult survivors six months after the Wenchuan earthquake.* Compr Psychiatry, 2013. **54**(5): p. 493-9.

32. Chan, C.L., et al., *Posttraumatic stress disorder symptoms among adult survivors of the 2008 Sichuan earthquake in China.* J Trauma Stress, 2011. **24**(3): p. 295-302.

33. Jin, Y., et al., *Posttraumatic stress disorder and posttraumatic growth among adult survivors of Wenchuan earthquake after 1 year: prevalence and correlates.* Arch Psychiatr Nurs, 2014. **28**(1): p. 67-73.

34. Xu, J. and Q. Liao, *Prevalence and predictors of posttraumatic growth among adult survivors one year following 2008 Sichuan earthquake.* J Affect Disord, 2011. **133**(1-2): p. 274-80.

35. Guo, J., et al., *Post-traumatic stress disorder among adult survivors of the Wenchuan earthquake in China: a repeated cross-sectional study.* J Anxiety Disord, 2014. **28**(1): p. 75-82.

36. Wang, L., et al., *Symptoms of posttraumatic stress disorder among health care workers in earthquake-affected areas in southwest China.* Psychol Rep, 2010. **106**(2): p. 555-61.

37. Tian, F., et al., *Psychological and behavioural impacts of the 2008 China earthquake on blood donors.* Vox Sang, 2010. **99**(2): p. 142-8.

38. Qu, Z., et al., *Posttraumatic stress disorder and depression among new mothers at 8 months later of the 2008 Sichuan earthquake in China.* Arch Womens Ment Health, 2012. **15**(1): p. 49-55.

39. Zhang, Z., et al., *Post-traumatic stress disorder, anxiety and depression among the elderly: a survey of the hard-hit areas a year after the Wenchuan earthquake.* Stress Health, 2012. **28**(1): p. 61-8.

40. Qu, Z., et al., *The impact of the catastrophic earthquake in China's Sichuan province on the mental health of pregnant women.* J Affect Disord, 2012. **136**(1-2): p. 117-23.

41. Hong, C. and T. Efferth, *Systematic review on post-traumatic stress disorder among survivors of the wenchuan earthquake.* Trauma, Violence, & Abuse, 2016. **17**(5): p. 542-561.

42. Glynn, L.M., E.P. Davis, and C.A. Sandman, *New insights into the role of perinatal HPA-axis dysregulation in postpartum depression.* Neuropeptides, 2013. **47**(6): p. 363-70.

43. Maniam, J., C. Antoniadis, and M.J. Morris, *Early-Life Stress, HPA Axis Adaptation, and Mechanisms Contributing to Later Health Outcomes.* Front Endocrinol (Lausanne), 2014. **5**: p. 73.

44. Nicolaides, N.C., et al., *Circadian endocrine rhythms: the hypothalamic-pituitary-adrenal axis and its actions.* Ann N Y Acad Sci, 2014. **1318**: p. 71-80.

45. Amstadter, A.B., et al., *Corticotrophin-releasing hormone type 1 receptor gene (CRHR1) variants predict posttraumatic stress disorder onset and course in pediatric injury patients.* Dis Markers, 2011. **30**(2-3): p. 89-99.

46. White, S., et al., *Association of CRHR1 variants and posttraumatic stress symptoms in hurricane exposed adults.* J Anxiety Disord, 2013. **27**(7): p. 678-83.

47. Wolf, E.J., et al., *Corticotropin releasing hormone receptor 2 (CRHR-2) gene is associated with decreased risk and severity of posttraumatic stress disorder in women.* Depress Anxiety, 2013. **30**(12): p. 1161-9.

48. Horn, C.A., et al., *Linking plasma cortisol levels to phenotypic heterogeneity of posttraumatic stress symptomatology.* Psychoneuroendocrinology, 2014. **39**: p. 88-93.

49. Lehrner, A., et al., *Maternal PTSD associates with greater glucocorticoid sensitivity in offspring of Holocaust survivors.* Psychoneuroendocrinology, 2014. **40**: p. 213-20.

50. Peters, J., P.W. Kalivas, and G.J. Quirk, *Extinction circuits for fear and addiction overlap in prefrontal cortex.* Learning & memory, 2009. **16**(5): p. 279-288.

51. Olszewski, T.M. and J.F. Varrasse, *The neurobiology of PTSD: implications for nurses.* J Psychosoc Nurs Ment Health Serv, 2005. **43**(6): p. 40-7.

52. Norrholm, S.D., et al., *Differential Genetic and Epigenetic Regulation of catechol-O-methyltransferase is Associated with Impaired Fear Inhibition in Posttraumatic Stress Disorder.* Front Behav Neurosci, 2013. **7**: p. 30.

53. Roth, T.L., et al., *Epigenetic modification of hippocampal Bdnf DNA in adult rats in an animal model of post-traumatic stress disorder.* J Psychiatr Res, 2011. **45**(7): p. 919-26.

54. Rusiecki, J.A., et al., *PTSD and DNA Methylation in Select Immune Function Gene Promoter Regions: A Repeated Measures Case-Control Study of U.S. Military Service Members.* Front Psychiatry, 2013. **4**: p. 56.

55. Luster, A.D., R. Alon, and U.H. von Andrian, *Immune cell migration in inflammation: present and future therapeutic targets.* Nature immunology, 2005. **6**(12): p. 1182-1190.

56. Rabin, B.S., *Stress, immune function, and health: The connection*. 1999: Wiley-Liss.

57. Glaser, R. and J.K. Kiecolt-Glaser, *Stress-induced immune dysfunction: implications for health.* Nature Reviews Immunology, 2005. **5**(3): p. 243-251.

58. Howren, M.B., D.M. Lamkin, and J. Suls, *Associations of depression with C-reactive protein, IL-1, and IL-6: a meta-analysis.* Psychosomatic medicine, 2009. **71**(2): p. 171-186.

59. Gimeno, D., et al., *Associations of C-reactive protein and interleukin-6 with cognitive symptoms of depression: 12-year follow-up of the Whitehall II study.* Psychological medicine, 2009. **39**(3): p. 413-423.

60. Ghosh, S., M.J. May, and E.B. Kopp, *NF-κB and Rel proteins: evolutionarily conserved mediators of immune responses.* Annual review of immunology, 1998. **16**(1): p. 225-260.

61. Bonizzi, G. and M. Karin, *The two NF-κB activation pathways and their role in innate and adaptive immunity.* Trends in immunology, 2004. **25**(6): p. 280-288.

62. Gilmore, T.D., *The Rel/NF-kB signal transduction pathway: introduction.* Oncogene, 1999. **18**(49): p. 6842-6844.

63. Kunsch, C., S.M. Ruben, and C.A. Rosen, *Selection of optimal kappa B/Rel DNA-binding motifs: interaction of both subunits of NF-kappa B with DNA is required for transcriptional activation.* Molecular and cellular biology, 1992. **12**(10): p. 4412-4421.

64. Chen-Ming, F. and T. Maniatis, *Generation of p50 Subunit of NF-(Kappa) B by Processing of p105 Through an ATP-Dependent Pathway.* Nature, 1991. **354**(6352): p. 395.

65. Betts, J.C. and G.J. Nabel, *Differential regulation of NF-kappaB2 (p100) processing and control by amino-terminal sequences.* Molecular and cellular biology, 1996. **16**(11): p. 6363-6371.

66. Schmitz, M.L. and P.A. Baeuerle, *The p65 subunit is responsible for the strong transcription activating potential of NF-kappa B.* The EMBO journal, 1991. **10**(12): p. 3805.

67. Chen, F.E. and G. Ghosh, *Regulation of DNA binding by Rel/NF-kB transcription factors: structural views.* Oncogene, 1999. **18**(49): p. 6845-6852.

68. Urban, M.B. and P.A. Baeuerle, *The 65-kD subunit of NF-kappa B is a receptor for I kappa B and a modulator of DNA-binding specificity.* Genes & Development, 1990. **4**(11): p. 1975-1984.

69. Chow, J.C., et al., *Toll-like receptor-4 mediates lipopolysaccharide-induced signal transduction.* Journal of Biological Chemistry, 1999. **274**(16): p. 10689-10692.

70. Gil, J., J. Alcami, and M. Esteban, *Activation of NF-kB by the dsRNA-dependent protein kinase, PKR involves the IkB kinase complex.* Oncogene, 2000. **19**(11): p. 1369-1378.

71. Hoshino, T., R.H. Wiltrout, and H.A. Young, *IL-18 is a potent coinducer of IL-13 in NK and T cells: a new potential role for IL-18 in modulating the immune response.* The Journal of Immunology, 1999. **162**(9): p. 5070-5077.

72. Li, X.-J., et al., *Xiaoyaosan exerts anxiolytic-like effects by down-regulating the TNF-α/JAK2-STAT3 pathway in the rat hippocampus.* Scientific Reports, 2017. **7**.

73. Durand, J.K. and A.S. Baldwin, *Targeting IKK and NF-kappaB for Therapy.* (1876-1623 (Print)).

74. Liu, F., et al., *IKK biology.* Immunological reviews, 2012. **246**(1): p. 239-253.

75. Kanarek, N. and Y. Ben‐Neriah, *Regulation of NF‐κB by ubiquitination and degradation of the IκBs.* Immunological reviews, 2012. **246**(1): p. 77-94.

76. Chen, Z.J., L. Parent, and T. Maniatis, *Site-specific phosphorylation of IκBα by a novel ubiquitination-dependent protein kinase activity.* Cell, 1996. **84**(6): p. 853-862.

77. Yamaoka, S., et al., *Complementation cloning of NEMO, a component of the IκB kinase complex essential for NF-κB activation.* Cell, 1998. **93**(7): p. 1231-1240.

78. Regnier, C.H., et al., *Identification and characterization of an IkappaB kinase.* (0092-8674 (Print)).

79. Woronicz, J.D., et al., *IkappaB kinase-beta: NF-kappaB activation and complex formation with IkappaB kinase-alpha and NIK.* (0036-8075 (Print)).

80. Mercurio, F., et al., *IKK-1 and IKK-2: cytokine-activated IκB kinases essential for NF-κB activation.* Science, 1997. **278**(5339): p. 860-866.

81. Ling, L., D.V. Cao Z Fau - Goeddel, and D.V. Goeddel, *NF-kappaB-inducing kinase activates IKK-alpha by phosphorylation of Ser-176.* (0027-8424 (Print)).

82. Bassères, D.S., et al., *Requirement of the NF-κB subunit p65/RelA for K-Ras–induced lung tumorigenesis.* Cancer research, 2010. **70**(9): p. 3537-3546.

83. Rushe, M., et al., *Structure of a NEMO/IKK-associating domain reveals architecture of the interaction site.* Structure, 2008. **16**(5): p. 798-808.

84. Marienfeld, R.B., L. Palkowitsch, and S. Ghosh, *Dimerization of the IκB kinase-binding domain of NEMO is required for tumor necrosis factor alpha-induced NF-κB activity.* Molecular and cellular biology, 2006. **26**(24): p. 9209-9219.

85. May, M.J., S. Marienfeld Rb Fau - Ghosh, and S. Ghosh, *Characterization of the Ikappa B-kinase NEMO binding domain.* (0021-9258 (Print)).

86. Schomer-Miller, B., et al., *Regulation of IkappaB kinase (IKK) complex by IKKgamma-dependent phosphorylation of the T-loop and C terminus of IKKbeta.* (0021-9258 (Print)).

87. Strickland, I. and S. Ghosh, *Use of cell permeable NBD peptides for suppression of inflammation.* Annals of the rheumatic Diseases, 2006. **65**(suppl 3): p. iii75-iii82.

88. Cross, S.A., et al., *Dimethyl fumarate, an immune modulator and inducer of the antioxidant response, suppresses HIV replication and macrophage-mediated neurotoxicity: a novel candidate for HIV neuroprotection.* The Journal of Immunology, 2011. **187**(10): p. 5015-5025.

89. Kastrati, I., et al., *Dimethyl fumarate inhibits the nuclear factor κB pathway in breast cancer cells by covalent modification of p65 protein.* Journal of Biological Chemistry, 2016. **291**(7): p. 3639-3647.

90. Karin, M., Y. Yamamoto, and Q.M. Wang, *The IKK NF-κB system: a treasure trove for drug development.* Nature reviews Drug discovery, 2004. **3**(1): p. 17-26.

91. Flint, M.S., et al., *Genomic profiling of restraint stress-induced alterations in mouse T lymphocytes.* Journal of neuroimmunology, 2005. **167**(1): p. 34-44.

92. Ng, F., et al., *Oxidative stress in psychiatric disorders: evidence base and therapeutic implications.* International Journal of Neuropsychopharmacology, 2008. **11**(6): p. 851-876.

93. Wilson, C.B., et al., *Inflammation and oxidative stress are elevated in the brain, blood, and adrenal glands during the progression of post-traumatic stress disorder in a predator exposure animal model.* PLoS One, 2013. **8**(10): p. e76146.

94. Logue, M.W., et al., *A genome-wide association study of post-traumatic stress disorder identifies the retinoid-related orphan receptor alpha (RORA) gene as a significant risk locus.* Molecular psychiatry, 2013. **18**(8): p. 937-942.

95. Miller, M.W., et al., *A novel locus in the oxidative stress-related gene ALOX12 moderates the association between PTSD and thickness of the prefrontal cortex.* Psychoneuroendocrinology, 2015. **62**: p. 359-65.

96. Bouvier E, B.F., Molet J, Claverie D, Cabungcal JH, Cresto N, Doligez N, Rivat C, Do KQ, Bernard C, Benoliel JJ, Becker C, *Nrf2-dependent persistent oxidative stress results in stress-induced vulnerability to depression.* Mol Psychiatry, 2016(1476-5578 (Electronic)).

97. Itoh, K., et al., *Keap1 represses nuclear activation of antioxidant responsive elements by Nrf2 through binding to the amino-terminal Neh2 domain.* Genes & development, 1999. **13**(1): p. 76-86.

98. Loboda, A., et al., *Role of Nrf2/HO-1 system in development, oxidative stress response and diseases: an evolutionarily conserved mechanism.* Cell Mol Life Sci, 2016. **73**(17): p. 3221-47.

99. Jiang, Z.-Y., M.-C. Lu, and Q.-D. You, *Discovery and Development of Kelch-like ECH-Associated Protein 1. Nuclear Factor Erythroid 2-Related Factor 2 (KEAP1: NRF2) Protein–Protein Interaction Inhibitors: Achievements, Challenges, and Future Directions.* Journal of Medicinal Chemistry, 2016. **59**(24): p. 10837-10858.

100. Fourquet, S., et al., *Activation of NRF2 by nitrosative agents and H2O2 involves KEAP1 disulfide formation.* J Biol Chem, 2010. **285**(11): p. 8463-71.

101. Suzuki, T., H. Motohashi, and M. Yamamoto, *Toward clinical application of the Keap1-Nrf2 pathway.* Trends Pharmacol Sci, 2013. **34**(6): p. 340-6.

102. Deshmukh, P., et al., *The Keap1–Nrf2 pathway: promising therapeutic target to counteract ROS-mediated damage in cancers and neurodegenerative diseases.* Biophysical reviews, 2017: p. 1-16.

103. Kang, M.-I., et al., *Scaffolding of Keap1 to the actin cytoskeleton controls the function of Nrf2 as key regulator of cytoprotective phase 2 genes.* Proceedings of the National Academy of Sciences, 2004. **101**(7): p. 2046-2051.

104. Tong, K.I., et al., *Two-site substrate recognition model for the Keap1-Nrf2 system: a hinge and latch mechanism.* Biological chemistry, 2006. **387**(10/11): p. 1311-1320.

105. Beamer, L.J., et al., *Conserved solvent and side-chain interactions in the 1.35 Angstrom structure of the Kelch domain of Keap1.* Acta Crystallogr D Biol Crystallogr, 2005. **61**(Pt 10): p. 1335-42.

106. Horer, S., et al., *Crystal-contact engineering to obtain a crystal form of the Kelch domain of human Keap1 suitable for ligand-soaking experiments.* Acta Crystallogr Sect F Struct Biol Cryst Commun, 2013. **69**(Pt 6): p. 592-6.

107. Lo, S.C., et al., *Structure of the Keap1:Nrf2 interface provides mechanistic insight into Nrf2 signaling.* EMBO J, 2006. **25**(15): p. 3605-17.

108. Tong, K.I., et al., *Different electrostatic potentials define ETGE and DLG motifs as hinge and latch in oxidative stress response.* Mol Cell Biol, 2007. **27(21)**(0270-7306 (Print)): p. 7511-21.

109. D'Autréaux, B. and M.B. Toledano, *ROS as signalling molecules: mechanisms that generate specificity in ROS homeostasis.* Nature reviews Molecular cell biology, 2007. **8**(10): p. 813-824.

110. Haroon, E., et al., *Conceptual convergence: increased inflammation is associated with increased basal ganglia glutamate in patients with major depression.* Molecular psychiatry, 2016. **21**(10): p. 1351-1357.

111. Wong, M., et al., *Inflammasome signaling affects anxiety-and depressive-like behavior and gut microbiome composition.* Molecular psychiatry, 2016. **21**(6): p. 797-805.

112. Lee, J.-M. and J.A. Johnson, *An important role of Nrf2-ARE pathway in the cellular defense mechanism.* BMB Reports, 2004. **37**(2): p. 139-143.

113. Taguchi, K., H. Motohashi, and M. Yamamoto, *Molecular mechanisms of the Keap1–Nrf2 pathway in stress response and cancer evolution.* Genes to Cells, 2011. **16**(2): p. 123-140.

114. Cleasby, A., et al., *Structure of the BTB domain of Keap1 and its interaction with the triterpenoid antagonist CDDO.* PloS one, 2014. **9**(6): p. e98896.

115. Marcotte, D., et al., *Small molecules inhibit the interaction of Nrf2 and the Keap1 Kelch domain through a non-covalent mechanism.* Bioorganic & medicinal chemistry, 2013. **21**(14): p. 4011-4019.

116. Sun, H.-P., et al., *Novel protein–protein interaction inhibitor of Nrf2–Keap1 discovered by structure-based virtual screening.* MedChemComm, 2014. **5**(1): p. 93-98.

117. Lu, M.C., et al., *The Keap1-Nrf2-ARE Pathway As a Potential Preventive and Therapeutic Target: An Update.* Med Res Rev, 2016. **36**(5): p. 924-63.

118. Ehlers, A., et al., *Do all psychological treatments really work the same in posttraumatic stress disorder?* Clin Psychol Rev, 2010. **30**(2): p. 269-76.

119. Goncalves, R., et al., *Efficacy of virtual reality exposure therapy in the treatment of PTSD: a systematic review.* PLoS One, 2012. **7**(12): p. e48469.

120. Wu, S., et al., *A new psychological intervention: "512 Psychological Intervention Model" used for military rescuers in Wenchuan Earthquake in China.* Soc Psychiatry Psychiatr Epidemiol, 2012. **47**(7): p. 1111-9.

121. Wang, Z., J. Wang, and A. Maercker, *Chinese My Trauma Recovery, a Web-based intervention for traumatized persons in two parallel samples: randomized controlled trial.* J Med Internet Res, 2013. **15**(9): p. e213.

122. Chen, Y., et al., *Effectiveness RCT of a CBT intervention for youths who lost parents in the Sichuan, China, earthquake.* Psychiatr Serv, 2014. **65**(2): p. 259-62.

123. Zang, Y., N. Hunt, and T. Cox, *A randomised controlled pilot study: the effectiveness of narrative exposure therapy with adult survivors of the Sichuan earthquake.* BMC Psychiatry, 2013. **13**: p. 41.

124. Jiang, R.F., et al., *Interpersonal psychotherapy versus treatment as usual for PTSD and depression among Sichuan earthquake survivors: a randomized clinical trial.* Confl Health, 2014. **8**: p. 14.

125. Jeffreys, M., B. Capehart, and M.J. Friedman, *Pharmacotherapy for posttraumatic stress disorder: review with clinical applications.* J Rehabil Res Dev, 2012. **49**(5): p. 703-15.

126. Ipser, J.C. and D.J. Stein, *Evidence-based pharmacotherapy of post-traumatic stress disorder (PTSD).* Int J Neuropsychopharmacol, 2012. **15**(6): p. 825-40.

127. Kerbage, H. and S. Richa, *Non-Antidepressant Long-Term Treatment in Post-Traumatic Stress Disorder (PTSD).* Curr Clin Pharmacol, 2013.

128. Brady, K., et al., *Efficacy and safety of sertraline treatment of posttraumatic stress disorder: a randomized controlled trial.* Jama, 2000. **283**(14): p. 1837-44.

129. Brady, K.T. and C.M. Clary, *Affective and anxiety comorbidity in post-traumatic stress disorder treatment trials of sertraline.* Compr Psychiatry, 2003. **44**(5): p. 360-9.

130. Robb, A.S., et al., *Sertraline treatment of children and adolescents with posttraumatic stress disorder: a double-blind, placebo-controlled trial.* J Child Adolesc Psychopharmacol, 2010. **20**(6): p. 463-71.

131. Catani, C., et al., *Treating children traumatized by war and Tsunami: a comparison between exposure therapy and meditation-relaxation in North-East Sri Lanka.* BMC Psychiatry, 2009. **9**: p. 22.

132. Descilo, T., et al., *Effects of a yoga breath intervention alone and in combination with an exposure therapy for post-traumatic stress disorder and depression in survivors of the 2004 South-East Asia tsunami.* Acta Psychiatr Scand, 2010. **121**(4): p. 289-300.

133. Rosenthal, J.Z., et al., *Effects of transcendental meditation in veterans of Operation Enduring Freedom and Operation Iraqi Freedom with posttraumatic stress disorder: a pilot study.* Mil Med, 2011. **176**(6): p. 626-30.

134. Kim, S.H., et al., *Mind-body practices for posttraumatic stress disorder.* J Investig Med, 2013. **61**(5): p. 827-34.

135. Bormann, J.E., et al., *Spiritual wellbeing mediates PTSD change in veterans with military-related PTSD.* Int J Behav Med, 2012. **19**(4): p. 496-502.

136. Grodin, M.A., et al., *Treating survivors of torture and refugee trauma: a preliminary case series using qigong and t'ai chi.* J Altern Complement Med, 2008. **14**(7): p. 801-6.

137. Zhu, Z., et al., *Effect of calligraphy training on hyperarousal symptoms for childhood survivors of the 2008 China earthquakes.* Neuropsychiatr Dis Treat, 2014. **10**: p. 977-985.

138. Khandelwal, A., V.M. Crowley, and B.S. Blagg, *Natural Product Inspired N-Terminal Hsp90 Inhibitors: From Bench to Bedside?* Med Res Rev, 2016. **36**(1): p. 92-118.

139. Houghton, P.J. and M.J. Howes, *Natural products and derivatives affecting neurotransmission relevant to Alzheimer's and Parkinson's disease.* Neurosignals, 2005. **14**(1-2): p. 6-22.

140. Kong, L.Y. and R.X. Tan, *Artemisinin, a miracle of traditional Chinese medicine.* Nat Prod Rep, 2015. **32**(12): p. 1617-21.

141. Mishra, B.B. and V.K. Tiwari, *Natural products: an evolving role in future drug discovery.* Eur J Med Chem, 2011. **46**(10): p. 4769-807.

142. Li, L.F. and J.H. Lu, *Clinical observation on acupuncture treatment of intractable insomnia.* J Tradit Chin Med, 2010. **30**(1): p. 21-2.

143. Zhu, T.M., R.J. Jin, and X.M. Zhong, *[Clinical effect of electroacupuncture combined with psychologic interference on patient with Internet addiction disorder].* Zhongguo Zhong Xi Yi Jie He Za Zhi, 2009. **29**(3): p. 212-4.

144. Manber, R., et al., *Acupuncture for depression during pregnancy: a randomized controlled trial.* Obstet Gynecol, 2010. **115**(3): p. 511-20.

145. Spence, D.W., et al., *Acupuncture increases nocturnal melatonin secretion and reduces insomnia and anxiety: a preliminary report.* J Neuropsychiatry Clin Neurosci, 2004. **16**(1): p. 19-28.

146. Pilkington, K., et al., *Acupuncture for anxiety and anxiety disorders--a systematic literature review.* Acupunct Med, 2007. **25**(1-2): p. 1-10.

147. Hollifield, M., et al., *Acupuncture for posttraumatic stress disorder: a randomized controlled pilot trial.* J Nerv Ment Dis, 2007. **195**(6): p. 504-13.

148. Lee, C., et al., *The effectiveness of acupuncture research across components of the trauma spectrum response (tsr): a systematic review of reviews.* Syst Rev, 2012. **1**: p. 46.

149. Zhang, Y., et al., *Clinical study on treatment of the earthquake-caused post-traumatic stress disorder by cognitive-behavior therapy and acupoint stimulation.* J Tradit Chin Med, 2011. **31**(1): p. 60-3.

150. Wang, Y., et al., *Clinical studies on treatment of earthquake-caused posttraumatic stress disorder using electroacupuncture.* Evid Based Complement Alternat Med, 2012. **2012**: p. 431279.

151. Head, K.A. and G.S. Kelly, *Nutrients and botanicals for treatment of stress: adrenal fatigue, neurotransmitter imbalance, anxiety, and restless sleep.* Altern Med Rev, 2009. **14**(2): p. 114-40.

152. Mao, Q.Q., et al., *Anti-depressant-like effect of peony: a mini-review*. Pharm Biol, 2012. **50**(1): p. 72-7.

153. Qin, F., et al., *Meta-analysis of randomized controlled trials to assess the effectiveness and safety of Free and Easy Wanderer Plus, a polyherbal preparation for depressive disorders.* J Psychiatr Res, 2011. **45**(11): p. 1518-24.

154. Wang, Y., R. Fan, and X. Huang, *Meta-analysis of the clinical effectiveness of traditional Chinese medicine formula Chaihu-Shugan-San in depression.* J Ethnopharmacol, 2012. **141**(2): p. 571-7.

155. Meng, X.Z., et al., *A chinese herbal formula to improve general psychological status in posttraumatic stress disorder: a randomized placebo-controlled trial on sichuan earthquake survivors.* Evid Based Complement Alternat Med, 2012. **2012**: p. 691258.

156. Li, N., et al., *TCM formula Xiaoyaosan decoction improves depressive-like behaviors in rats with type 2 diabetes.* Evidence-Based Complementary and Alternative Medicine, 2015. **2015**.

157. Meng, Z.-z., et al., *Xiaoyaosan decoction, a traditional chinese medicine, inhibits oxidative-stress-induced hippocampus neuron apoptosis in vitro.* Evidence-Based Complementary and Alternative Medicine, 2012. **2012**.

158. Liang, Y., et al., *Effects of the Chinese traditional prescription Xiaoyaosan decoction on chronic immobilization stress-induced changes in behavior and ultrastructure in rat hippocampus.* Evidence-Based Complementary and Alternative Medicine, 2013. **2013**.

159. Meng, Z.-Z., et al., *Effect of xiaoyaosan decoction on learning and memory deficit in rats induced by chronic immobilization stress.* Evidence-Based Complementary and Alternative Medicine, 2013. **2013**.

160. Liu, C.-C., et al., *Plasma-metabolite-biomarkers for the therapeutic response in depressed patients by the traditional Chinese medicine formula Xiaoyaosan: A 1 H NMR-based metabolomics approach.* Journal of affective disorders, 2015. **185**: p. 156-163.

161. Tylee, D.S., et al., *Blood-based gene-expression biomarkers of post-traumatic stress disorder among deployed marines: A pilot study*. Psychoneuroendocrinology, 2015. **51**: p. 472-494.

162. Segman, R.H., et al., *Peripheral blood mononuclear cell gene expression profiles identify emergent post-traumatic stress disorder among trauma survivors.* Molecular Psychiatry, 2005. **10**(5): p. 500-513.

163. Neylan, T.C., et al., *Suppressed monocyte gene expression profile in men versus women with PTSD.* Brain Behav Immun, 2011. **25**(3): p. 524-31.

164. Su, Y.A., et al., *Dysregulated mitochondrial genes and networks with drug targets in postmortem brain of patients with posttraumatic stress disorder (PTSD) revealed by human mitochondria-focused cDNA microarrays.* Int J Biol Sci, 2008. **4**(4): p. 223-35.

165. Holland, R. and J.C. Fishbein, *Chemistry of the cysteine sensors in Kelch-like ECH-associated protein 1.* Antioxidants & redox signaling, 2010. **13**(11): p. 1749-1761.

166. Klomsiri, C., P.A. Karplus, and L.B. Poole, *Cysteine-based redox switches in enzymes.* Antioxidants & redox signaling, 2011. **14**(6): p. 1065-1077.

167. Dong, H., et al., *Paeoniflorin inhibition of 6-hydroxydopamine-induced apoptosis in PC12 cells via suppressing reactive oxygen species-mediated PKCdelta/NF-kappaB pathway.* Neuroscience, 2015. **285**: p. 70-80.

168. Mao, Q.Q., et al., *Protective effects of paeoniflorin against corticosterone-induced neurotoxicity in PC12 cells.* Phytother Res, 2012. **26**(7): p. 969-73.

169. Yang, N., et al., *Paeoniflorin inhibits human pancreatic cancer cell apoptosis via suppression of MMP-9 and ERK signaling.* Oncol Lett, 2016. **12**(2): p. 1471-1476.

170. Gu, X., et al., *Protective effect of paeoniflorin on inflammation and apoptosis in the cerebral cortex of a transgenic mouse model of Alzheimer's disease.* Mol Med Rep, 2016. **13**(3): p. 2247-52.

171. Huang, H., et al., *Paeoniflorin improves menopause depression in ovariectomized rats under chronic unpredictable mild stress.* Int J Clin Exp Med, 2015. **8**(4): p. 5103-11.

172. Zhou, J., et al., *Paeoniflorin and Albiflorin Attenuate Neuropathic Pain via MAPK Pathway in Chronic Constriction Injury Rats.* Evid Based Complement Alternat Med, 2016. **2016**: p. 8082753.

173. Ma, Z., et al., *Paeoniflorin alleviates non-alcoholic steatohepatitis in rats: Involvement with the ROCK/NF-kappaB pathway.* Int Immunopharmacol, 2016. **38**: p. 377-84.

174. Chen, L., et al., *The new use of an ancient remedy: a double-blinded randomized study on the treatment of rheumatoid arthritis.* Am J Chin Med, 2013. **41**(2): p. 263-80.

175. Sadakane, C., et al., *Pharmacokinetic Profiles of Active Components After Oral Administration of a Kampo Medicine, Shakuyakukanzoto, to Healthy Adult Japanese Volunteers.* J Pharm Sci, 2015. **104**(11): p. 3952-9.

176. Shang, Q.H., et al., *A multi-center randomized double-blind placebo-controlled trial of Xiongshao Capsule in preventing restenosis after percutaneous coronary intervention: a subgroup analysis of senile patients.* Chin J Integr Med, 2011. **17**(9): p. 669-74.

177. Suh, K.S., et al., *Protective effect of albiflorin against oxidative-stress-mediated toxicity in osteoblast-like MC3T3-E1 cells.* Fitoterapia, 2013. **89**: p. 33-41.

178. Kim, S.H., et al., *Chemical constituents isolated from Paeonia lactiflora roots and their neuroprotective activity against oxidative stress in vitro.* J Enzyme Inhib Med Chem, 2009. **24**(5): p. 1138-40.

179. Song, J., et al., *Not only serotonergic system, but also dopaminergic system involved in albiflorin against chronic unpredictable mild stress-induced depression-like behavior in rats.* Chem Biol Interact, 2015. **242**: p. 211-7.

180. Ho, S.L., et al., *Inhibition of beta-amyloid Aggregation By Albiflorin, Aloeemodin And Neohesperidin And Their Neuroprotective Effect On Primary Hippocampal Cells Against beta-amyloid Induced Toxicity.* Curr Alzheimer Res, 2015. **12**(5): p. 424-33.

181. Zhang, Y., et al., *Calcium channels contribute to albiflorin-mediated antinociceptive effects in mouse model.* Neurosci Lett, 2016. **628**: p. 105-9.

182. Min, W., et al., *Baicalin Protects Keratinocytes from Toll-like Receptor-4 Mediated DNA Damage and Inflammation Following Ultraviolet Irradiation.* Photochem Photobiol, 2015. **91**(6): p. 1435-43.

183. Li, X., et al., *Effect of baicalin-copper on the induction of apoptosis in human hepatoblastoma cancer HepG2 cells.* Med Oncol, 2015. **32**(3): p. 72.

184. Zheng, W.X., et al., *Baicalin protects PC-12 cells from oxidative stress induced by hydrogen peroxide via anti-apoptotic effects.* Brain Inj, 2014. **28**(2): p. 227-34.

185. Buelna-Chontal, M. and C. Zazueta, *Redox activation of Nrf2 & NF-κB: a double end sword?* Cellular signalling, 2013. **25**(12): p. 2548-2557.

186. Yu, F.Y., et al., *[Effect of baicalin on signal transduction and activating transcription factor expression in ulcerative colitis patients].* Zhongguo Zhong Xi Yi Jie He Za Zhi, 2015. **35**(4): p. 419-24.

187. Teng, L., et al., *Liquiritin modulates ERK and AKT/GSK3betadependent pathways to protect against glutamateinduced cell damage in differentiated PC12 cells.* Mol Med Rep, 2014. **10**(2): p. 818-24.

188. Jia, S.L., et al., *Neuroprotective effects of liquiritin on cognitive deficits induced by soluble amyloid-beta1-42 oligomers injected into the hippocampus.* J Asian Nat Prod Res, 2016: p. 1-14.

189. Huang, X., Y. Wang, and K. Ren, *Protective Effects of Liquiritin on the Brain of Rats with Alzheimer's Disease.* West Indian Med J, 2016.

190. Farahani, M.S., et al., *Plant-derived natural medicines for the management of depression: an overview of mechanisms of action.* Rev Neurosci, 2015. **26**(3): p. 305-21.

191. Sun, Y.X., et al., *Neuroprotective effect of liquiritin against focal cerebral ischemia/reperfusion in mice via its antioxidant and antiapoptosis properties.* J Asian Nat Prod Res, 2010. **12**(12): p. 1051-60.

192. Amer, M. and M. Metwalli, *Topical liquiritin improves melasma.* Int J Dermatol, 2000. **39**(4): p. 299-301.

193. Rafi, M.M., et al., *Novel polyphenol molecule isolated from licorice root (Glycrrhiza glabra) induces apoptosis, G2/M cell cycle arrest, and Bcl-2 phosphorylation in tumor cell lines.* J Agric Food Chem, 2002. **50**(4): p. 677-84.

194. Kaur, P., et al., *Evaluation of antigenotoxic activity of isoliquiritin apioside from Glycyrrhiza glabra L.* Toxicol In Vitro, 2009. **23**(4): p. 680-6.

195. Wang, W., et al., *Antidepressant-like effects of liquiritin and isoliquiritin from Glycyrrhiza uralensis in the forced swimming test and tail suspension test in mice.* Prog Neuropsychopharmacol Biol Psychiatry, 2008. **32**(5): p. 1179-84.

196. Luo, J., et al., *Antifungal Activity of Isoliquiritin and Its Inhibitory Effect against Peronophythora litchi Chen through a Membrane Damage Mechanism.* Molecules, 2016. **21**(2): p. 237.

197. Su, G.Y., et al., *Antidepressant-like effects of Xiaochaihutang in a rat model of chronic unpredictable mild stress.* J Ethnopharmacol, 2014. **152**(1): p. 217-26.

198. Wang, X., et al., *Oroxyloside prevents dextran sulfate sodium-induced experimental colitis in mice by inhibiting NF-kappaB pathway through PPARgamma activation.* Biochem Pharmacol, 2016. **106**: p. 70-81.

199. Fong, S.Y., et al., *Herb-drug interactions between Scutellariae Radix and mefenamic acid: Simultaneous investigation of pharmacokinetics, anti-inflammatory effect and gastric damage in rats.* J Ethnopharmacol, 2015. **170**: p. 106-16.

200. Liu, H., et al., *Synergistic protective effect of paeoniflorin and beta-ecdysterone against rotenone-induced neurotoxicity in PC12 cells.* Apoptosis, 2016. **21**(12): p. 1354-1365.

201. Zhai, T., et al., *Unique immunomodulatory effect of paeoniflorin on type I and II macrophages activities.* J Pharmacol Sci, 2016. **130**(3): p. 143-50.

202. Liu, H., et al., *Paeoniflorin attenuates Abeta1-42-induced inflammation and chemotaxis of microglia in vitro and inhibits NF-kappaB- and VEGF/Flt-1 signaling pathways.* Brain Res, 2015. **1618**: p. 149-58.

203. Jiang, C., et al., *Selective suppression of microglial activation by paeoniflorin attenuates morphine tolerance.* Eur J Pain, 2015. **19**(7): p. 908-19.

204. Gan, Y., et al., *Paeoniflorin upregulates beta-defensin-2 expression in human bronchial epithelial cell through the p38 MAPK, ERK, and NF-kappaB signaling pathways.* Inflammation, 2014. **37**(5): p. 1468-75.

205. Zhang, Q., et al., *Paeoniflorin reduced BLP-induced inflammatory response by inhibiting the NF-kappaB signal transduction in pathway THP-1 cells.* Cent Eur J Immunol, 2014. **39**(4): p. 461-7.

206. Kong, P., et al., *Effects of paeoniflorin on tumor necrosis factor-alpha-induced insulin resistance and changes of adipokines in 3T3-L1 adipocytes.* Fitoterapia, 2013. **91**: p. 44-50.

207. Zhou, H., et al., *Paeoniflorin attenuates pressure overload-induced cardiac remodeling via inhibition of TGFbeta/Smads and NF-kappaB pathways.* J Mol Histol, 2013. **44**(3): p. 357-67.

208. Liu, Q., et al., *Paeoniflorin ameliorates renal function in cyclophosphamide-induced mice via AMPK suppressed inflammation and apoptosis.* Biomed Pharmacother, 2016. **84**: p. 1899-1905.

209. Zhai, J. and Y. Guo, *Paeoniflorin attenuates cardiac dysfunction in endotoxemic mice via the inhibition of nuclear factor-kappaB.* Biomed Pharmacother, 2016. **80**: p. 200-6.

210. Zhang, L.G., et al., *Paeoniflorin improves regional cerebral blood flow and suppresses inflammatory factors in the hippocampus of rats with vascular dementia.* Chin J Integr Med, 2015.

211. Zhang, H.R., et al., *Paeoniflorin Atttenuates Amyloidogenesis and the Inflammatory Responses in a Transgenic Mouse Model of Alzheimer's Disease.* Neurochem Res, 2015. **40**(8): p. 1583-92.

212. Yi, J.F., *[Effect of paeoniflorin on level of glucocorticoid receptor of peripheral blood monocytes in rats of collagen-induced arthritis].* Zhongguo Zhong Yao Za Zhi, 2014. **39**(5): p. 907-10.

213. Chen, M., et al., *Paeoniflorin protects against concanavalin A-induced hepatitis in mice.* Int Immunopharmacol, 2015. **24**(1): p. 42-9.

214. Zhang, J., et al., *Paeoniflorin abrogates DSS-induced colitis via a TLR4-dependent pathway.* Am J Physiol Gastrointest Liver Physiol, 2014. **306**(1): p. G27-36.

215. Guo, R.B., et al., *Paeoniflorin protects against ischemia-induced brain damages in rats via inhibiting MAPKs/NF-kappaB-mediated inflammatory responses.* PLoS One, 2012. **7**(11): p. e49701.

216. Zhou, H., et al., *Paeoniflorin protects against lipopolysaccharide-induced acute lung injury in mice by alleviating inflammatory cell infiltration and microvascular permeability.* Inflamm Res, 2011. **60**(10): p. 981-90.

217. Shin, J.M., et al., *Baicalin Down-Regulates IL-1beta-Stimulated Extracellular Matrix Production in Nasal Fibroblasts.* PLoS One, 2016. **11**(12): p. e0168195.

218. Wang, B., et al., *Baicalin and geniposide inhibit the development of atherosclerosis by increasing Wnt1 and inhibiting dickkopf-related protein-1 expression.* J Geriatr Cardiol, 2016. **13**(10): p. 846-854.

219. Fu, S., et al., *Baicalin suppresses NLRP3 inflammasome and nuclear factor-kappa B (NF-kappaB) signaling during Haemophilus parasuis infection.* Vet Res, 2016. **47**(1): p. 80.

220. Guo, M., et al., *Baicalin plays an anti-inflammatory role through reducing nuclear factor-kappaB and p38 phosphorylation in S. aureus-induced mastitis.* Int Immunopharmacol, 2013. **16**(2): p. 125-30.

221. Yang, W., et al., *Baicalin attenuates lipopolysaccharide induced inflammation and apoptosis of cow mammary epithelial cells by regulating NF-kappaB and HSP72.* Int Immunopharmacol, 2016. **40**: p. 139-145.

222. Liu, J., et al., *Baicalin attenuates inflammation in mice with OVA-induced asthma by inhibiting NF-kappaB and suppressing CCR7/CCL19/CCL21.* Int J Mol Med, 2016. **38**(5): p. 1541-1548.

223. Sun, J.Y., et al., *Baicalin inhibits toll-like receptor 2/4 expression and downstream signaling in rat experimental periodontitis.* Int Immunopharmacol, 2016. **36**: p. 86-93.

224. Zhou, Y.J., et al., *Inhibitory effect of baicalin on allergic response in ovalbumin-induced allergic rhinitis guinea pigs and lipopolysaccharide-stimulated human mast cells.* Inflamm Res, 2016. **65**(8): p. 603-12.

225. Wang, H.Z., et al., *Inhibitory effect of baicalin on collagen-induced arthritis in rats through the nuclear factor-kappaB pathway.* J Pharmacol Exp Ther, 2014. **350**(2): p. 435-43.

226. Zhou, Q.B., et al., *Baicalin attenuates brain edema in a rat model of intracerebral hemorrhage.* Inflammation, 2014. **37**(1): p. 107-15.

227. Ding, X.M., et al., *Baicalin exerts protective effects against lipopolysaccharide-induced acute lung injury by regulating the crosstalk between the CX3CL1-CX3CR1 axis and NF-kappaB pathway in CX3CL1-knockout mice.* Int J Mol Med, 2016. **37**(3): p. 703-15.

228. Wan, J.Y., et al., *Protective effect of baicalin against lipopolysaccharide/D-galactosamine-induced liver injury in mice by up-regulation of heme oxygenase-1.* Eur J Pharmacol, 2008. **587**(1-3): p. 302-8.

229. Singh, D.P. and K. Chopra, *Flavocoxid, dual inhibitor of cyclooxygenase-2 and 5-lipoxygenase, exhibits neuroprotection in rat model of ischaemic stroke.* Pharmacol Biochem Behav, 2014. **120**: p. 33-42.

230. Tu, X.K., et al., *Baicalin inhibits TLR2/4 signaling pathway in rat brain following permanent cerebral ischemia.* Inflammation, 2011. **34**(5): p. 463-70.

231. Kim, J.Y., et al., *Isoliquiritigenin isolated from the roots of Glycyrrhiza uralensis inhibits LPS-induced iNOS and COX-2 expression via the attenuation of NF-kappaB in RAW 264.7 macrophages.* Eur J Pharmacol, 2008. **584**(1): p. 175-84.

232. Zhang, X., et al., *Liquiritin attenuates advanced glycation end products-induced endothelial dysfunction via RAGE/NF-kappaB pathway in human umbilical vein endothelial cells.* Mol Cell Biochem, 2013. **374**(1-2): p. 191-201.

233. Zhang, Y., et al., *The protective role of liquiritin in high fructose-induced myocardial fibrosis via inhibiting NF-kappaB and MAPK signaling pathway.* Biomed Pharmacother, 2016. **84**: p. 1337-1349.

234. Tao, J., et al., *Chemomics-Integrated Proteomics Analysis of Jie-Geng-Tang to Ameliorate Lipopolysaccharide-Induced Acute Lung Injury in Mice.* Evid Based Complement Alternat Med, 2016. **2016**: p. 7379146.

235. Bryan, H.K., et al., *The Nrf2 cell defence pathway: Keap1-dependent and-independent mechanisms of regulation.* Biochemical pharmacology, 2013. **85**(6): p. 705-717.

236. Kong, L., et al., *Paeoniflorin attenuates ultraviolet B-induced apoptosis in human keratinocytes by inhibiting the ROS-p38-p53 pathway.* Mol Med Rep, 2016. **13**(4): p. 3553-8.

237. Li, J.Z., et al., *Paeoniflorin protects myocardial cell from doxorubicin-induced apoptosis through inhibition of NADPH oxidase.* Can J Physiol Pharmacol, 2012. **90**(12): p. 1569-75.

238. Yang, X., et al., *Paeoniflorin protects Schwann cells against high glucose induced oxidative injury by activating Nrf2/ARE pathway and inhibiting apoptosis.* J Ethnopharmacol, 2016. **185**: p. 361-9.

239. Li, C.R., et al., *Protective effect of paeoniflorin on irradiation-induced cell damage involved in modulation of reactive oxygen species and the mitogen-activated protein kinases.* Int J Biochem Cell Biol, 2007. **39**(2): p. 426-38.

240. Choi, E.M. and Y.S. Lee, *Paeoniflorin isolated from Paeonia lactiflora attenuates osteoblast cytotoxicity induced by antimycin A.* Food Funct, 2013. **4**(9): p. 1332-8.

241. Zhao, Y., et al., *Paeoniflorin protects against ANIT-induced cholestasis by ameliorating oxidative stress in rats.* Food and chemical toxicology, 2013. **58**: p. 242-248.

242. Lin, J., et al., *Paeoniflorin Attenuated Oxidative Stress in Rat COPD Model Induced by Cigarette Smoke.* Evid Based Complement Alternat Med, 2016. **2016**: p. 1698379.

243. Yang, X., et al., *Mechanism of Tang Luo Ning effect on attenuating of oxidative stress in sciatic nerve of STZ-induced diabetic rats.* J Ethnopharmacol, 2015. **174**: p. 1-10.

244. Li, C.T., et al., *Baicalin attenuates oxygen-glucose deprivation-induced injury by inhibiting oxidative stress-mediated 5-lipoxygenase activation in PC12 cells.* Acta Pharmacol Sin, 2010. **31**(2): p. 137-44.

245. Ai, Z.L., et al., *[Effect of baicalin on liver fatty acid binding protein in oxidative stress model in vitro].* Zhonghua Gan Zang Bing Za Zhi, 2011. **19**(12): p. 927-31.

246. Song, J.X., et al., *Baicalein antagonizes rotenone-induced apoptosis in dopaminergic SH-SY5Y cells related to Parkinsonism.* Chin Med, 2012. **7**(1): p. 1.

247. Yao, J., et al., *Protective Effect of Baicalin Against Experimental Colitis via Suppression of Oxidant Stress and Apoptosis.* Pharmacogn Mag, 2016. **12**(47): p. 225-34.

248. Ku, S.K. and J.S. Bae, *Baicalin, baicalein and wogonin inhibits high glucose-induced vascular inflammation in vitro and in vivo.* BMB Rep, 2015. **48**(9): p. 519-24.

249. Xu, M., et al., *Baicalin can scavenge peroxynitrite and ameliorate endogenous peroxynitrite-mediated neurotoxicity in cerebral ischemia-reperfusion injury.* J Ethnopharmacol, 2013. **150**(1): p. 116-24.

250. Zhou, B.R., et al., *Baicalin protects human skin fibroblasts from ultraviolet A radiation-induced oxidative damage and apoptosis.* Free Radic Res, 2012. **46**(12): p. 1458-71.

251. Zhou, Y.Z., et al., *Protective effect of isoliquiritin against corticosterone-induced neurotoxicity in PC12 cells.* Food Funct, 2017.

252. Zhao, Z., et al., *Antidepressant-like effect of liquiritin from Glycyrrhiza uralensis in chronic variable stress induced depression model rats.* Behav Brain Res, 2008. **194**(1): p. 108-13.

253. Guan, Y., et al., *Protective effects of liquiritin apioside on cigarette smoke-induced lung epithelial cell injury.* Fundam Clin Pharmacol, 2012. **26**(4): p. 473-83.

254. Jia, S.L., et al., *Neuroprotective effects of liquiritin on cognitive deficits induced by soluble amyloid-beta1-42 oligomers injected into the hippocampus.* J Asian Nat Prod Res, 2016. **18**(12): p. 1186-1199.

255. McMahon, M., et al., *Keap1-dependent proteasomal degradation of transcription factor Nrf2 contributes to the negative regulation of antioxidant response element-driven gene expression.* Journal of Biological Chemistry, 2003. **278**(24): p. 21592-21600.

256. Li, H., et al., *Blood-brain barrier permeability of Gualou Guizhi granules and neuroprotective effects in ischemia/reperfusion injury.* Mol Med Rep, 2015. **12**(1): p. 1272-8.

257. Yao, W., et al., *Role of Keap1-Nrf2 signaling in depression and dietary intake of glucoraphanin confers stress resilience in mice.* Sci Rep, 2016. **6**: p. 30659.

258. Yin, S.-H., et al., *Room-temperature super-extraction system (RTSES) optimizes the anxiolytic-and antidepressant-like behavioural effects of traditional Xiao-Yao-San in mice.* Chinese medicine, 2012. **7**(1): p. 24.

259. Sun, G. and G. Ding, *Establishment of capillary electrophoresis fingerprints of Xiaoyao pills.* Se pu= Chinese journal of chromatography, 2011. **29**(10): p. 1020-1026.

260. Zhu, X., et al., *Xiao Yao San improves depressive-like behavior in rats through modulation of β-arrestin 2-mediated pathways in hippocampus.* Evidence-Based Complementary and Alternative Medicine, 2014. **2014**.

261. Ding, X.-F., et al., *Xiao yao san improves depressive-like behaviors in rats with chronic immobilization stress through modulation of locus coeruleus-norepinephrine system.* Evidence-Based Complementary and Alternative Medicine, 2014. **2014**.

262. Cao, G., et al., *Xiao Yao San against Corticosterone-Induced Stress Injury via Upregulating Glucocorticoid Receptor Reaction Element Transcriptional Activity.* Evidence-Based Complementary and Alternative Medicine, 2016. **2016**.

263. Zhao, H.-B., et al., *Xiao Yao San Improves the Anxiety-Like Behaviors of Rats Induced by Chronic Immobilization Stress: The Involvement of the JNK Signaling Pathway in the Hippocampus.* Biological and Pharmaceutical Bulletin, 2017. **40**(2): p. 187-194.

264. Tian, J.-s., et al., *Dynamic analysis of the endogenous metabolites in depressed patients treated with TCM formula Xiaoyaosan using urinary 1 H NMR-based metabolomics.* Journal of ethnopharmacology, 2014. **158**: p. 1-10.

265. Qiu, J.-J., et al., *Gut microbial diversity analysis using Illumina sequencing for functional dyspepsia with liver depression-spleen deficiency syndrome and the interventional Xiaoyaosan in a rat model.* World journal of gastroenterology, 2017. **23**(5): p. 810.

266. Jimenez-Marin, A., et al., *Biological pathway analysis by ArrayUnlock and Ingenuity Pathway Analysis.* BMC Proc, 2009. **3 Suppl 4**: p. S6.

267. Liu, T., et al., *Cistrome: an integrative platform for transcriptional regulation studies.* Genome Biol, 2011. **12**(8): p. R83.

268. Karolchik, D., et al., *The UCSC Genome Browser database: 2014 update.* Nucleic Acids Res, 2014. **42**(Database issue): p. D764-70.

269. Bass, D.A., et al., *Flow cytometric studies of oxidative product formation by neutrophils: a graded response to membrane stimulation.* J Immunol, 1983. **130**(4): p. 1910-7.

270. Bass, D.A., et al., *Pillars Article: Flow Cytometric Studies of Oxidative Product Formation by Neutrophils: A Graded Response to Membrane Stimulation.* J Immunol, 2016. **197**(3): p. 683-90.

271. Cossarizza, A., et al., *Simultaneous analysis of reactive oxygen species and reduced glutathione content in living cells by polychromatic flow cytometry*. Nat Protoc, 2009. **4**(12): p. 1790-7.

272. Zhao, Q., et al., *Inhibition of c-MYC with involvement of ERK/JNK/MAPK and AKT pathways as a novel mechanism for shikonin and its derivatives in killing leukemia cells.* Oncotarget, 2015. **6**(36): p. 38934.

273. Wang, Y., et al., *Therapeutic effect of MG-132 on diabetic cardiomyopathy is associated with its suppression of proteasomal activities: roles of Nrf2 and NF-kappaB.* Am J Physiol Heart Circ Physiol, 2013. **304**(4): p. H567-78.

274. Qiaoli Zhao MZ, T.E., Jennifer Herrmann, Rolf Müller, Thomas Efferth, *Molecular docking studies of myxobacterial disorazoles and tubulysins to tubulin* J Biosci Med., 2013. **3**(1): p. 37-44.

7 Supplementary data

7.1 Isolation

Standardized HPLC/MS method:

Column:	Agilent XDB Phenyl, 3.5 µm, 150 x 3 mm
Temperature:	40 °C (column oven)
Solvents:	H_2O with 0.1% HCOOH and MeCN
Gradient:	1% MeCN to 50 % MeCN in 40 min
	50% MeCN to 100 % MeCN in 5min
	100% MeCN isocratic for 2 min
	100% MeCN to 1 % MeCN in 1 min
Flow:	0.45 ml/min
MS:	Ion source: APCI
	Capillary voltage: 3500 V (pos.)/2200 V (neg.)
	Corona current: 4.0 µA (pos.)/12 µA (neg.)
	Drying Gas Flow: 6.0 l/min
	Nebulizer pressure: 50 psig
	Drying Gas Temperature: 350 °C
	Vaporizer Temperature: 400 °C

Crude extract “*free and easy wanderer*“(HPLC-MS chromatogram, 250 nm)

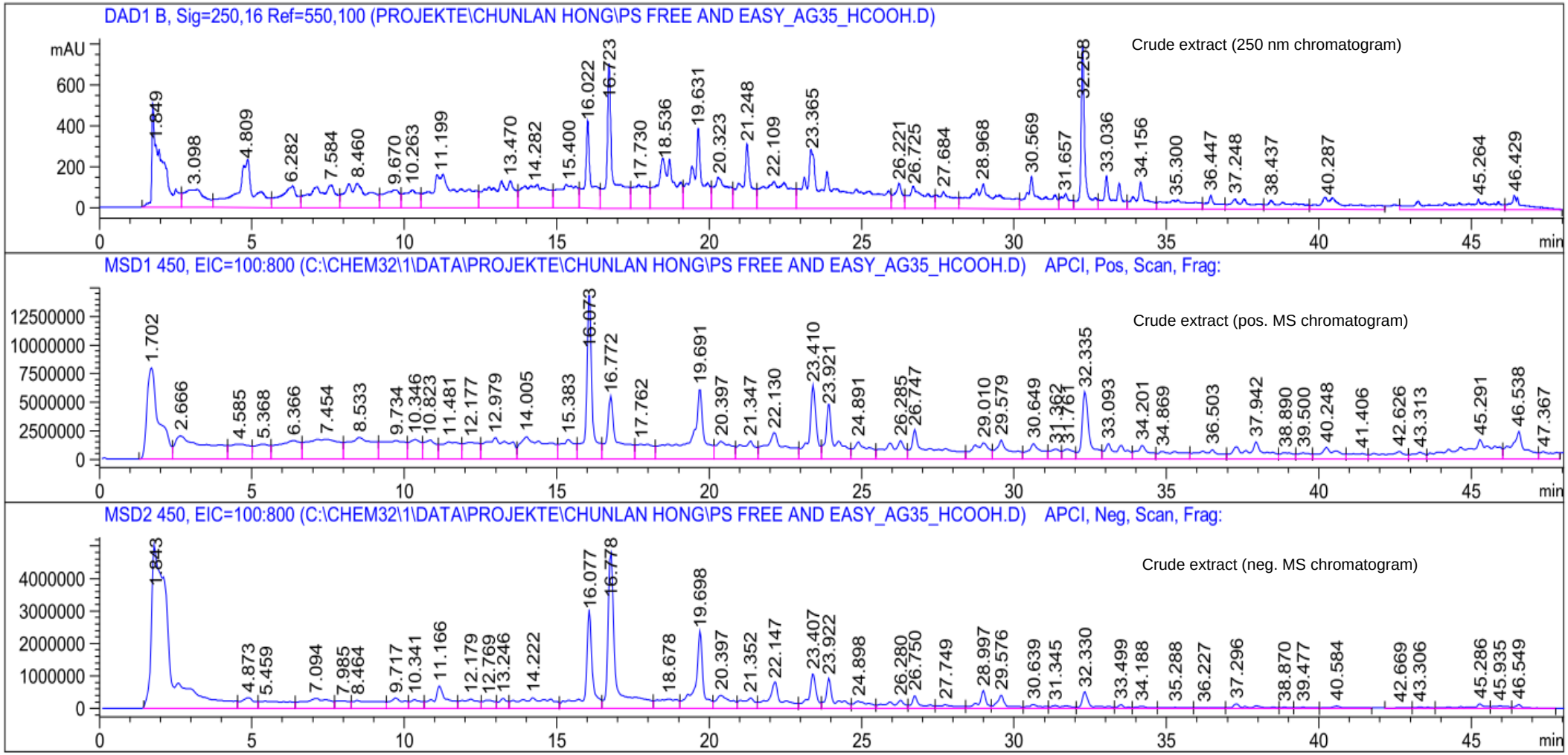

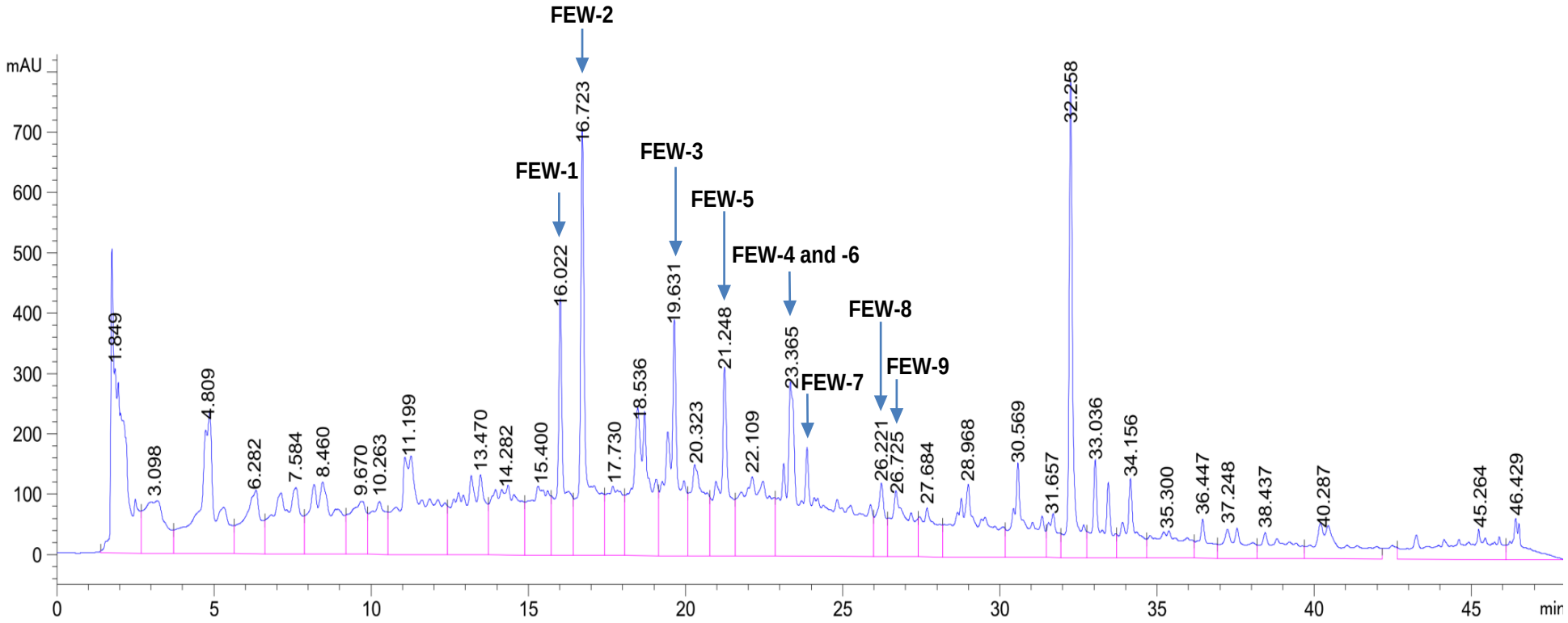

HPLC chromatogram (250 nm) of the crude extract (*Free and Easy Wanderer*), isolated compounds are marked

7.2 Structure identification

7.2.1 FAEW-1 Albiflorin

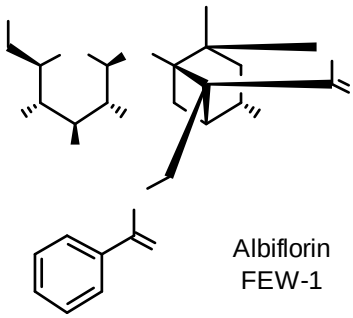

Albiflorin
FEW-1

Brown oil, [α]D29= –7.3 (c = 0.07, MeOH), ESI-MS m/z = 481.2 [M+H]+, HR-ESI-MS m/z = 503.1529 calculated for [C23H28O11+Na]+; found: 503.1546.

1H NMR, COSY (600 MHz, Methanol-d4) δ 8.11 – 8.07 (m, 2H, H-2‘‘/H-6‘‘), 7.64 – 7.60 (m, 1H, H-4‘‘), 7.52 – 7.48 (m, 2H, H-3‘‘/H-5‘‘), 4.80 (d, J = 12.2 Hz, 1H, H-8), 4.68 (d, J = 12.2 Hz, 1H, H-8), 4.53 (d, J = 7.6 Hz, 1H, H-1‘), 4.27 (dd, J = 6.6, 4.9 Hz, 1H, H-4), 3.85 (dd, J = 11.8, 1.5 Hz, 1H, H-6‘), 3.61 – 3.58 (m, 1H, H-6‘), 3.27 – 3.24 (m, 1H, H-3‘), 3.24 – 3.19 (m, 3H, H-2‘, H-4‘, H-5‘), 2.92 (dd, J = 7.8, 4.9 Hz, 1H, H-5), 2.80 (dd, J = 11.0, 7.8 Hz, 1H, H-7), 2.41 (dd, J = 15.4, 6.6 Hz, 1H, H-3), 2.05 (d, J = 11.0 Hz, 1H, H-7), 2.00 (dd, J = 15.4, 1.5 Hz, 1H, H-3), 1.52 (s, 3H, C-2-Me).

13C NMR, HSQC, HMBC (151 MHz, MeOD) δ 178.0 (C-9), 167.9 (C-1‘‘-CO), 134.4 (C-4’’), 131.2 (C-1’’), 130.8 (C-2’’/C-6’’), 129.7 (C-3’’/C-5’’), 100.1 (C-1’), 93.5 (C-2), 86.9 (C-1), 78.2 (C-5’), 78.0 (C-3’), 74.8 (C-2’), 71.6 (C-4’), 68.4 (C-4), 62.8 (C-6’), 62.0 (C-8), 56.9 (C-6), 41.7 (C-5), 41.6 (C-3), 28.5 (C-7), 20.6 (C-2-Me).

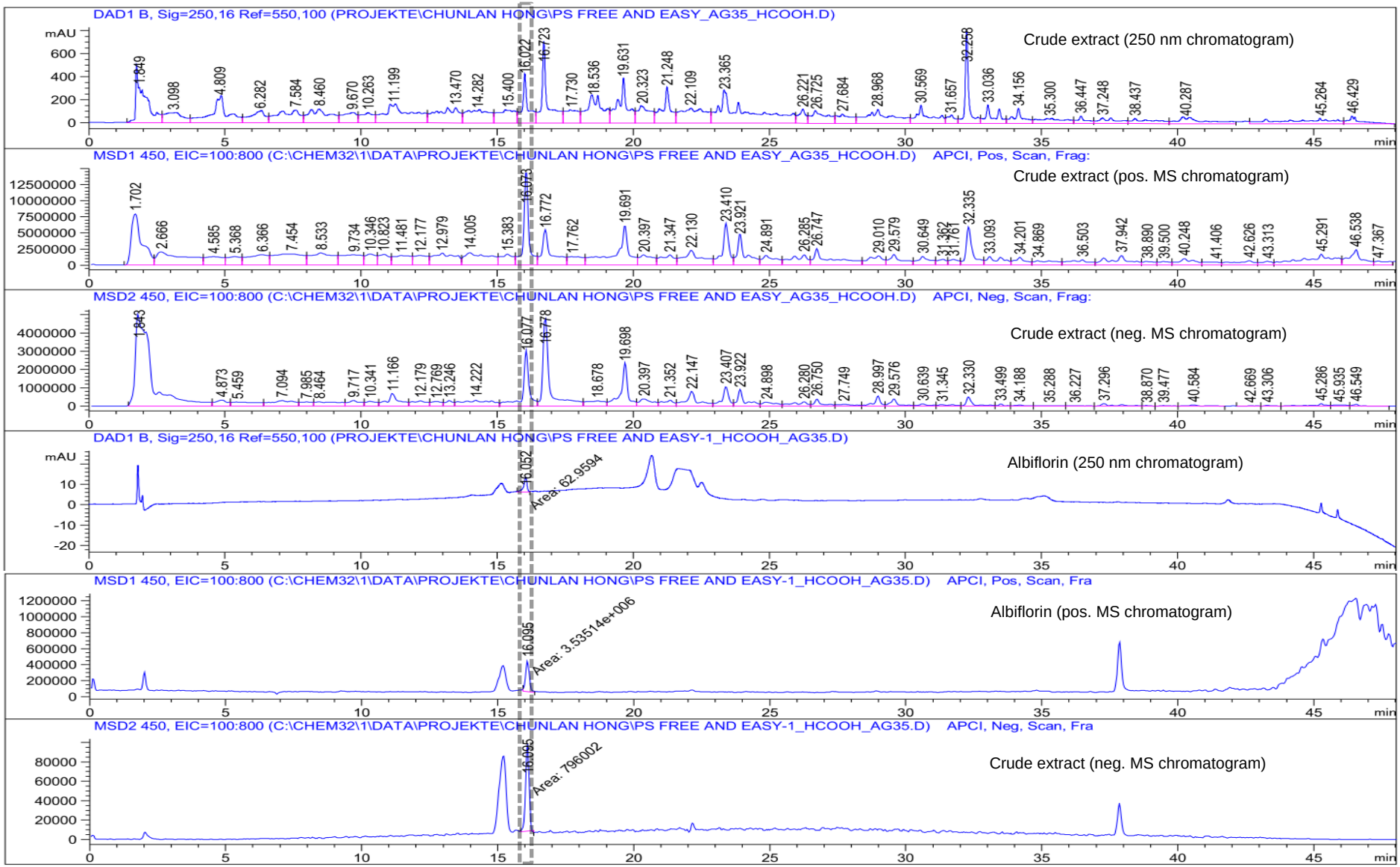
DAD1 B, Sig=250,16 Ref=550,100 (PROJEKTE\CHUNLAN HONG\PS FREE AND EASY_AG35_HCOOH.D)
Crude extract (250 nm chromatogram)
MSD1 450, EIC=100:800 (C:\CHEM32\1\DATA\PROJEKTE\CHUNLAN HONG\PS FREE AND EASY_AG35_HCOOH.D) APCI, Pos, Scan, Frag:
Crude extract (pos. MS chromatogram)
MSD2 450, EIC=100:800 (C:\CHEM32\1\DATA\PROJEKTE\CHUNLAN HONG\PS FREE AND EASY_AG35_HCOOH.D) APCI, Neg, Scan, Frag:
Crude extract (neg. MS chromatogram)
DAD1 B, Sig=250,16 Ref=550,100 (PROJEKTE\CHUNLAN HONG\PS FREE AND EASY-1_HCOOH_AG35.D)
Albiflorin (250 nm chromatogram)
Area: 62.9594
MSD1 450, EIC=100:800 (C:\CHEM32\1\DATA\PROJEKTE\CHUNLAN HONG\PS FREE AND EASY-1_HCOOH_AG35.D) APCI, Pos, Scan, Fra
Albiflorin (pos. MS chromatogram)
Area: 3.53514e+006
MSD2 450, EIC=100:800 (C:\CHEM32\1\DATA\PROJEKTE\CHUNLAN HONG\PS FREE AND EASY-1_HCOOH_AG35.D) APCI, Neg, Scan, Fra
Crude extract (neg. MS chromatogram)
Area: 796002
mAU
min

Albiflorin MS-spectra (comparison of corresponding MS spectra)

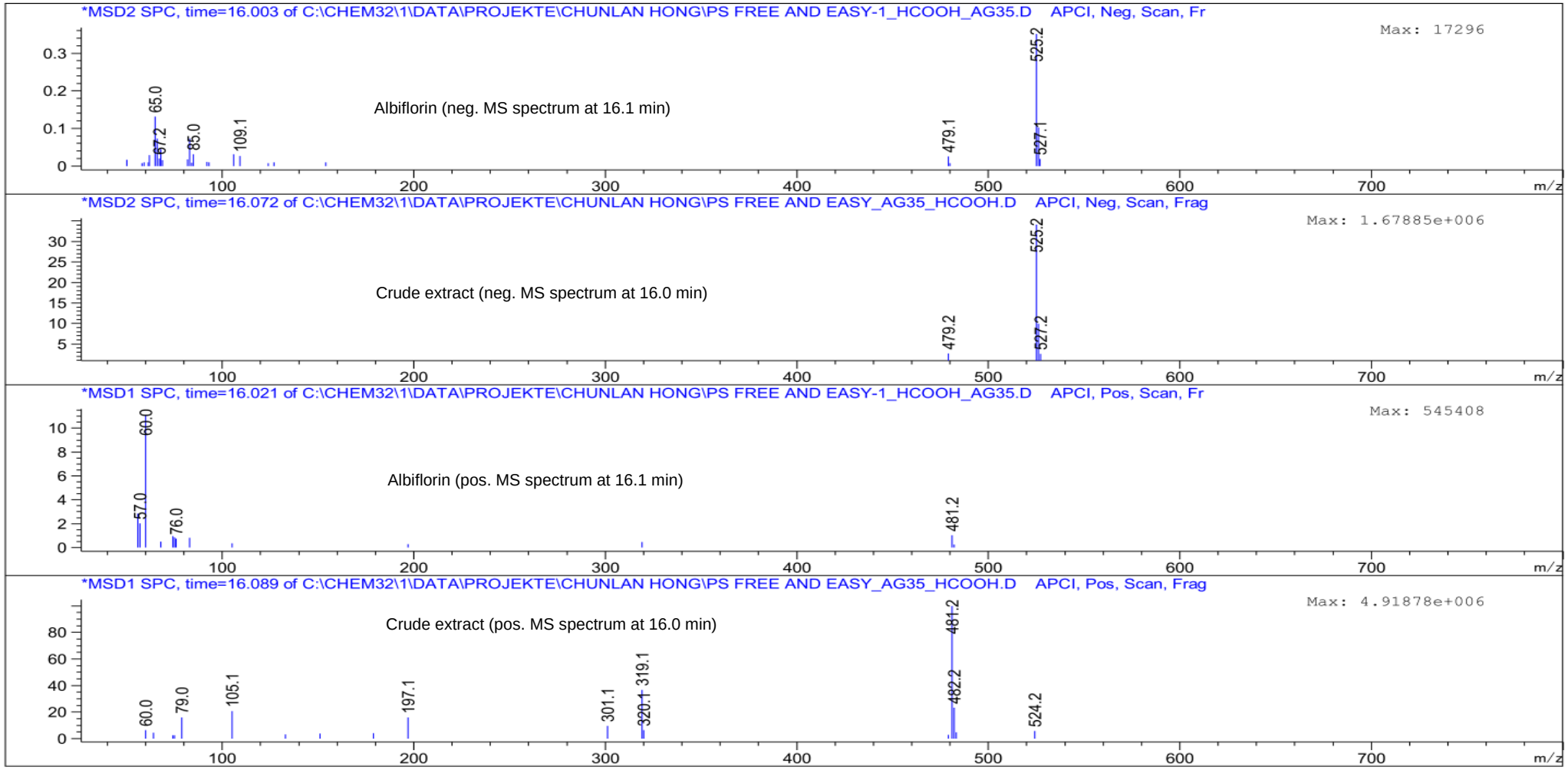

7.2.2 FAEW-2 Paeoniflorin

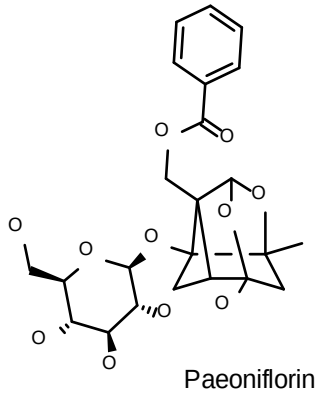

Paeoniflorin
FEW-2

Brown oil, [α]D29= –23.2 (c = 0.17, MeOH), ESI-MS m/z = 503.2 [M+Na]+, HR-ESI-MS m/z = 503.1529 calculated for [C23H28O11+Na]+; found: 503.1523

1H NMR, COSY (600 MHz, Methanol-d4) δ 8.09 – 8.04 (m, 2H, H-2‘‘/H-6‘‘), 7.66 – 7.60 (m, 1H, H-4‘‘), 7.52 – 7.48 (m, H-3‘‘/H-5‘‘), 5.42 (s, 1H, H-9), 4.78 – 4.72 (m, 2H, H-8), 4.53 (d, J = 7.7 Hz, 1H, H-1‘), 3.85 (dd, J = 11.9, 1.5 Hz, 1H, H-6‘), 3.63 – 3.58 (m, 1H, H-6‘), 3.31 (m, 1H, H-3‘), 3.25 – 3.20 (m, 3H, H-2‘, H-4‘, H-5‘), 2.62 – 2.57 (m, 1H, H-5), 2.50 (dd, J = 11.0, 6.9 Hz, 1H, H-7), 2.20 (d, J = 12.6 Hz, 1H, H-3), 1.96 (d, J = 11.0 Hz, 1H, H-7), 1.81 (d, J = 12.6, 1H, H-3), 1.37 (s, 3H, C-2-Me).

13C NMR, HSQC, HMBC (151 MHz, MeOD) δ 167.95 (C-1‘‘-CO), 134.43 (C-4’’), 131.21 (C-1’’), 130.68 (C-2’’/C-6’’), 129.64)C-3’’/C-5’’), 106.40 (C-4), 102.30 (C-9), 100.19 (C-1’), 89.33 (C-1), 87.25 (C-2), 78.05 (C-3’), 77.98 (C-5’), 75.01 (C-2’), 72.25 (C-6), 71.74 (C-4’), 62.87 (C-6’), 61.70 (C-8), 44.53 (C-3), 43.95 (C-5), 23.40 (C-7), 19.61 (C-2-Me).

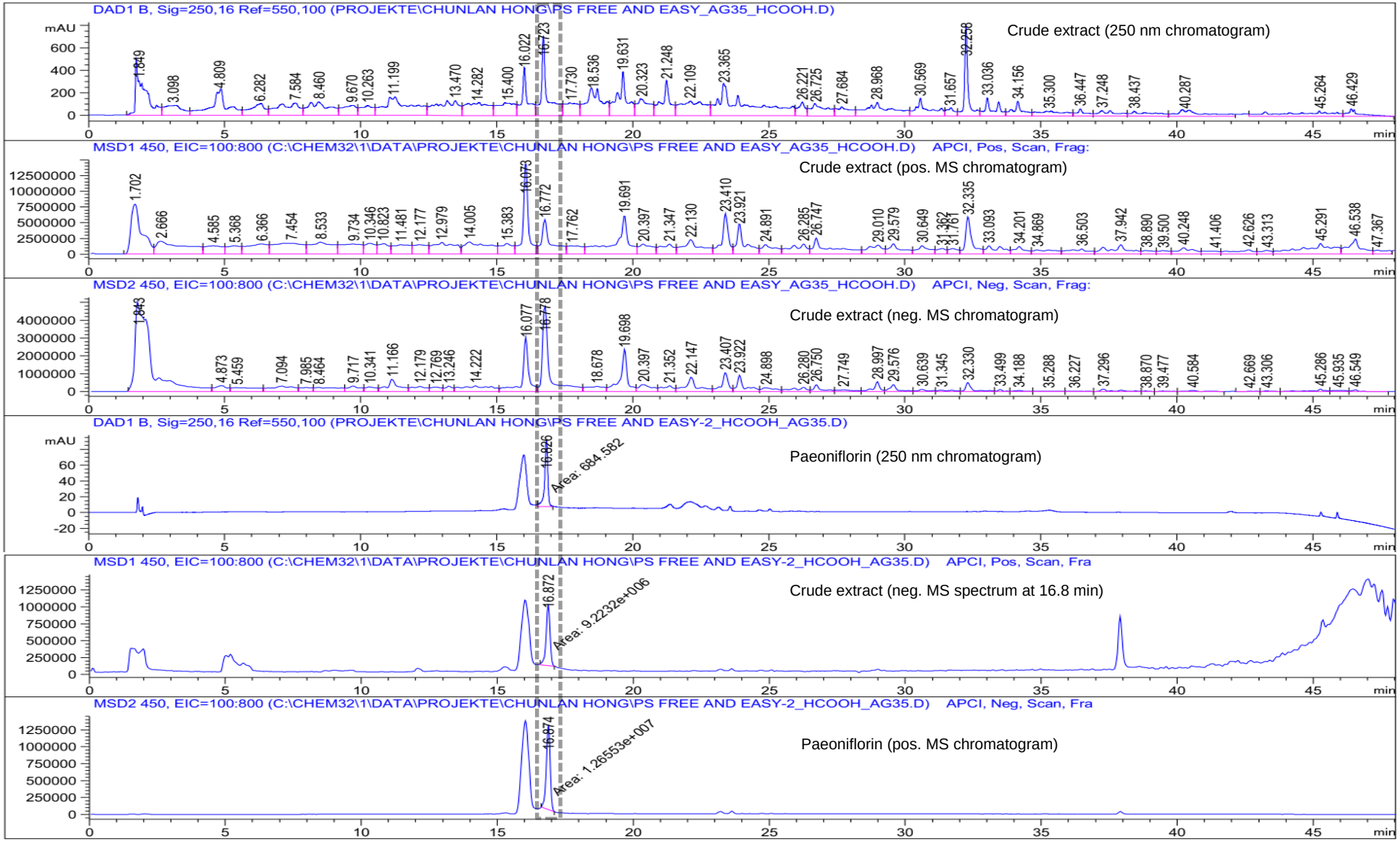
DAD1 B, Sig=250,16 Ref=550,100 (PROJEKTE\CHUNLAN HONG\PS FREE AND EASY_AG35_HCOOH.D)
Crude extract (250 nm chromatogram)
MSD1 450, EIC=100:800 (C:\CHEM32\1\DATA\PROJEKTE\CHUNLAN HONG\PS FREE AND EASY_AG35_HCOOH.D) APCI, Pos, Scan, Frag:
Crude extract (pos. MS chromatogram)
MSD2 450, EIC=100:800 (C:\CHEM32\1\DATA\PROJEKTE\CHUNLAN HONG\PS FREE AND EASY_AG35_HCOOH.D) APCI, Neg, Scan, Frag:
Crude extract (neg. MS chromatogram)
DAD1 B, Sig=250,16 Ref=550,100 (PROJEKTE\CHUNLAN HONG\PS FREE AND EASY-2_HCOOH_AG35.D)
Paeoniflorin (250 nm chromatogram)
Area: 684.582
MSD1 450, EIC=100:800 (C:\CHEM32\1\DATA\PROJEKTE\CHUNLAN HONG\PS FREE AND EASY-2_HCOOH_AG35.D) APCI, Pos, Scan, Fra
Crude extract (neg. MS spectrum at 16.8 min)
Area: 9.2232e+006
MSD2 450, EIC=100:800 (C:\CHEM32\1\DATA\PROJEKTE\CHUNLAN HONG\PS FREE AND EASY-2_HCOOH_AG35.D) APCI, Neg, Scan, Fra
Paeoniflorin (pos. MS chromatogram)
Area: 1.26553e+007
mAU
min

Paeoniflorin: negative MS-spectrum (comparison of corresponding MS spectrum)

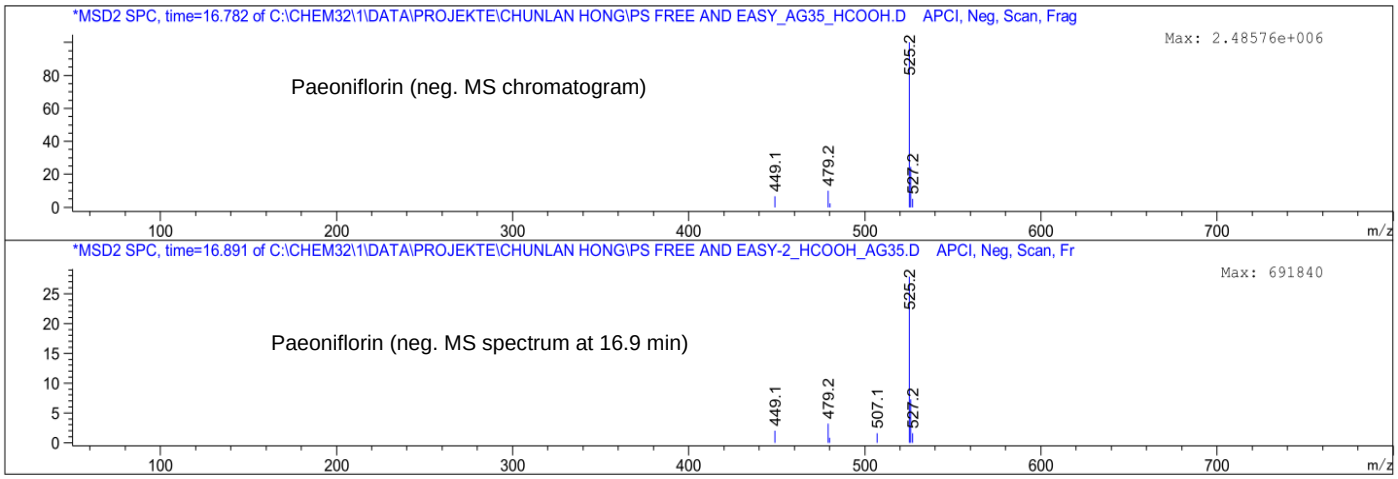

7.2.3 FAEW-3 Liquiritin

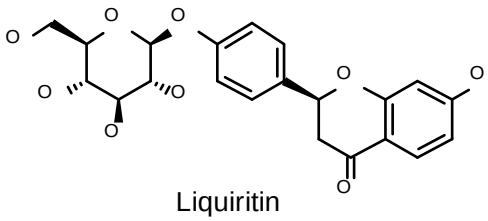

Liquiritin
FEW-3

Yellow oil, [α]D29= –41.8 (c = 0.10, MeOH), ESI-MS m/z = 441.1 [M+Na]+ , HR-ESI-MS m/z = 441.1161 calculated for [C21H22O9+Na]+; found: 441.1169

1H NMR, COSY (600 MHz, Methanol-d4) δ 7.74 (d, J = 8.7 Hz, 1H, H-5), 7.48 – 7.39 (m, 2H, H-2‘/H-6‘), 7.16 – 7.13 (m, 2H, H-3‘/H-5‘), 6.51 (dd, J = 8.7, 2.3 Hz, 1H, H-6), 6.37 (d, J = 2.3 Hz, 1H, H-8), 5.49 – 5.43 (m, 1H, H-2), 4.95 – 4.93 (m, 1H, H-1‘‘), 3.98 – 3.91 (m, 1H, H-6‘‘), 3.70 (dd, J = 12.1, 5.8 Hz, 1H, H-6‘‘), 3.49 – 3.43 (m, 3H, H-3‘‘, H-2‘‘, H-5‘‘), 3.41 – 3.37 (m, 1H, H-4‘‘), 3.05 (dd, J = 16.9, 12.9 Hz, 1H, H-3), 2.74 (dd, J = 16.9, 3.0 Hz, 1H, H-3).

13C NMR, HSQC, HMBC (151 MHz, MeOD) δ 193.19 (C-4), 166.82 (C-7), 165.42 (C-8a), 159.25 (C-4‘), 134.44 (C-1‘), 129.87 (C-5), 128.78 (C-2‘/C-6‘), 117.78, 117.76 (C-3‘/C-5‘), 115.00 (C-4a), 111.80 (C-6), 103.81 (C-8), 102.17 (C-1‘‘), 80.74 (C-2), 78.19 (C-5‘‘), 77.97 (C-3‘‘), 74.89 (C-2‘‘), 71.35 (C-4‘‘), 62.48 (C-6‘‘), 45.00 (C-3).

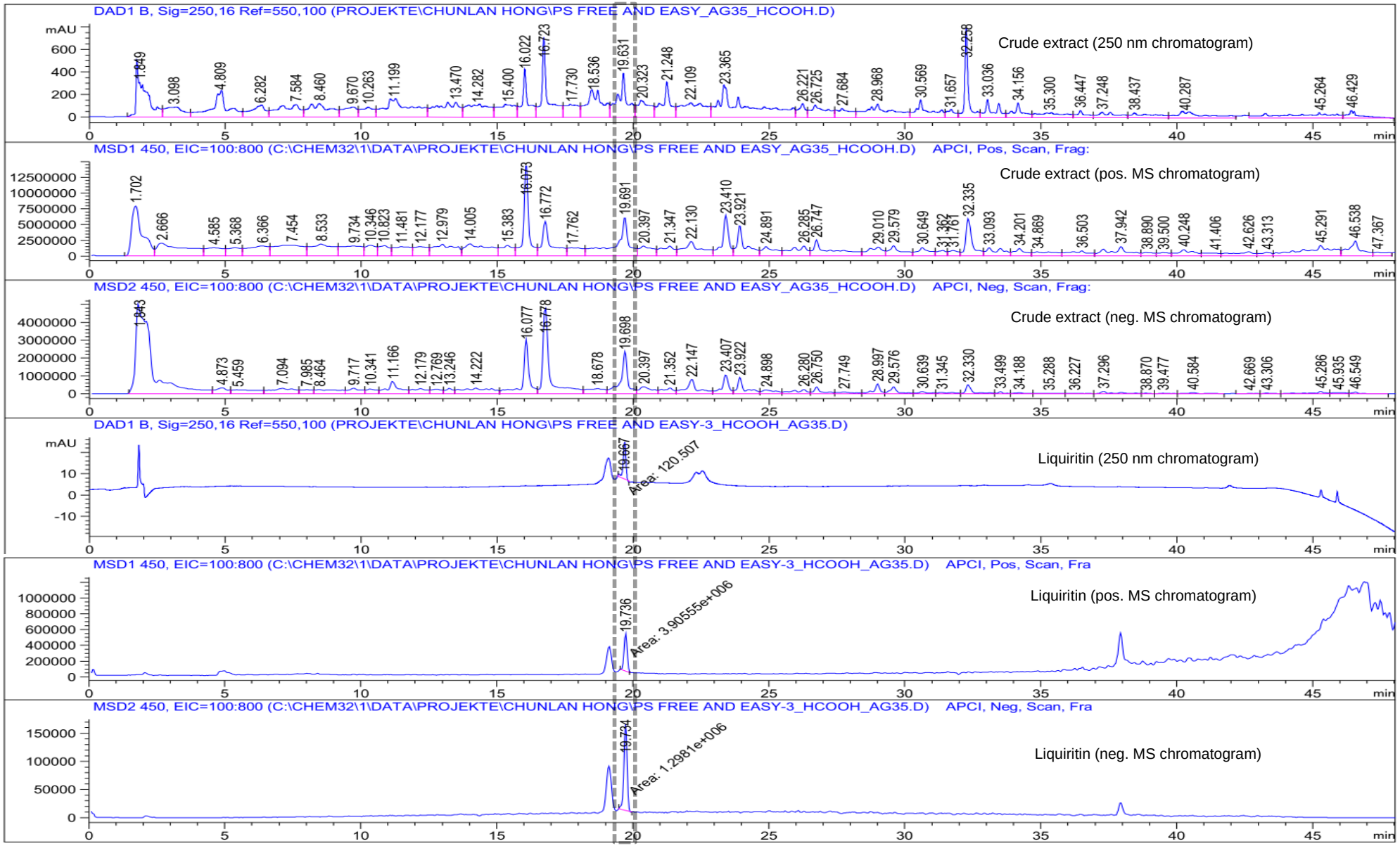
DAD1 B, Sig=250,16 Ref=550,100 (PROJEKTE\CHUNLAN HONG\PS FREE AND EASY_AG35_HCOOH.D)
Crude extract (250 nm chromatogram)
MSD1 450, EIC=100:800 (C:\CHEM32\1\DATA\PROJEKTE\CHUNLAN HONG\PS FREE AND EASY_AG35_HCOOH.D) APCI, Pos, Scan, Frag:
Crude extract (pos. MS chromatogram)
MSD2 450, EIC=100:800 (C:\CHEM32\1\DATA\PROJEKTE\CHUNLAN HONG\PS FREE AND EASY_AG35_HCOOH.D) APCI, Neg, Scan, Frag:
Crude extract (neg. MS chromatogram)
DAD1 B, Sig=250,16 Ref=550,100 (PROJEKTE\CHUNLAN HONG\PS FREE AND EASY-3_HCOOH_AG35.D)
Area: 120.507
Liquiritin (250 nm chromatogram)
MSD1 450, EIC=100:800 (C:\CHEM32\1\DATA\PROJEKTE\CHUNLAN HONG\PS FREE AND EASY-3_HCOOH_AG35.D) APCI, Pos, Scan, Fra
Area: 3.90555e+006
Liquiritin (pos. MS chromatogram)
MSD2 450, EIC=100:800 (C:\CHEM32\1\DATA\PROJEKTE\CHUNLAN HONG\PS FREE AND EASY-3_HCOOH_AG35.D) APCI, Neg, Scan, Fra
Area: 1.29816e+006
Liquiritin (neg. MS chromatogram)
mAU
min

Liquiritin: MS-spectra (comparison of corresponding MS spectra)

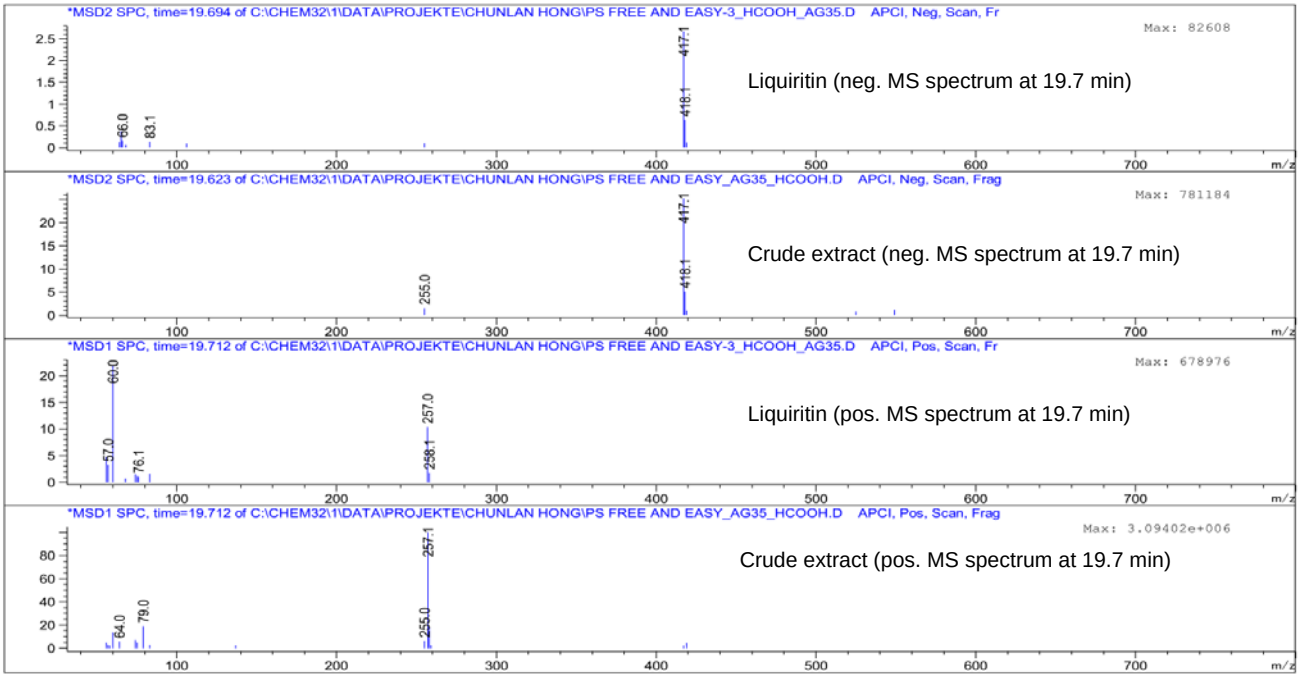

7.2.4 FAEW-4 Baicalin

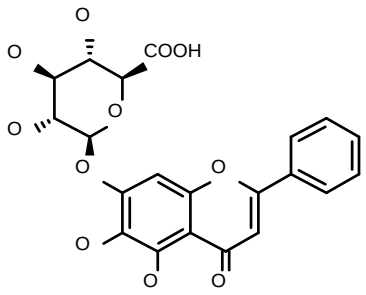

Baicalin
FEW-4

Yellow oil, [α]D29= –46.0 (c = 0.05, H2O), ESI-MS m/z = 447.1 [M+H]+ , HR-ESI-MS m/z = 469.0747 calculated for [C21H18O11+Na]+; found: 469.0744

1H NMR, COSY (600 MHz, Deuterium Oxide) δ 7.86 (br, 1H, H-2'/H-6'), 7.53 (br, 1H, H-4'), 7.47 (br, 2H, H-3'/H-5'), 6.90 (s, 1H, H-8), 6.69 (s, 1H, H-3), 5.19 (d, J = 7.7 Hz, 1H, H-1''), 3.96 (d, J = 9.5 Hz, 1H, H-5''), 3.72 (t, J = 8.5 Hz, 1H, H-2''), 3.69 – 3.65 (m, 1H, H-3''), 3.62 (t, J = 9.5 Hz, H-4'').

13C NMR, HSQC, HMBC (151 MHz, D2O) δ 175.18 (COOH), 150.26 (C-7 or 8a), 132.08 (C-4') , 128.94 (C-3'/C-5'), 126.25 (C-2'/C-6'), 106.55 (C-4a), 104.17 (C-3), 99.73 (C-1''), 94.29 (C-8), 76.48 (C-5''), 74.94 (C-3''), 72.39 (C-2''), 71.59 (C-4'').

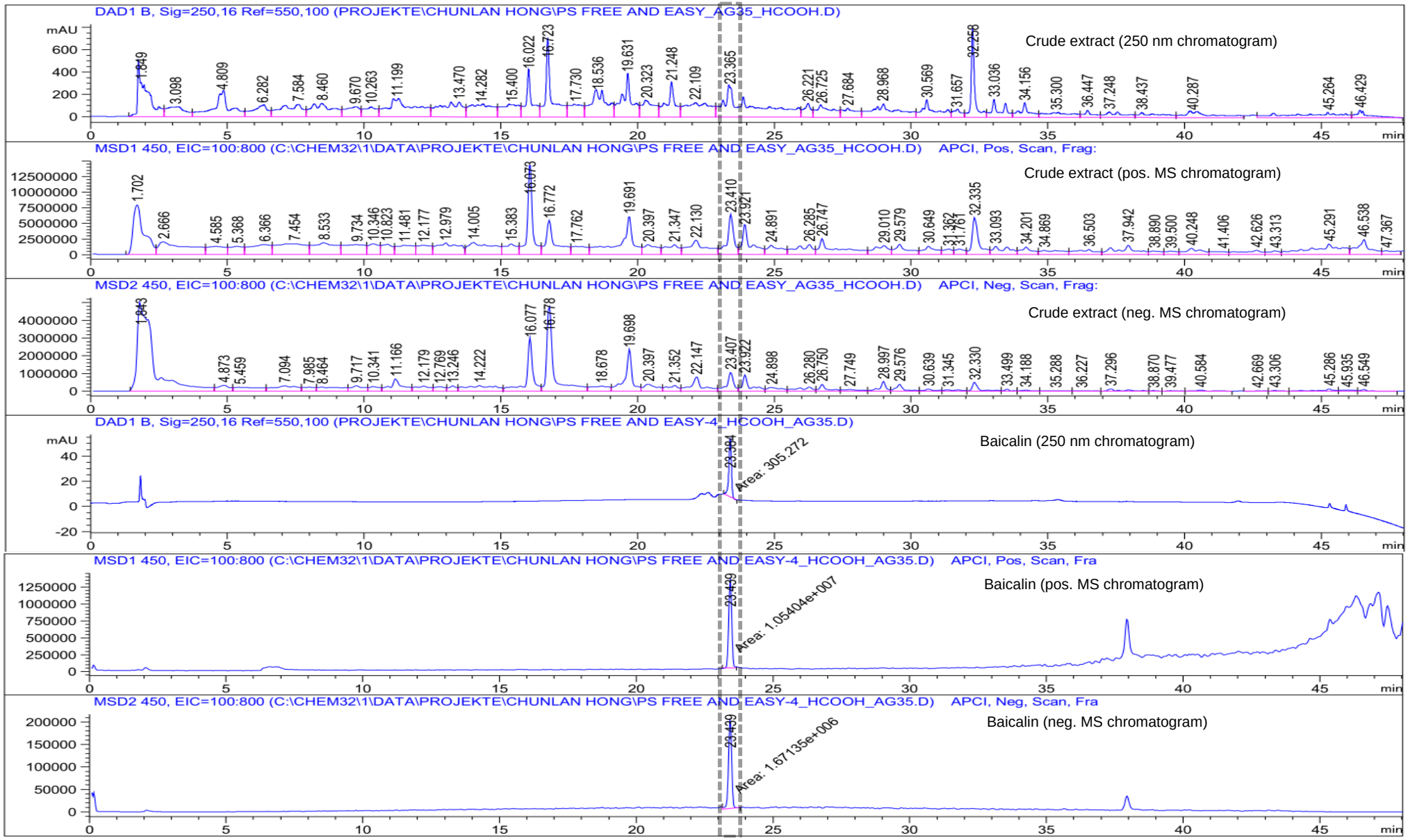
DAD1 B, Sig=250,16 Ref=550,100 (PROJEKTE\CHUNLAN HONG\PS FREE AND EASY_AG35_HCOOH.D)
Crude extract (250 nm chromatogram)
MSD1 450, EIC=100:800 (C:\CHEM32\1\DATA\PROJEKTE\CHUNLAN HONG\PS FREE AND EASY_AG35_HCOOH.D) APCI, Pos, Scan, Frag:
Crude extract (pos. MS chromatogram)
MSD2 450, EIC=100:800 (C:\CHEM32\1\DATA\PROJEKTE\CHUNLAN HONG\PS FREE AND EASY_AG35_HCOOH.D) APCI, Neg, Scan, Frag:
Crude extract (neg. MS chromatogram)
DAD1 B, Sig=250,16 Ref=550,100 (PROJEKTE\CHUNLAN HONG\PS FREE AND EASY-4_HCOOH_AG35.D)
Baicalin (250 nm chromatogram)
Area: 305.272
MSD1 450, EIC=100:800 (C:\CHEM32\1\DATA\PROJEKTE\CHUNLAN HONG\PS FREE AND EASY-4_HCOOH_AG35.D) APCI, Pos, Scan, Fra
Baicalin (pos. MS chromatogram)
Area: 1.05404e+007
MSD2 450, EIC=100:800 (C:\CHEM32\1\DATA\PROJEKTE\CHUNLAN HONG\PS FREE AND EASY-4_HCOOH_AG35.D) APCI, Neg, Scan, Fra
Baicalin (neg. MS chromatogram)
Area: 1.67135e+006
mAU
min

Baicalin: MS-spectra (comparison of corresponding MS spectra)

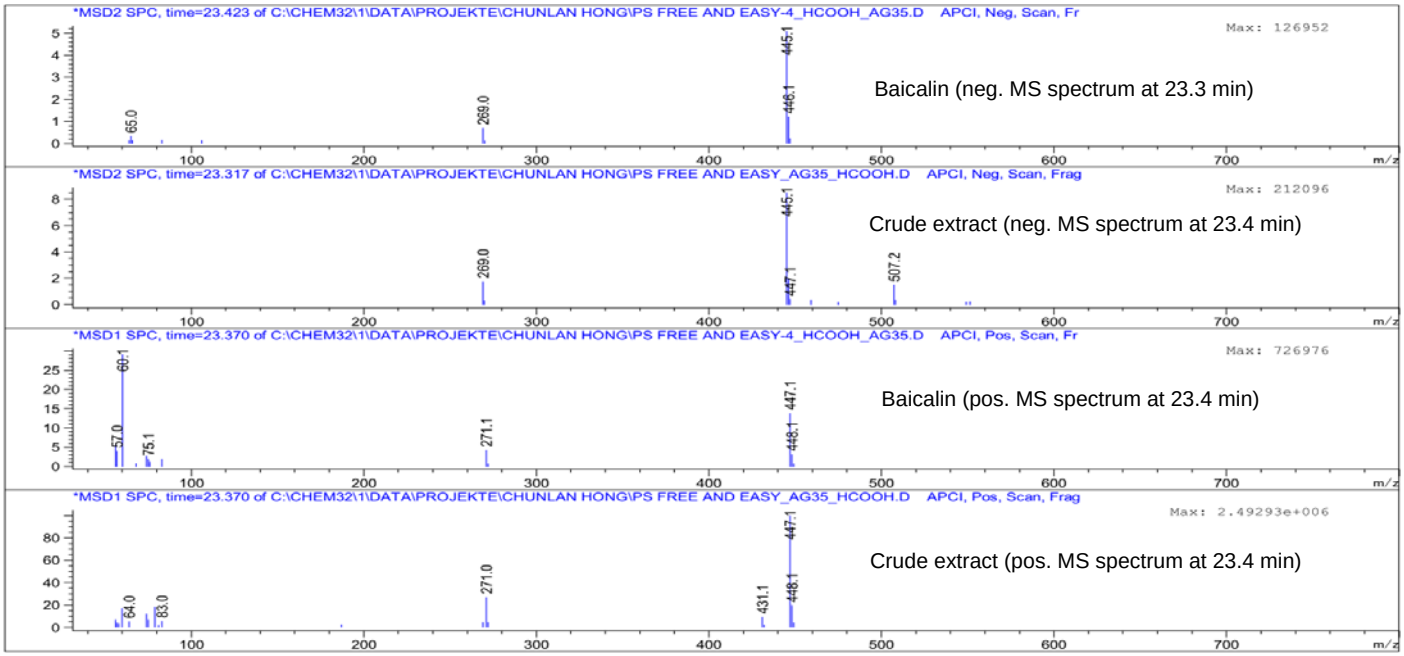

7.2.5 FAEW-5 Pentagalloyl-glucopyranose

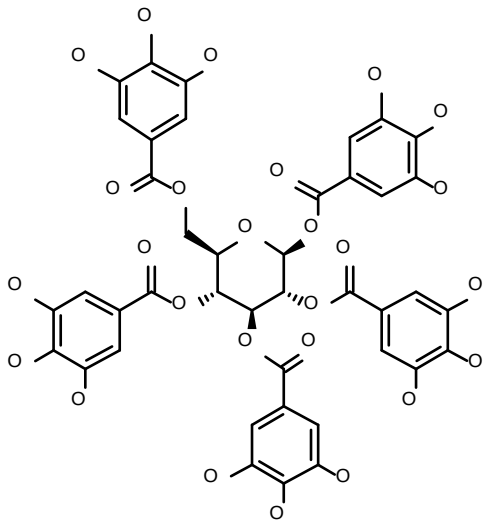

Pentagalloyl-glucopyranose
FEW-5

Brown oil, $[\alpha]_D^{29}$= +17.4 (*c* = 0.13, MeOH), ESI-MS *m/z* = 941.1 $[M+H]^+$, HR-ESI-MS *m/z* = 963.1079 calculated for $[C_{41}H_{32}O_{26}+Na]^+$; found: 963.1052

^{1}H NMR, COSY (600 MHz, Methanol-*d*$_4$) δ 7.11 (s, 2H, H-2e/H-6e), 7.05 (s, 1H, H-2a/H-6a), 6.98 (s, 2H, H-2d/H-6d), 6.95 (s, 2H, H-2b/H-6b), 6.90 (s, 2H, H-2c/H-6c), 6.24 (d, *J* = 8.3 Hz, 1H, H-1), 5.91 (t, *J* = 9.7 Hz, 1H, H-3), 5.64 – 5.57 (m, 2H, H-4, H-2), 4.51 (dd, *J* = 12.3, 1.9 Hz, 1H, H-6), 4.43 – 4.36 (m, 2H, H-5, H-6).

^{13}C NMR, HSQC, HMBC (151 MHz, MeOD) δ 167.91 (C-1e-*C*O), 167.28 (C-1c-*C*O), 167.01 (C-1b-*C*O), 166.91 (C-1d-*C*O), 166.20 (C-1a-*C*O), 146.54 (C-

3a/C-5a), 146.47 (C-3e/C-5e), 146.43 (C-3d/C-5d), 146.37 (C-3b/C-5b), 146.27 (C-3c/C-5c), 140.75 (C-4a), 140.34 (C-4d), 140.29 (C-4b), 140.11 (C-4c), 140.00 (C-4e), 121.01 (C-1e), 120.33 (C-1c), 120.21 (C-1d), 120.17 (C-1b), 119.70 (C-1a), 110.58 (C-2a/C-6a), 110.43 (C-2d/C-6d), 110.37 (C-2b/C-6b), 110.34 (C-2c/C-6c), 110.30 (C-2e/C-6e), 93.80 (C-1), 74.40 (C-5), 74.10 (C-3), 72.17 (C-2), 69.77 (C-4), 63.10 (C-6).

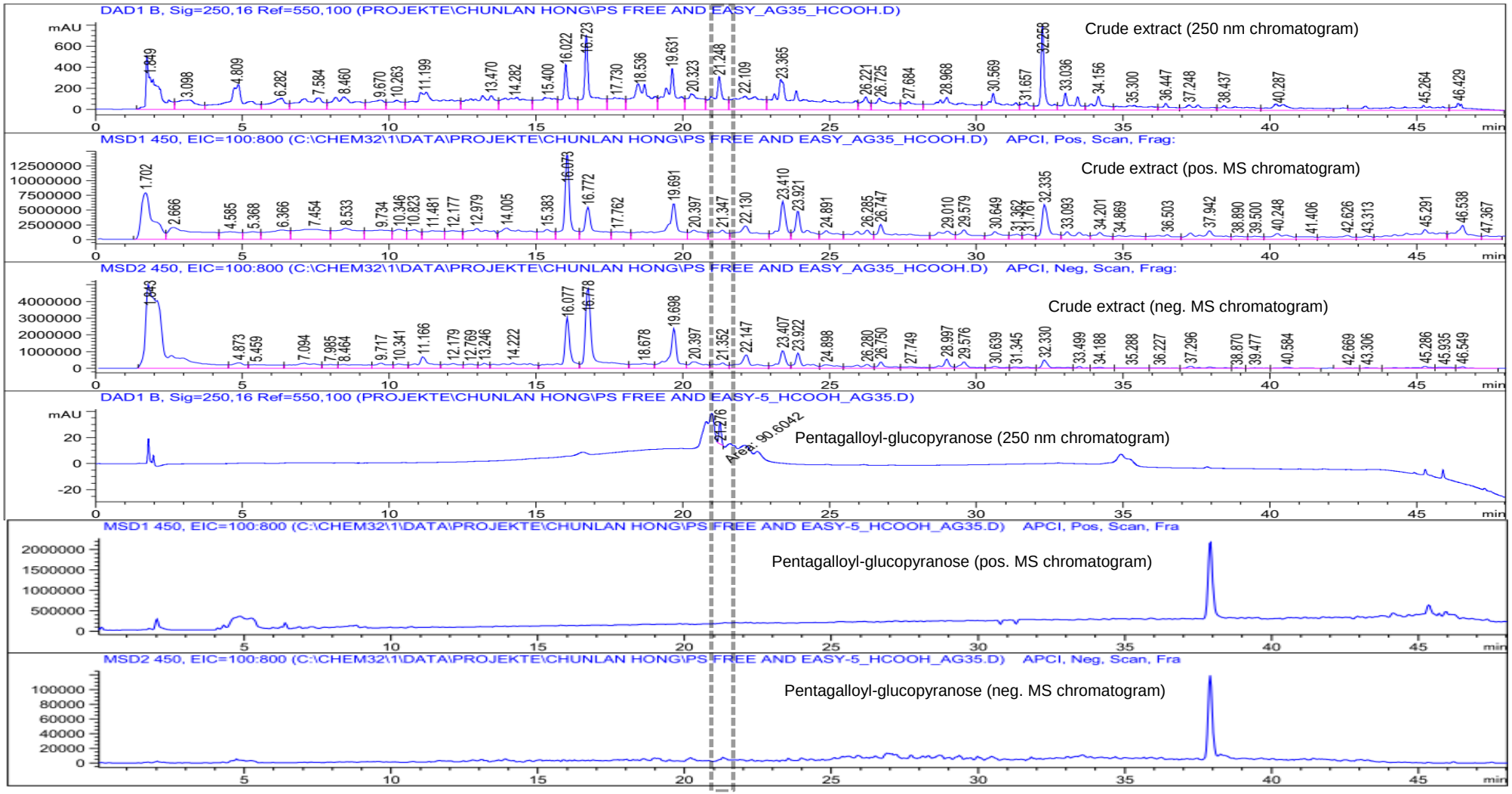

Pentagalloyl-glucopyranose: UV/vis-spectra (comparison of corresponding UV/vis spectra, no mass data was available)

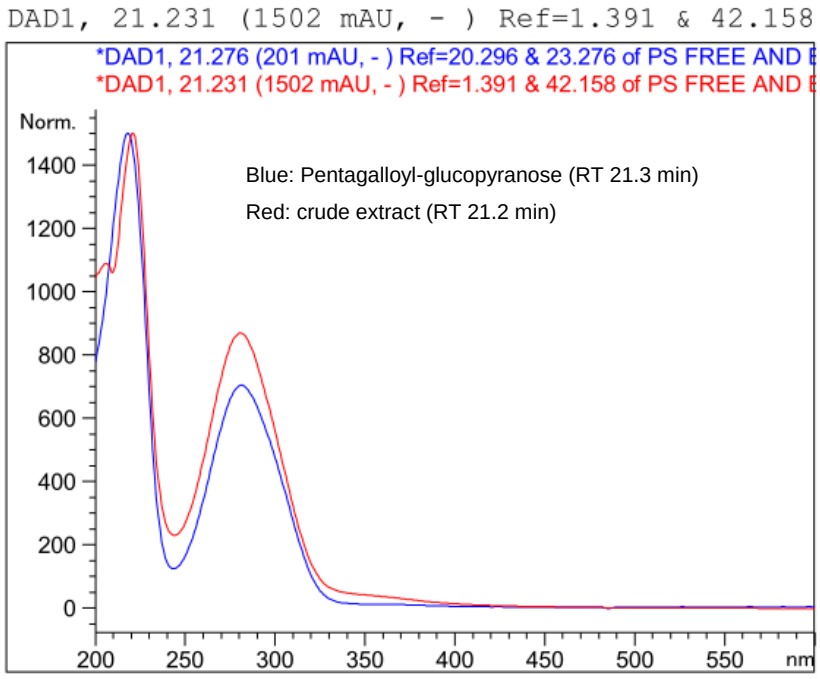

7.2.6 FAEW-6 Isoliquiritin apioside / Ononin

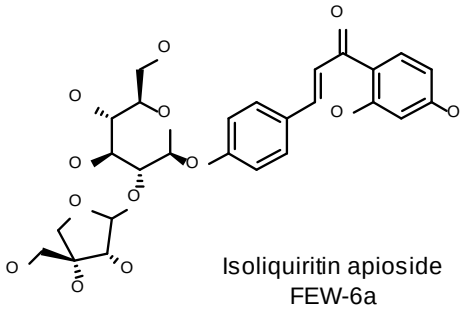

Isoliquiritin apioside
FEW-6a

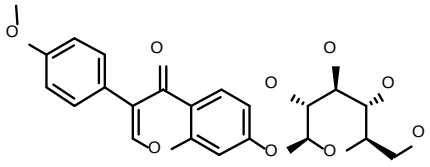

Ononin
FEW-6b

Brown oil, ESI-MS *m/z* = 551.3 $[M+H]^+$, HR-ESI-MS *m/z* = 573.1584 calculated for $[C_{26}H_{30}O_{13}+Na]^+$; found: 573.1595

^{1}H NMR, COSY (600 MHz, Methanol-d_4) δ 8.00 (d, *J* = 8.9 Hz, 1H, H-6‘), 7.82 (d, *J* = 15.3 Hz, 1H, H-3), 7.75 – 7.69 (m, 3H, H-2‘‘/H-6‘‘, H-2), 7.15 – 7.12 (m, 2H, H-3‘‘/H-5‘‘), 6.43 (dd, *J* = 8.9, 2.4 Hz, 1H, H-5‘), 6.30 (d, *J* = 2.4 Hz, 1H, H-3‘), 5.47 (d, *J* = 1.6 Hz, 1H, H-1^{iv}), 5.06 (d, *J* = 7.6 Hz, 1H, H-1’’’), 4.06 (d, J = 9.6 Hz, 1H, H-4^{iv}), 3.95 (d, *J* = 1.6 Hz, 1H, H-2^{iv}), 3.94 – 3.89 (m, 1H, H-6’’’), 3.81 (d, *J* = 9.6 Hz, 1H, H-4d), 3.74 – 3.69 (m, 1H, H-6’’’), 3.67 (dd, *J* = 9.0 Hz, 7.6 Hz, 1H, H-2c), 3.62 (t, *J* = 9.0 Hz, 1H, H-3c), 3.58 – 3.54 (m, 1H, H-5’’’ or H-5‘‘ Ononin), 3.54 (d, *J* = 2.1 Hz, 2H, H-5^{iv}), 3.50 – 3.46 (m, 1H, H-5’’’ or H-5‘‘ Ononin), 3.43 – 3.38 (m, 1H, H-4’’’).

^{13}C NMR, HSQC, HMBC (151 MHz, MeOD) δ 193.36 (C-1), 167.61 (C-2‘), 166.54 (C-4‘), 160.95 (C-4‘‘), 144.82 (C-3), 133.50 (C-6‘), 131.46 (C-2‘‘/C-6‘‘), 130.49 (C-1‘‘), 120.03 (C-2), 117.84 (C-3‘‘/C-5‘‘), 114.67 (C-1‘), 110.82 (C-1^{iv}), 109.20 (C-5‘), 103.79 (C-3‘), 100.43 (C-1‘‘‘),

80.76 (C-3^{iv}), 78.60 (C-3‘‘‘), 78.57 (C-2‘‘‘), 78.42 (C-5’’ Ononin or C-5‘‘‘), 78.17 (C-5’’ Ononin or C-5‘‘‘), 78.05 (C-2^{iv}), 75.47 (C-4^{iv}), 71.33 (C-4‘‘‘ or C-4‘‘ Ononin), 71.23 (C-4‘‘‘ or C-4‘‘ Ononin), 66.00 (C-5d^{iv}), 62.43 (C-6’’’).

ESI-MS *m/z* = 431.2 $[M+H]^+$, HR-ESI-MS *m/z* = 453.1161 calculated for $[C_{22}H_{22}O_9+Na]^+$; found: 453.1172

^{1}H NMR, COSY (600 MHz, Methanol-d_4) δ 8.24 (s, 1H, H-2), 8.16 (d, *J* = 8.9 Hz, 1H, H-5), 7.52 – 7.48 (m, 2H, H-2‘/H-6‘), 7.26 (d, *J* = 2.3 Hz, 1H, H-8), 7.23 (dd, *J* = 8.9, 2.3 Hz, 1H, H-6), 7.02 – 6.98 (m, 2H, H-3‘/H-5‘), 5.13 – 5.10 (m, 1H, H-1‘‘), 3.94 – 3.89 (m, 1H, H-6‘‘), 3.83 (s, 3H, C-4‘-OMe), 3.74 – 3.69 (m, 1H, H-6‘‘), 3.58 – 3.54 (m, 1H, H-5’’ or H-5‘‘’ FEW-6a), 3.53 – 3.51 (m, 2H, H-2‘‘, H-3‘‘), 3.50 – 3.46 (m, 1H, H-5’’ or H-5‘‘‘ FEW-6a), 3.43 – 3.38 (m, 1H, H-4‘‘).

^{13}C NMR, HSQC, HMBC (151 MHz, MeOD) δ 177.97 (C-4), 163.53 (C-7), 161.20 (C-4‘), 159.25 (C-8a), 155.26 (C-2), 131.37 (C-2’/C-6’), 128.30 (C-5), 125.97 (C-3), 125.29 (C-1’), 120.21 (C-4a), 117.08 (C-6), 114.86 (C-3’/C-5’), 104.94 (C-8), 101.79 (C-1‘‘), 78.42 (C-5’’ or C-5‘‘‘ FEW-6a), 78.17 (C-5’’ or C-5’’’ FEW-6a), 77.84 (C-3‘‘), 74.73 (C-2‘‘), 71.33 (C-4’’ or C-4‘‘’ FEW-6a), 71.23 (C-4’’ or C-4’‘‘ FEW-6a), 62.43 (C-6‘‘), 55.73 (C-4‘-*Me*).

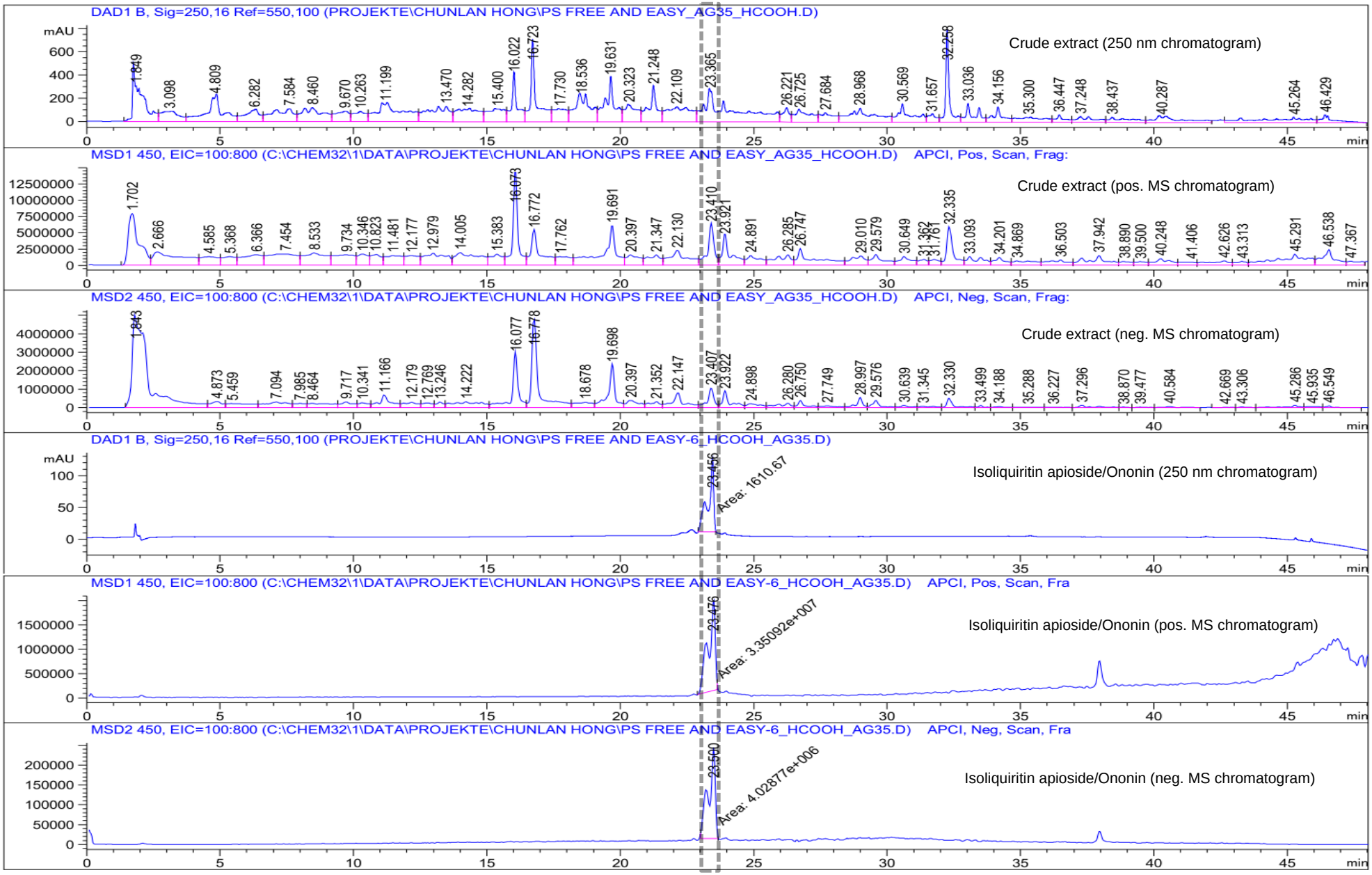
DAD1 B, Sig=250,16 Ref=550,100 (PROJEKTE\CHUNLAN HONG\PS FREE AND EASY_AG35_HCOOH.D)
Crude extract (250 nm chromatogram)
MSD1 450, EIC=100:800 (C:\CHEM32\1\DATA\PROJEKTE\CHUNLAN HONG\PS FREE AND EASY_AG35_HCOOH.D) APCI, Pos, Scan, Frag:
Crude extract (pos. MS chromatogram)
MSD2 450, EIC=100:800 (C:\CHEM32\1\DATA\PROJEKTE\CHUNLAN HONG\PS FREE AND EASY_AG35_HCOOH.D) APCI, Neg, Scan, Frag:
Crude extract (neg. MS chromatogram)
DAD1 B, Sig=250,16 Ref=550,100 (PROJEKTE\CHUNLAN HONG\PS FREE AND EASY-6_HCOOH_AG35.D)
Isoliquiritin apioside/Ononin (250 nm chromatogram)
Area: 1610.67
MSD1 450, EIC=100:800 (C:\CHEM32\1\DATA\PROJEKTE\CHUNLAN HONG\PS FREE AND EASY-6_HCOOH_AG35.D) APCI, Pos, Scan, Fra
Isoliquiritin apioside/Ononin (pos. MS chromatogram)
Area: 3.35092e+007
MSD2 450, EIC=100:800 (C:\CHEM32\1\DATA\PROJEKTE\CHUNLAN HONG\PS FREE AND EASY-6_HCOOH_AG35.D) APCI, Neg, Scan, Fra
Isoliquiritin apioside/Ononin (neg. MS chromatogram)
Area: 4.02877e+006
mAU
min

Isoliquiritin apioside/Ononin: negative MS-spectrum (comparison of corresponding MS spectrum)

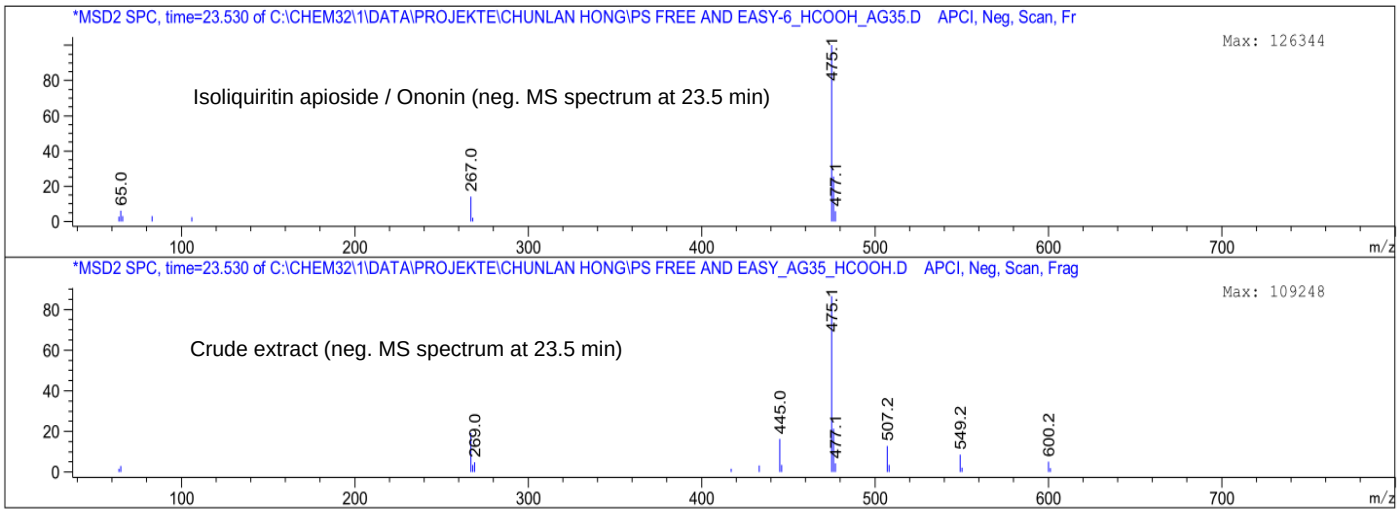

7.2.7 FAEW-7 Isoliquiritin

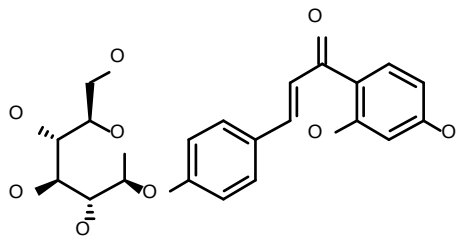

Isoliquiritin
FEW-7

Brown oil, [α]D29= –35.4 (c = 0.16, MeOH), ESI-MS m/z = 419.2 [M+H]+, HR-ESI-MS m/z = 441.1161 calculated for [C21H22O9+Na]+; found: 441.1167

1H NMR, COSY (600 MHz, Methanol-d4) δ 8.00 (d, J = 9.0 Hz, 1H, H-6‘), 7.82 (d, J = 15.4 Hz, 1H, H-3), 7.75 – 7.69 (m, 3H, H-2‘‘/H-6‘‘, H-2), 7.19 – 7.14 (m, 2H, H-3‘‘/H-5‘‘), 6.43 (dd, J = 9.0, 2.4 Hz, 1H, H-5‘), 6.30 (d, J = 2.4 Hz, 1H, H-3‘), 5.00 (dd, J = 5.4, 2.2 Hz, 1H, H-1‘‘‘), 3.91 (dd, J = 12.1, 2.3 Hz, 1H, H-6‘‘‘), 3.71 (dd, J = 12.1, 5.7 Hz, 1H, H-6‘‘‘), 3.51 – 3.46 (m, 3H, H-2’’’, H-3’’’, H-5’’’), 3.43 – 3.37 (m, 1H, H-4’’’).

13C NMR, HSQC, HMBC (151 MHz, MeOD) δ 193.37 (C-1), 167.62 (C-2‘), 166.54 (C-4‘), 161.08 (C-4‘‘), 144.83 (C-3), 133.50 (C-6‘), 131.42 (C-2‘‘/C-6‘‘), 130.53 (C-1‘‘), 120.03 (C-2), 117.99 (C-3‘‘/C-5‘‘), 114.67 (C-1‘), 109.20 (C-5‘), 103.78 (C-3‘), 101.80 (C-1‘‘‘), 78.28 (C-5‘‘‘), 77.95 (C-3‘‘‘), 74.83 (C-2‘‘‘), 71.29 (C-4‘‘‘), 62.46 (C-6‘‘‘).

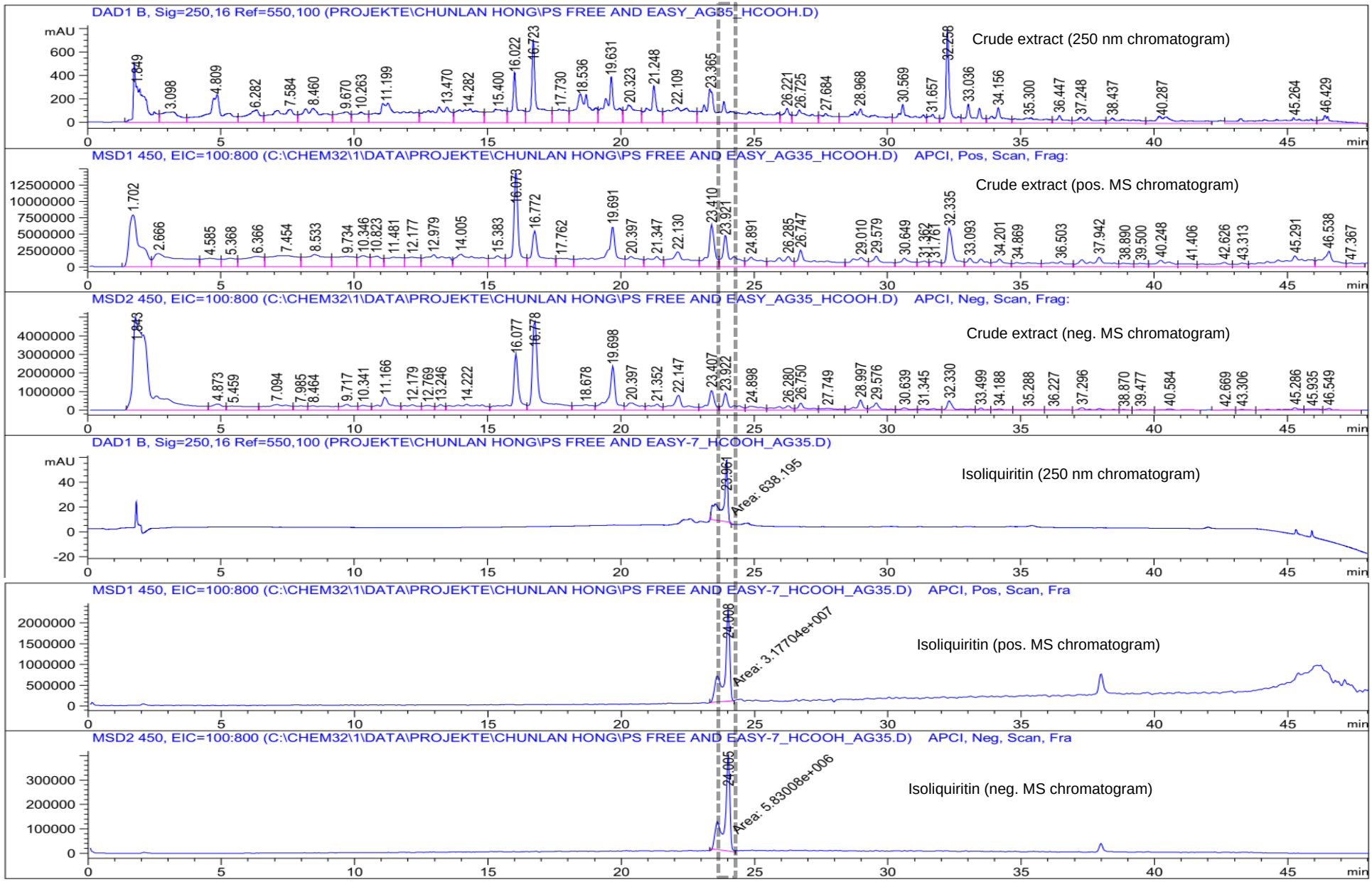
DAD1 B, Sig=250,16 Ref=550,100 (PROJEKTE\CHUNLAN HONG\PS FREE AND EASY_AG35_HCOOH.D)
Crude extract (250 nm chromatogram)
MSD1 450, EIC=100:800 (C:\CHEM32\1\DATA\PROJEKTE\CHUNLAN HONG\PS FREE AND EASY_AG35_HCOOH.D) APCI, Pos, Scan, Frag:
Crude extract (pos. MS chromatogram)
MSD2 450, EIC=100:800 (C:\CHEM32\1\DATA\PROJEKTE\CHUNLAN HONG\PS FREE AND EASY_AG35_HCOOH.D) APCI, Neg, Scan, Frag:
Crude extract (neg. MS chromatogram)
DAD1 B, Sig=250,16 Ref=550,100 (PROJEKTE\CHUNLAN HONG\PS FREE AND EASY-7_HCOOH_AG35.D)
Area: 638.195
Isoliquiritin (250 nm chromatogram)
MSD1 450, EIC=100:800 (C:\CHEM32\1\DATA\PROJEKTE\CHUNLAN HONG\PS FREE AND EASY-7_HCOOH_AG35.D) APCI, Pos, Scan, Fra
Area: 3.17704e+007
Isoliquiritin (pos. MS chromatogram)
MSD2 450, EIC=100:800 (C:\CHEM32\1\DATA\PROJEKTE\CHUNLAN HONG\PS FREE AND EASY-7_HCOOH_AG35.D) APCI, Neg, Scan, Fra
Area: 5.83008e+006
Isoliquiritin (neg. MS chromatogram)
mAU
min

Isoliquiritin: MS-spectra (comparison of corresponding MS spectra)

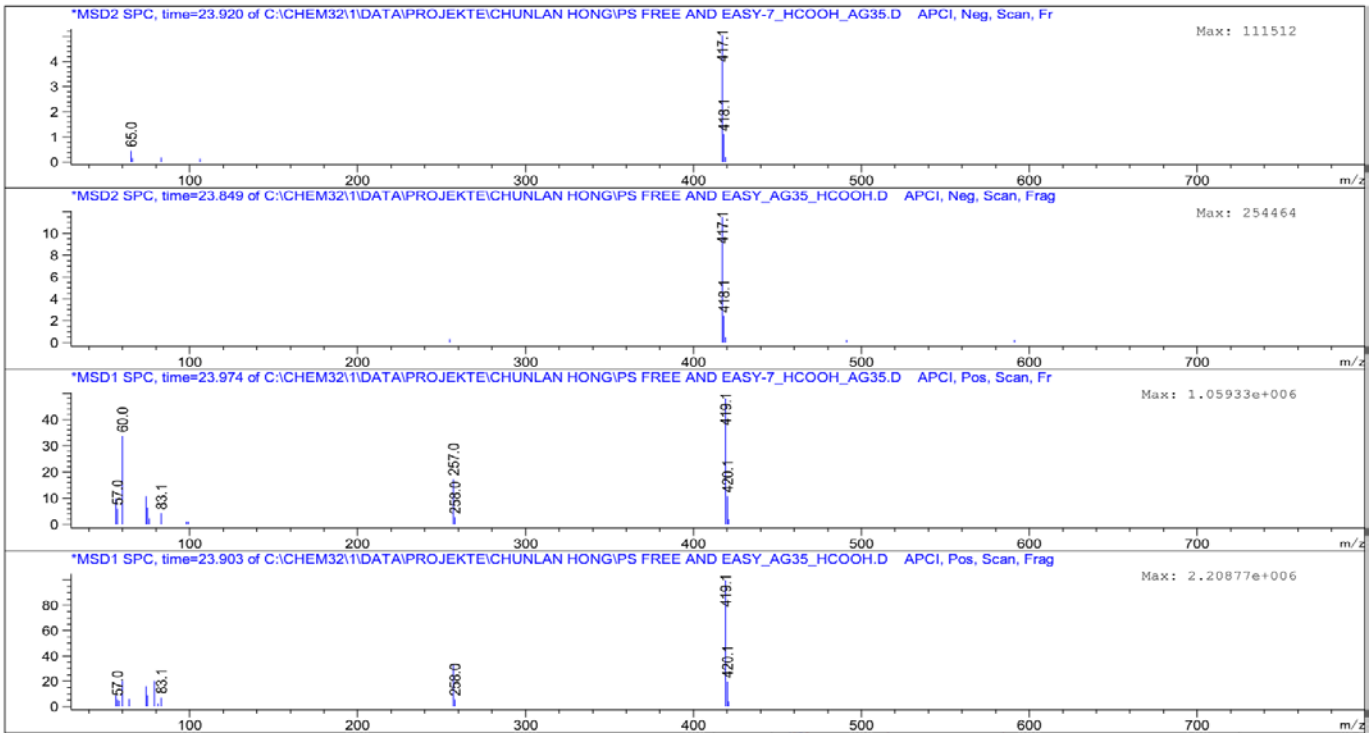

7.2.8 FAEW-8 β-Hydroxy-DHP

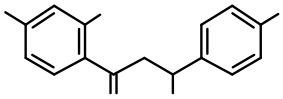

β-Hydroxy-DHP
FEW-8

Yellow oil, [α]D29= –8.9 (c = 0.06, MeOH), ESI-MS m/z = 256.1 [M-H2O +H]+ , HR-ESI-MS m/z = 279.0633 calculated for [C15H14O5–H2O +Na]+; found: 279.0645

1H NMR, COSY (600 MHz, Methanol-d4) δ 7.74 (d, J = 8.7 Hz, 1H, H-6), 7.35 – 7.31 (m, 2H, H-2‘/H-6‘), 6.86 – 6.79 (m, 2H, H-3‘/H-5‘), 6.50 (dd, J = 8.7, 2.3 Hz, 1H, H-5), 6.36 (d, J = 2.3 Hz, 1H, H-3), 5.39 (dd, J = 13.2, 2.9 Hz, 1H, H-β), 3.06 (dd, J = 16.9, 13.1 Hz, 1H, H-α), 2.70 (dd, J = 16.9, 2.9 Hz, 1H, H-α).

13C NMR, HSQC, HMBC (151 MHz, MeOD) δ 193.54 (C=O), 166.79 (C-2), 165.58 (C-4), 158.99 (C-4’), 131.34 (C-1’), 129.85 (C-6), 129.02 (C-2’/C-6’), 116.28 (C-3’/C-5‘), 114.97 (C-1), 111.72 (C-5), 103.79 (C-3), 81.07 (Cβ), 44.97 (Cα)

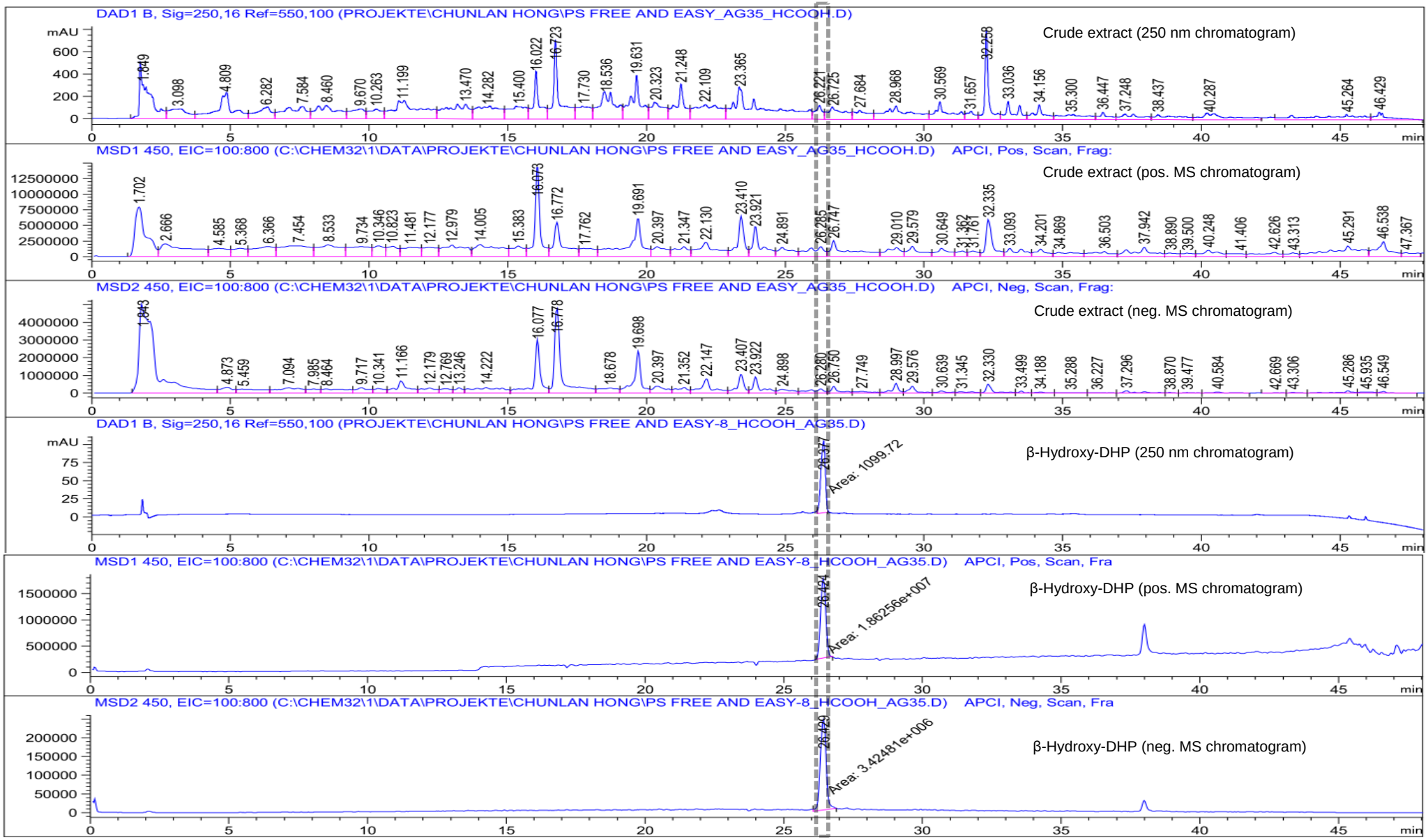
DAD1 B, Sig=250,16 Ref=550,100 (PROJEKTE\CHUNLAN HONG\PS FREE AND EASY_AG35_HCOOH.D)
Crude extract (250 nm chromatogram)
MSD1 450, EIC=100:800 (C:\CHEM32\1\DATA\PROJEKTE\CHUNLAN HONG\PS FREE AND EASY_AG35_HCOOH.D) APCI, Pos, Scan, Frag:
Crude extract (pos. MS chromatogram)
MSD2 450, EIC=100:800 (C:\CHEM32\1\DATA\PROJEKTE\CHUNLAN HONG\PS FREE AND EASY_AG35_HCOOH.D) APCI, Neg, Scan, Frag:
Crude extract (neg. MS chromatogram)
DAD1 B, Sig=250,16 Ref=550,100 (PROJEKTE\CHUNLAN HONG\PS FREE AND EASY-8_HCOOH_AG35.D)
Area: 1099.72
β-Hydroxy-DHP (250 nm chromatogram)
MSD1 450, EIC=100:800 (C:\CHEM32\1\DATA\PROJEKTE\CHUNLAN HONG\PS FREE AND EASY-8_HCOOH_AG35.D) APCI, Pos, Scan, Fra
Area: 1.86256e+007
β-Hydroxy-DHP (pos. MS chromatogram)
MSD2 450, EIC=100:800 (C:\CHEM32\1\DATA\PROJEKTE\CHUNLAN HONG\PS FREE AND EASY-8_HCOOH_AG35.D) APCI, Neg, Scan, Fra
Area: 3.42481e+006
β-Hydroxy-DHP (neg. MS chromatogram)
min

β-Hydroxy-DHP: MS-spectra (comparison of corresponding MS spectra)

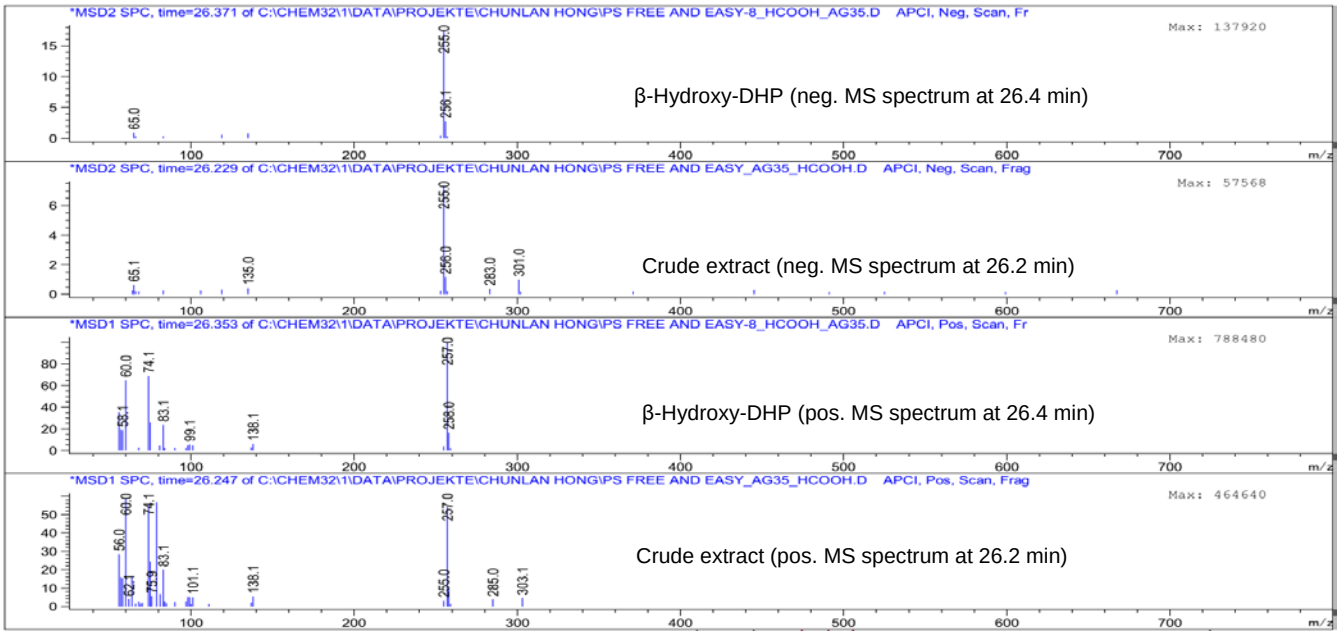

7.2.9 FAEW-9 Oroxyloside

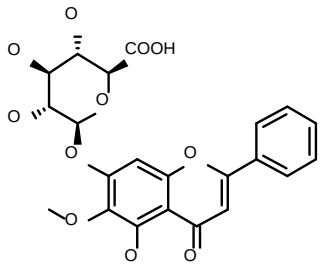

Oroxyloside
FEW-9

Brown oil, $[\alpha]_D^{29}$= –10.0 (*c* = 0.05, MeOH), ESI-MS *m/z* = 461.2 $[M+H]^+$, HR-ESI-MS *m/z* = 483.0903 calculated for $[C_{22}H_{20}O_{11}+Na]^+$; found: 483.0923

^{1}H NMR, COSY (600 MHz, Methanol-d_4) δ 8.07 (d, *J* = 7.4 Hz, 2H, H-2‘/H-6‘), 7.64 – 7.57 (m, 2H, H-3‘/H-5‘), 6.85 (s, 1H, H-3), 6.67 (s, 1H, H-8), 5.21 (d, *J* = 7.3 Hz, 1H, H-1‘‘), 4.06 (d, *J* = 7.8 Hz, H-5‘‘), 3.99 (s, 3H, C-6-O*Me*), 3.67 – 3.59 (m, 2H, H-2‘‘, H-4‘‘), 3.58 – 3.52 (m, 1H, H-3‘‘).

^{13}C NMR, HSQC, HMBC (151 MHz, MeOD) δ 184.32 (C-4), (C6‘‘ not observed), 165.97 (C-2), 158.11 (C-7), 157.73 (C-5), 151.14 (C-8a), 133.34 (C-4’), 132.48 (C-1’), 131.27 (C-6), 130.35 (C-3’/C-5’), 127.57 (C-2’/C-6’), 107.23 (C-4a), 106.20 (C-3), 101.84 (C-1‘‘), 100.34 (C-8), 77.40 (C-3‘‘), 76.67 (C-5‘‘), 74.51 (C-2‘‘), 72.93 (C-4‘‘), 62.50 (C-6-O*Me*).

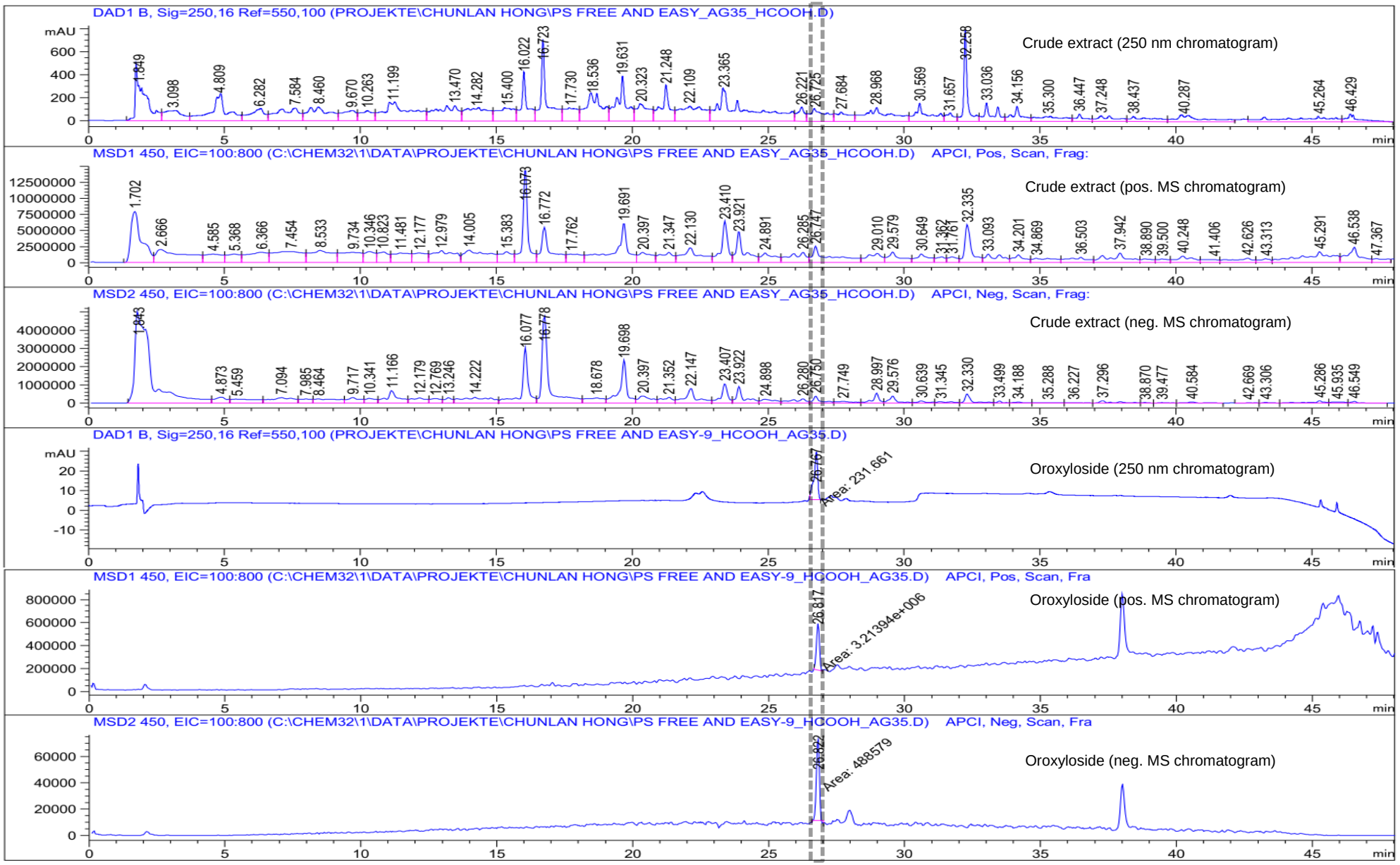
DAD1 B, Sig=250,16 Ref=550,100 (PROJEKTE\CHUNLAN HONG\PS FREE AND EASY_AG35_HCOOH.D)
Crude extract (250 nm chromatogram)
MSD1 450, EIC=100:800 (C:\CHEM32\1\DATA\PROJEKTE\CHUNLAN HONG\PS FREE AND EASY_AG35_HCOOH.D) APCI, Pos, Scan, Frag:
Crude extract (pos. MS chromatogram)
MSD2 450, EIC=100:800 (C:\CHEM32\1\DATA\PROJEKTE\CHUNLAN HONG\PS FREE AND EASY_AG35_HCOOH.D) APCI, Neg, Scan, Frag:
Crude extract (neg. MS chromatogram)
DAD1 B, Sig=250,16 Ref=550,100 (PROJEKTE\CHUNLAN HONG\PS FREE AND EASY-9_HCOOH_AG35.D)
Oroxyloside (250 nm chromatogram)
Area: 231.661
MSD1 450, EIC=100:800 (C:\CHEM32\1\DATA\PROJEKTE\CHUNLAN HONG\PS FREE AND EASY-9_HCOOH_AG35.D) APCI, Pos, Scan, Fra
Oroxyloside (pos. MS chromatogram)
Area: 3.21394e+006
MSD2 450, EIC=100:800 (C:\CHEM32\1\DATA\PROJEKTE\CHUNLAN HONG\PS FREE AND EASY-9_HCOOH_AG35.D) APCI, Neg, Scan, Fra
Oroxyloside (neg. MS chromatogram)
Area: 488579
mAU
min

Oroxyloside: MS-spectra (comparison of corresponding MS spectra)

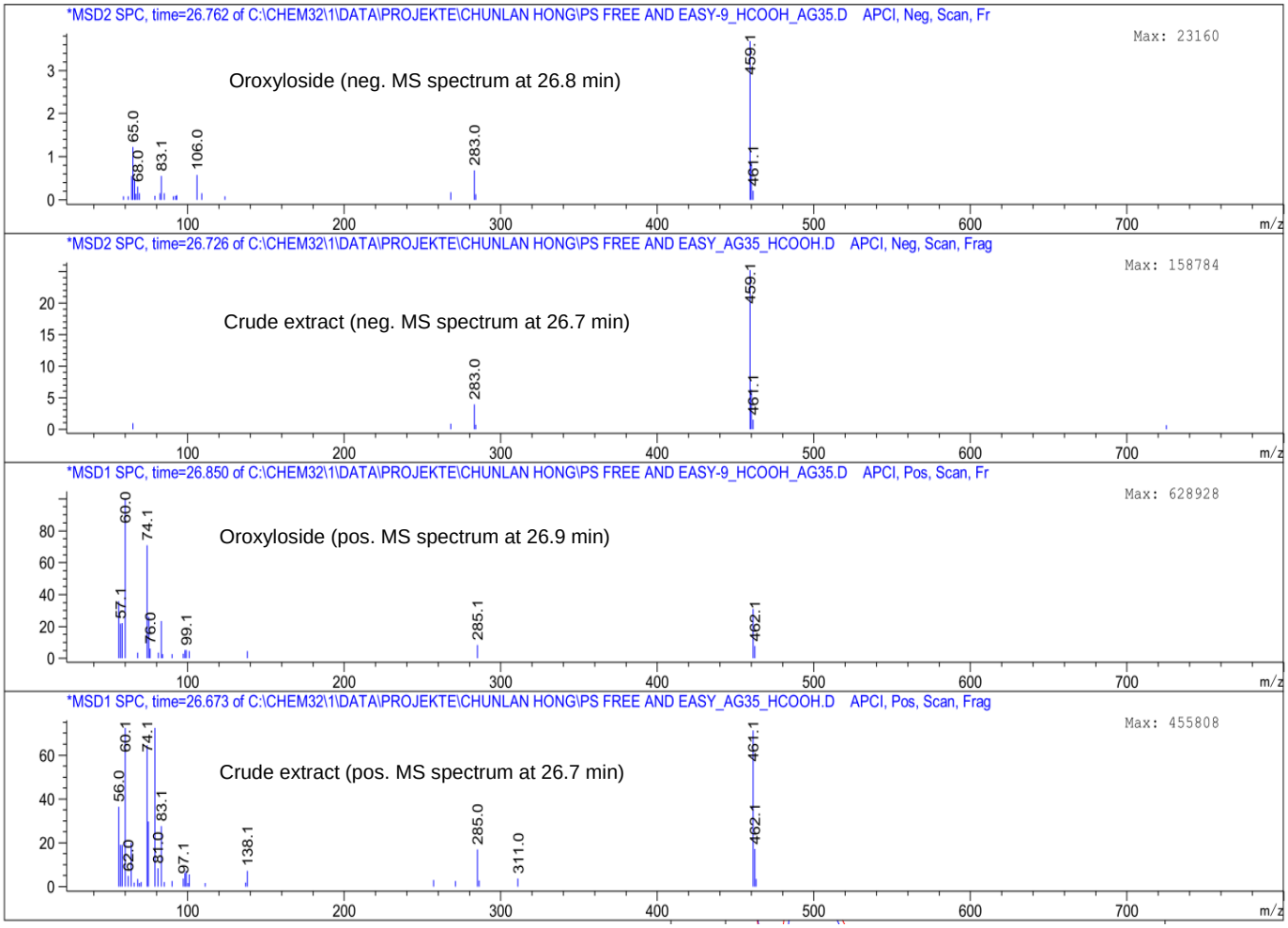

8 Appendix

8.1 Publications

Original publications as first author

- **Hong C**, Cao J, Wu CF, Kadioglu O, Schüffler A, Kauhl U, Klauck SM, Opatz T, Thines E, Paul NW, Efferth T. The Chinese herbal formula *Free and Easy Wanderer* ameliorates oxidative stress through KEAP1-NRF2/HO-1 pathway. *Sci Rep*. 2017, 7(1):11551.

- **Hong C**, Schüffler A, Kauhl U, Cao J, Wu CF, Opatz T, Thines E, Efferth T. Identification of NF-κB as Determinant of Posttraumatic Stress Disorder and Its Inhibition by the Chinese Herbal Remedy *Free and Easy Wanderer*. *Front Pharmacol*. 2017, 8: 181.

- **Hong C**, Efferth T. Systematic Review on Post-Traumatic Stress Disorder among Survivors of the Wenchuan Earthquake. *Trauma Violence Abuse*. 2016, 17(5): 542-561.

Original publications as co-author

- Efferth T, Banerjee M, Paul NW, Abdelfatah S, Arend J, Elhassan G, Hamdoun S, Hamm R, **Hong C**, Kadioglu O, Naß J, et al. Biopiracy of natural products and good bioprospecting practice. *Phytomedicine*. 2016, 23(2): 166-73

- Wu CF, **Hong C**, Klauck SM, Lin YL, Efferth T. Molecular mechanisms of rosmarinic acid from Salvia miltiorrhiza in acute lymphoblastic leukemia cells. *J Ethnopharmacol*. 2015, 176: 55-68.

Conference paper

- **Hong C**, Cao J, Efferth T. Posttraumatic stress disorder among earthquake survivors of the Wenchuan area (Sichuan, China). *Eur J Psychotraumatol*. 2014, 5: 26531.

Poster

- Sep 2-5, 2017, Paris: 30th ECNP Congress of Applied and Translational Neuroscience

Poster presentation: The application of TCM to the treatment of psychiatric disorders: *in vitro* antioxidative and anti-inflammatory effect of *free and easy wanderer*

- Jul 24-28, 2017, Mainz: International Conference on Science and Society: Biopiracy and Phytomedicine

Oral presentation: The Chinese herbal formula *Free and Easy Wanderer* ameliorates oxidative stress through KEAP1-NRF2/HO-1 pathway

- Mar 14, 2016, Mainz: “Mensch und Medizin: Kosten - Nutzen - Gesundheit?” held by Deutsche Forschungsgemeinschaft (DFG, German Research Foundation) “Life Science - Life Writing” Research Training School

Poster presentation: Life Science and Humanities: Therapeutic Approach of Posttraumatic Stress Disorder by Traditional Chinese Medicine

- Sep 27-29, 2015, Barcelona: 12th World congress of Chinese medicine

Oral presentation: Temporality, Materiality and Traditional Chinese medicine

- Dec 2-4, 2015, Prague: 15th International Forum on Mood and Anxiety Disorders

Poster presentation: A meta-analysis on microarray-based transcriptome-wide mRNA expression profiling of patients with posttraumatic stress syndrome suggesting an important role of NFκB

- Oct 17-19, 2014, Hangzhou: “Post-Traumatic Stress: State of the Art Research and Clinical Implications for China” held by the International Society for Traumatic Stress Studies

Oral presentation: Posttraumatic stress disorder (PTSD) among earthquake survivors of the Wenchuan area (Sichuan, China)

8.2 Curriculum Vitae